UNIVERSITY OF CALIFORNIA

SANTA CRUZ

GENETIC AND BIOCHEMICAL ANALYSIS of the GTPase ASSOCIATED CENTER OF THE RIBOSOME

A dissertation submitted in partial satisfaction
of the requirements for the degree of

DOCTOR OF PHILOSOPHY
In

MOLECULAR, CELL AND DEVELOPMENTAL BIOLOGY

By

Eric J. Maklan

March 2012

The Dissertation of Eric J. Maklan is approved:

_____
Professor Harry F. Noller, Jr

_____
Professor Melissa Jurica

_____
Professor Michael Rexach

_____
Tyrus Miller
Vice Provost and Dean of Graduate Studies

TABLE of CONTENTS

List of Figures

List of Tables

ABSTRACT

Eric J. Maklan

GENETIC and BIOCHEMICAL ANALYSIS of the GTPase ASSOCIATED CENTER OF THE RIBOSOME

A macromolecular ribonucleoprotein complex called the ribosome is responsible for translation of the genetic code into proteins. The overall structure of the ribosome and its catalytic mechanisms are highly conserved across the three kingdoms of life. During all stages of protein synthesis ribosomes interact with a family of conserved protein factors that hydrolyze a bound molecule of GTP through an intrinsic GTPase mechanism and release GDP and inorganic phosphate. In isolation, the GTPase factors have very low GTPase activity. However, upon binding to the ribosome activity of their GTPase centers is highly stimulated. The hydrolysis of GTP is coupled to conformational rearrangements that promote various stages of protein synthesis. The protein factors interact with an overlapping binding site on the

large ribosomal subunit known as the GTPase Associated Center (GAC). The GAC is composed of two separate regions of the 23S rRNA known as the L11 stalk and the sarcin-ricin loop (SRL), which are proposed to individually contribute to the GTPase activation of the factors and the coupling of hydrolysis to the reactions of protein synthesis. In this work the role of the SRL and L11 stalk during protein synthesis have been explored. We find that the SRL is essential for the GTPase activity of elongation factor (EF) -G and the folding of 23S rRNA. Portions of the L11 stalk are dispensable for the GTPase activity of EF-G and EF-Tu; however, mutant ribosomes translate with reduced accuracy. A correlation between the position of the L11 stalk and the binding of translation factors is explored, and we suggest that the L11 stalk plays a direct role in controlling access of the factor's GTPase G domain to the SRL. We uncover a role for rRNA tertiary interactions in maintaining the architecture of the L11 stalk as well as a tertiary pathway between the SRL and L11 stalk. Additionally, we show that removal of the entire stalk inactivates ribosomes.

ACKNOWLEDGMENTS

I would like to thank my graduate advisor Professor Harry Noller and the current and past members of the Noller lab for creating an unforgettable experience.

I particularly would like to acknowledge Dr. Laura Lancaster for bench training and for the many hours she was available for discussions of both scientific and non-scientific topics. I would like to thank Dr. Iraj Ali for my start in the Noller lab, the training he provided, and his overall good-natured attitude. I would like to thank Dr. Martin Laurberg and John-Paul Donohue for their work on Tensor Analysis.

I thank my parents, Dr. David and Dr. Claire Maklan for always believing in me and for never accepting less than A(-) performance.

I extend special thanks to my wife and best friend Stephanie Maklan. Thank you for being my hardest critic and most ardent supporter throughout this process and all those that will follow.

The text of this dissertation includes reprints from Lancaster L, Lambert NJ, Maklan EJ, Horan LH, Noller HF (2008). The sarcin-ricin loop of 23S rRNA is essential for assembly of the functional core of the 50S ribosomal subunit. RNA 14, 1999-2012.

PREFACE: From Function to Structure

The central dogma of molecular biology lays the foundation for the sequential transfer of the genetic information, as encoded by deoxyribonucleic acid (DNA) within the genome, into ribonucleic acid (RNA), and finally into amino acids, which constitute the proteins (Figure 1) (Crick 1958). The translation of RNA into proteins occurs on the ribosome, a highly conserved macromolecular complex that is essential for all life on Earth.

Ribosomes were initially identified in electron micrographs of liver homogenates as small granules, which were found to contain a large proportion of RNA (Claude 1943) and to be active in the incorporation of amino acids into proteins (Zamecnik et al. 1954). Decades of research and development in the techniques of biochemical isolation and characterization have led to our current understanding of ribosome structure and function.

Robust translation activity requires the hydrolysis of guanosine-triphosphate (GTP) to guanosine-diphosphate (GDP) and inorganic phosphate (Pi) (Keller et al. 1956). This GTPase activity was first identified in cellular fractions of *E. coli*, and was found to depend on, and to be stimulated by the presence of active ribosomes (Conway et al. 1964). The specific proteins responsible for GTP binding and hydrolysis were identified as

elongation factor (EF) -Tu and -G (Allende et al. 1964; Nishizuka et al. 1966). These proteins assist in the binding of aminoacylated tRNA (aa-tRNA) and in the translocation of message and tRNAs through the ribosome during translation, for review see Wintermeyer et al (2004).

The elongation factors interact with a single overlapping region of the ribosome. As early as 1972 it was appreciated that EF-Tu and EF-G cannot be simultaneously bound to the ribosome (Richter 1972). Moazed et al. localized the binding site for both factors to loop 43 (L43) of 23S ribosomal RNA (rRNA) within the L11 stalk (helix 42, 43, and 44 of 23S rRNA) and helix 95 of 23S rRNA (Moazed et al. 1988). The ribosome targeting proteins, ricin and alpha-sarin (Endo et al. 1987; Endo et al. 1982), and the antibiotics thiostrepton, and micrococcin (Egebjerg et al. 1989), were found to inhibit or alter GTPase activities by specifically modifying or binding to these rRNA helices. In the last two decades of the millennium, groups around the world have worked to decipher the structure of the factor-binding site, specific interactions with the elongation factors, and mechanism of GTP hydrolysis.

The L11 stalk was determined to be an unexpectedly complex and dynamic component of the ribosome. In 1999, Wimberly et al. reported the first X-ray structure of the L11 stalk in isolation (Wimberly et al. 1999). The structure in context of complete ribosomes was not solved until 2001 (Yusupov et al. 2001). As crystallographers explored new crystallization

conditions, the technique of cryo-electron microscopy (cryo-EM) advanced to allow for resolution of individual ribosomal proteins and rRNA helices. Cryo-EM reconstructions were the first to identify the manner of interaction between the elongation factors and the ribosome, and to localize the specific domains involved therein. What emerged from multiple views of the ribosome, relying on independent techniques (Schuwirth et al. 2005), was that the L11 stalk occupies a range of positions in relation to the body of the 50S subunit (Frank et al. 2005; Valle et al. 2003). Surprisingly, both elongation factors were found to contact 23S rRNA loop 43 (L43) within the L11 stalk, and the nature of this interaction appeared to correlate with the position of the L11 stalk.

In nearly a half-century much has been determined about the structure and function of the ribosome. However, high-resolution structures and advanced biochemistry have not yet succeeded in providing a complete mechanism for protein synthesis. Questions of particular interest relate to the L11 stalk. What is the role of the L11 stalk in the process of translation? Is the L11 stalk required for the completion of one or multiple sub-reactions promoted by the elongation factors? Why is the L11 stalk observed in multiple orientations and how may these relate to elongation factor binding and GTP hydrolysis? Throughout my seven years in the Noller Lab I have worked to answer these questions, and my results are contained within this dissertation.

Figure 1. The Central Dogma of Molecular Biology

The genetic information is stored within double-stranded deoxyribonucleic acid (DNA) and is copied into single-stranded ribonucleic acid (RNA) by the process of transcription. RNA serves as the template molecule for protein synthesis, which occurs on the ribosome by the process of translation.

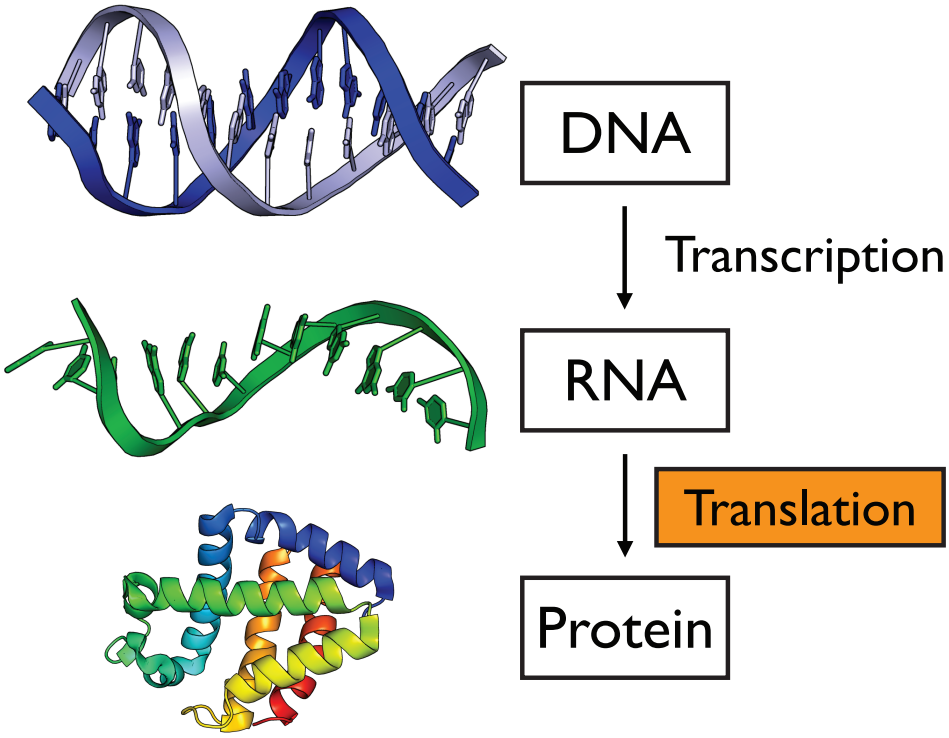
DNA
Transcription
RNA
Translation
Protein

CHAPTER I: Introduction

Proteins are an essential component of life on Earth and participate in nearly every process within cells. Many proteins are enzymes that function as catalysts in a diverse range of metabolic and catabolic reactions. Other proteins form intra and extra cellular structures or participate in cell signaling and ligand binding. Proteins are biological molecules that consist of one or more polypeptide chains typically folded into fibrous or globular structures. Polypeptide chains are composed of amino acid monomers connected one by one in an ordered sequence. The linear sequence of amino acids is defined according to the genetic code stored within a double-stranded polymer of DNA, known as a gene (Figure 1). To preserve the original DNA gene, a temporary copy is made of single-stranded RNA (Figure 1). The genetic code, which specifies 20 standard amino acids, is translated from RNA into protein (Figure 1) within a molecular machine called the ribosome. Despite the incredible diversity of life on Earth the ribosome is highly similar among all life forms.

Ribosome Structure

Universally, the ribosome consists of two ribonucleoprotein complexes termed the large and small ribosomal subunits. In both cases, rRNA accounts for approximately two-thirds the mass, while the remaining third is protein. In the Gram-negative prokaryote model organism *Escherichia coli*, the 1.5 megadalton large ribosomal subunit (50S) contains 23S (2904 nucleotides) and 5S (120 nucleotides) rRNAs (Figure 2), and thirty-four proteins. The 0.8 megadalton small subunit (30S) contains a single copy of the 16S rRNA (1542 nucleotides) and twenty-one proteins (Figure 3). 50S (Figure 4A) and 30S (Figure 4B) subunits associate to form the active 70S ribosome (Figure 4C).

Ribosomal Ligands

During the course of protein synthesis the ribosome interacts with multiple RNA ligands. The first RNA ligand is the messenger RNA (mRNA), which binds to the 30S subunit and serves as the template from which the target protein is generated. mRNAs range in size from tens to many hundreds of nucleotides in length. Nucleotide triplets known as codons specify the exact ordering of amino acids according to the genetic code (Matthaei et al. 1961;

Nirenberg et al. 1965). The ribosome translates mRNA codons one at a time with the aid of a special type of RNA ligand, the transfer RNA (tRNA). tRNAs are composed of a structured RNA (Figure 5A) that is covalently attached at its 3' end to an amino acid through an aminoacyl ester bond (Figure 5B). tRNAs also contain a 3-nucleotide anticodon that is responsible for base pairing interactions with the mRNA codon (Figure 5C). Each of the 20 amino acids is attached to a specific subset of tRNA isoacceptors by a protein aminoacyl tRNA synthetase (aaRS) (Figure 5D).

The ribosomal subunits each contain three tRNA binding sites that span the intersubunit space of the 70S ribosome (Watson 1964; Wettstein et al. 1965). These binding sites are known as the acceptor (A), peptidyl (P), and exit (E) sites (Figure 6A). The tRNA anticodon interacts with mRNA on the 30S subunit and the acceptor ends bind to the 50S subunit. Aminoacylated tRNAs (aa-tRNA) bind to the A site. The tRNA carrying the nascent polypeptide chain, known as the peptidyl tRNA, is bound to the P site. During the peptidyl transferase reaction the aminoacyl ester bond between the P-site tRNA and its amino acid is broken and a new peptide amino bond (amino acid-amino acid) is formed with the amino acid attached to the A site tRNA. In this manner the growing polypeptide is transferred from one tRNA to another, each step extending the final protein by a single amino acid.

Protein Synthesis

The process of protein synthesis occurs in three phases: initiation, elongation and termination (Figure 6B-G). In each phase the ribosome is assisted by multiple protein cofactors. A special class of GTP hydrolyzing (GTPase) protein factors function with the ribosome in each phase of protein synthesis. These factors share a similarly structured GTPase domain that is responsible for the hydrolysis of a bound molecule of GTP, forming GDP and inorganic phosphate. The GTPase activity of the factors is greatly stimulated by interaction with the ribosome.

Initiation

The initiation phase of protein synthesis brings the mRNA and ribosomal subunits together, establishes the reading frame, and prepares the ribosome for formation of the first peptide bond (Figure 6B). Initiation begins with mRNA binding to the 30S subunit. The first codon to be translated (start codon) is aligned into the 30S P site by base pairing interactions between the Shine-Dalgarno region of 16S rRNA and the 5' untranslated region of the mRNA (Shine et al. 1974). A special initiator tRNA carrying the modified

amino acid N-formyl-methionine (fMet) is bound to the P site of the 30S subunit with the aid of initiation factors (IF) 1, IF2, and IF3 (Mazumder et al. 1969). Binding of the initiator tRNA establishes the reading frame that will be used during translation. This 30S initiation complex is now prepared to associate with a 50S subunit. IF2 is a GTPase, and subunit association stimulates its GTPase activity. GTP hydrolysis triggers the release of IF2 as well as IF1 and IF3. The large and small subunits are now associated on an mRNA and contain the initiator tRNA bound to the start codon in the ribosomal P site.

Elongation

During the elongation phase of protein synthesis the template mRNA is sequentially decoded and the nascent polypeptide is extended. The elongation phase is a repetitive cycle of three reactions: aa-tRNA binding, peptidyl transferase, and translocation (Figure 6C-F). Elongation is aided by two GTPase protein factors, EF-Tu and EF-G. EF-Tu functions in a ternary complex of EF-Tu•aa-tRNA•GTP and is responsible for the binding of aa-tRNA to the ribosomal A site. EF-G catalyzes translocation, the 3-nucleotide movement of mRNA and transfer of tRNAs from the P and A to E and P sites, respectively.

Ternary complex binds to the ribosome when the A site is vacant (Figure 7A) and facilitates interaction between the tRNA anticodon and mRNA codon within the A site of the 30S subunit (Figure 7B). If the codon and anticodon are complementary, the aa-tRNA is cognate. The binding of cognate tRNA stimulates the GTPase activity of EF-Tu and leads to the release of EF-Tu•GDP and accommodation of the aa-tRNA into the A site of the 50S subunit (Figure 7C). Peptidyl transferase is catalyzed by the 50S subunit (Figure 7D). In this reaction, the peptidyl group is transferred from the P-site tRNA and a new peptide bond is formed between its carboxyl group and the amino group of the A-site tRNA. This pretranslocation complex contains a deacylated-tRNA in the P site and a peptidyl-tRNA in the A site (Figure 7D).

Translocation occurs in two steps. Following peptidyl transferase (Figure 7D) the deacylated-P- and peptidyl-A-site tRNAs reversibly translocate on the 50S subunit by a mechanism that is spontaneous, but promoted by the binding of EF-G (Figure 7E) (Cornish et al. 2008; Moazed et al. 1989; Pan et al. 2007; Spiegel et al. 2007). In this intermediate configuration tRNAs are bound in the hybrid P/E and A/P states (Moazed et al. 1989) and the 30S subunit is rotated approximately 6˚ counter clockwise relative to the stationary 50S subunit (Frank et al. 2000). The ribosome promotes the GTPase activity of EF-G and hydrolysis leads to conformational

rearrangements in the ribosome known as unlocking (Valle et al. 2003), which prepare the ribosome for translocation on the 50S subunit (Savelsbergh et al. 2003). The movement of mRNA and tRNAs is rapid following unlocking and may proceed or follow the release of Pi, which independently proceeds the release of EF-G•GDP. Following translocation, the peptidyl-tRNA is once again bound in the P site, the deacylated E-site tRNA is released (Spiegel et al. 2007), and the A site is once again vacant and prepared for binding of the next aa-tRNA (Figure 7F). The elongation cycle continues in this manner until the end of the mRNA coding region is reached, as indicated by presence of a stop codon in the A site.

Termination

Protein synthesis culminates in the termination phase, during which time the completed polypeptide is released and the 70S ribosome is recycled (Figure 6G). Unlike the sense codons that are recognized by tRNAs, the non-sense stop codons are recognized by a protein release factor (RF). The binding of RF1 or RF2 triggers the hydrolysis of the terminal peptidyl-tRNA bond, releasing the completed protein. The ribosome now contains deacylated-tRNAs in the E and P sites and is still bound by mRNA and the release factor. The release factor is removed with the help of another GTPase

factor, RF3. Finally, ribosomal recycling factor (RRF) and EF-G act together to split the ribosomal subunits, releasing the deacylated-tRNAs and mRNA. The subunits, tRNAs and factors are used repeatedly by the cell to generate its full compliment of proteins.

The Ribosome is a Ribozyme

The central activities of the elongation cycle (tRNA binding, peptidyl transferase and translocation) are catalyzed by the 23S and 16S rRNAs. However, because the ribosome contains both proteins and RNAs, there existed a debate as to which fraction was responsible for its catalytic activities. The solution emerged by characterization of the minimum components necessary for each reaction in which the ribosome partakes. In all cases the answer was the same. The protein fraction of the ribosome is dispensable and the rRNAs are essential; the ribosome is a ribozyme. For a review of RNA based catalysis see (Scott 1998).

Peptidyl Transferase

Studies of the peptidyl transferase reaction were greatly aided by the discovery of the antibiotic puromycin (Yarmolinsky et al. 1959). Puromycin

contains an analog of the aminoacyl-adenosine group naturally present on aa-tRNA. When added to ribosomes containing a peptidyl P-site tRNA, the amino group of puromycin functions similarly to the 3' terminus of an A-site aa-tRNA. Puromycin accepts the P-site peptide and is released from the ribosome as peptidyl-puromycin (Darken 1964; Gilbert 1963; Morris et al. 1961). This reaction is inhibited by the antibiotic chloramphenicol (Traut et al. 1964), which interferes with authentic peptide transfer from one tRNA to another, and does not occur when puromycin is added to isolated aa-tRNAs (Nathans et al. 1961). Therefore, the mechanism and kinetics of the ribosome's peptidyl transferase activity may be accurately modeled by the puromycin reaction.

The peptidyl transferase reaction is supported by the 70S ribosome and isolated 50S ribosomal subunit and does not require the presence of the 30S subunit, translation factors, or GTP. Maden et al (1968) demonstrated that 70-80% of polyphenylalanine-charged 70S or 50S ribosomes that were washed with salt to remove the translation factors were reactive towards puromycin. The reaction proceeded with normal kinetics in a minimum buffer free of GTP, ruling out the possibility that a translation factor GTPase responsible for peptidyl transfer remained bound to the ribosomes following salt washing (Maden et al. 1968). These experiments localized the peptidyl transferase activity to the 50S subunit but were not sufficient to determine if protein or RNA catalyzed it.

Final evidence for the rRNA origin of the peptidyl transferase activity came from chemical cross-linking and protein depletion experiments. tRNAs were synthesized to contain chemically reactive groups at their 3' ends that when bound to the ribosome would cross-link themselves to the closest macromolecular components. The theory behind this approach was simple. Because the 3' end of the tRNA must interact with the peptidyl transferase center, identification of the tRNA cross-linked species, be it protein or rRNA, would determine the source of the peptidyl transferase activity. Barta et al (1984) determined that a benzophenone-derivatized Phe-tRNA was efficiently cross-linked to the central loop of domain V of the 23S rRNA (Figure 2). These cross-links were noteworthy because mutations conferring resistance to chloramphenicol were located in the same region of domain V (Vester et al. 1988). Secondly, ribosomes were shown to maintain their peptidyl transferase activity following a procedure designed to degrade and remove the ribosomal proteins. Antibiotics or treatment with ribonuclease T1, EDTA, or phenol inhibited the activity (Noller et al. 1992). EDTA is a chelator of the divalent cation Mg^{2+}, which is critical for the structured folding of rRNAs, and phenol is used to specifically extract RNAs.

tRNA Binding

The ribosomal tRNA binding sites are framed by the 23S and 16S rRNAs and can be filled in the absence of GTPase translation factors. During *in vivo* protein synthesis tRNAs are bound to the ribosome with the aid of IF2 and EF-Tu. IF2 is responsible for the binding of initiator tRNA to the P site of the 30S subunit, and EF-Tu delivers aa-tRNAs to the A site of the 70S ribosome. The strict requirement for the factors and GTP can be circumvented *in vitro* by increased Mg^{2+} concentrations, once again demonstrating the centrality of the rRNAs in translation.

Translocation

The coupled movement of mRNA and tRNAs through the ribosomes during protein synthesis is promoted by EF-G and the hydrolysis of GTP. In the presence of EF-G•GTP translocation occurs at a rate greater than 35 s-1 (Savelsbergh et al. 2003), however, neither the protein factor nor its GTPase activity is strictly required. The first evidence for EF-G-independent translocation came from Gavrilova et al (1976) who demonstrated the translocation-dependent synthesis of polyphenylalanine peptides from a polyuridylic acid (poly(U)) mRNA template in a system lacking EF-G

(Gavrilova et al. 1976). EF-G-independent translocation is also promoted by the antibiotic sparsomycin (Fredrick et al. 2003), which binds to the peptidyl transferase center and stabilizes the binding of peptidyl-tRNA to the 50S P site (Monro et al. 1969). GTP hydrolysis is prevented when GTP is replaced with the non-hydrolyzable analogue GDPNP. This replacement slows translocation between 2.5- and 50-fold but does not prevent full extent of the reaction (Ermolenko et al. 2011; Pan et al. 2007; Rodnina et al. 1997). Finally, translocation may also be uncoupled from the release of inorganic phosphate by the antibiotic fusidic acid, which traps EF-G•GDP•P_i on the post-translocation ribosome (Savelsbergh et al. 2009).

The GTPase Factors EF-Tu and EF-G

Although the ribosome is a ribozyme, rapid translation elongation is dependent on the activity of the elongation factor GTPases, EF-Tu and EF-G. Both factors bind to an overlapping region of the ribosome, including the 50S subunit GAC and 30S subunit A-site (Agrawal et al. 1999; Moazed et al. 1988; Valle et al. 2003). As may be expected for two ligands sharing a common binding site, EF-Tu and EF-G share a high degree of structural homology and EF-Tu ternary complex and EF-G display properties of macromolecular

mimicry (Liljas 1996; Nissen et al. 1995). One major unsolved question is how does the ribosome distinguish between these two factors?

Structural homology and molecular mimicry between the elongation factors is apparent when comparing EF-Tu ternary complex in the GTP bound conformation (Kjeldgaard et al. 1993; Nissen et al. 1995) (Figure 5A) with EF-G in complex with GDP (Czworkowski et al. 1994) or a GTP analogue (Figure 5B) (Hansson et al. 2005). EF-Tu is composed of three domains and domain I and II are homologous to the first two domains of EF-G. Domain I, also known as the G domain, is the site of GTP binding and GTPase activity. The aa-tRNA is bound by EF-Tu such that tRNA body and anticodon stem extend away from protein (Figure 8A). EF-G is composed of five domains and contains a unique insertion within domain I known as the G' domain (Fgire 8B). Domains IV and V form an elongated structure that is molecularly analogous to the aa-tRNA as bound within ternary complex (Figure 8C). The elbow of aa-tRNA and domain V of EF-G form the site of interaction between the L11 stalk and EF-Tu ternary complex and EF-G, respectively. It is likely that these regions are of particular importance for interaction between the factors and ribosome.

Figure 2. Secondary Structures of the Large Ribosomal Subunit rRNAs

The large ribosomal subunit of *E. coli* contains 23S and 5S rRNAs. 23S rRNA is 2904 nucleotides and is divided into domains I through VI. 5S rRNA is composed of a single 120 nucleotide domain.

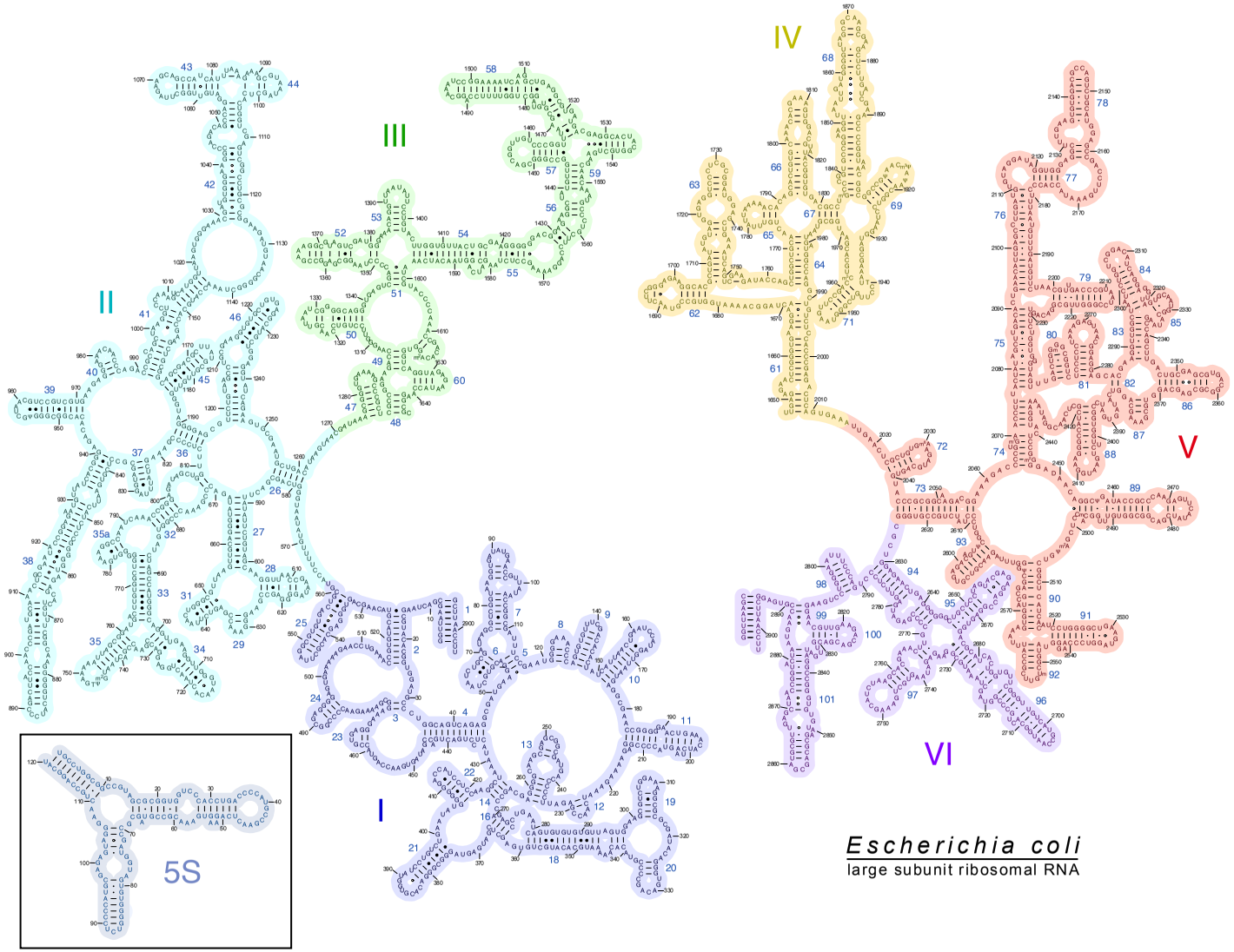
I
II
III
IV
V
VI
5S
Escherichia coli
large subunit ribosomal RNA

Figure 3. Secondary Structure of the Small Ribosomal Subunit rRNA

The small ribosomal subunit of *E. coli* contains a single copy of the 1542 nucleotide 16S rRNA. 16S rRNA is divided into 4 domains: 5', central (C), 3' major (3'M), and 3' minor (3'm).

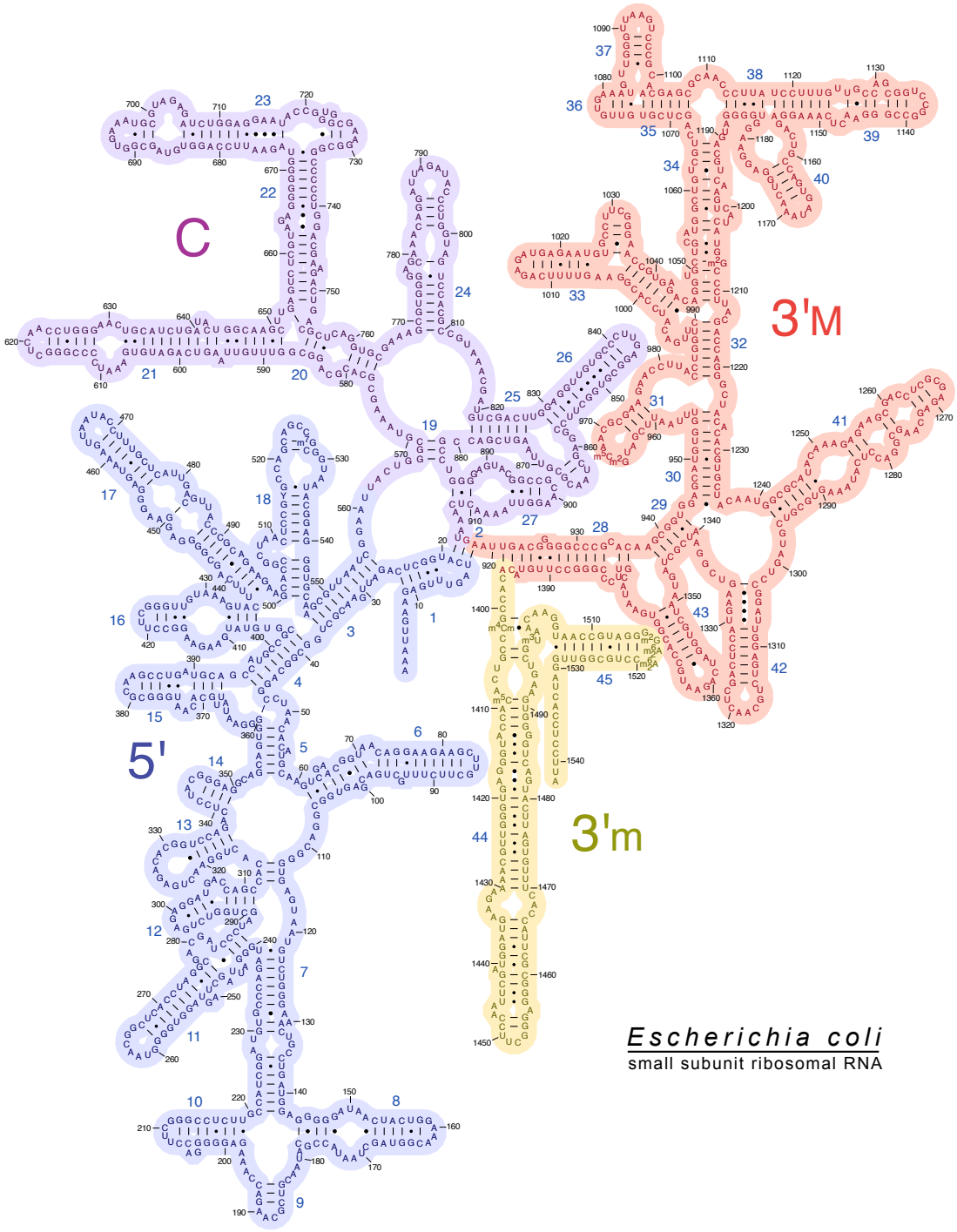
C
5'
3'M
3'm
Escherichia coli
small subunit ribosomal RNA

Figure 4. Ribosome Structure

Model of the (A) 50S subunit (B) 30S subunit and associated subunits in the (C) 70S ribosome as determined by X-ray crystallography at 5.5 Å resolution (Yusupova et al. 2006). The 70S ribosome is shown from the side with the A site oriented forward. The 23S rRNA is shown in grey, 16S rRNA teal, mRNA green, 50S proteins magenta, and 30S proteins in blue. A-, P-, and E-site tRNAs are shown bound to each subunit and the 70S ribosome in yellow, orange, and red, respectively.

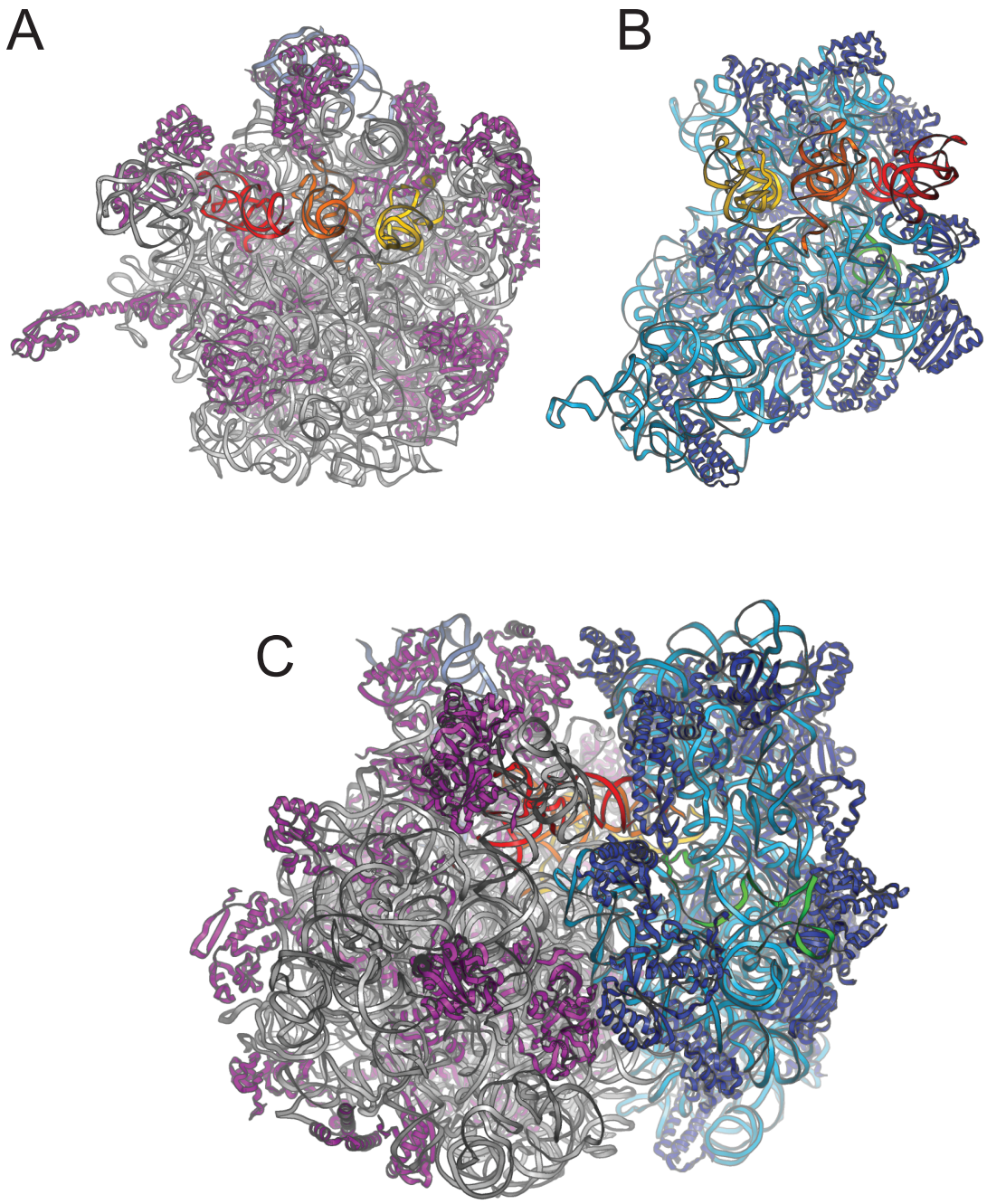
A
B
C

Figure 5. Structural Features of Transfer RNA

Transfer RNAs (tRNA) are formed from a single RNA of approximately 76 nucleotides. (A) Structure of aminoacylated Phe-tRNAPhe determined by X-ray crystallography at 2.70 Å resolution. The phosphate backbone is shown in cartoon (orange) and nucleotides are presented as cones (grey). The three nucleotides of the anticodon and terminal 3' adenosine (A76) with linked phenylalanine are shown as sticks. (B) Detail view of the 3' end showing A76 and phenylalanine (Phe); colored by element: carbon (white), nitrogen (blue), oxygen (red), and phosphorus (orange). Location of the aminoacyl bond is indicated with an arrow. (C) Details of the anticodon, colored as in (B). tRNAs are charged with their amino acid by specific aminoacyl tRNA synthetases (ARS). (D) De-acylated $tRNA^{Phe}$ reacts with ARS^{Phe}, Phe, and ATP to form Phe-$tRNA^{Phe}$. Reaction byproducts are adenosine monophosphate (AMP) and pyrophosphate (PP_i). Phe is indicated by the green sphere.

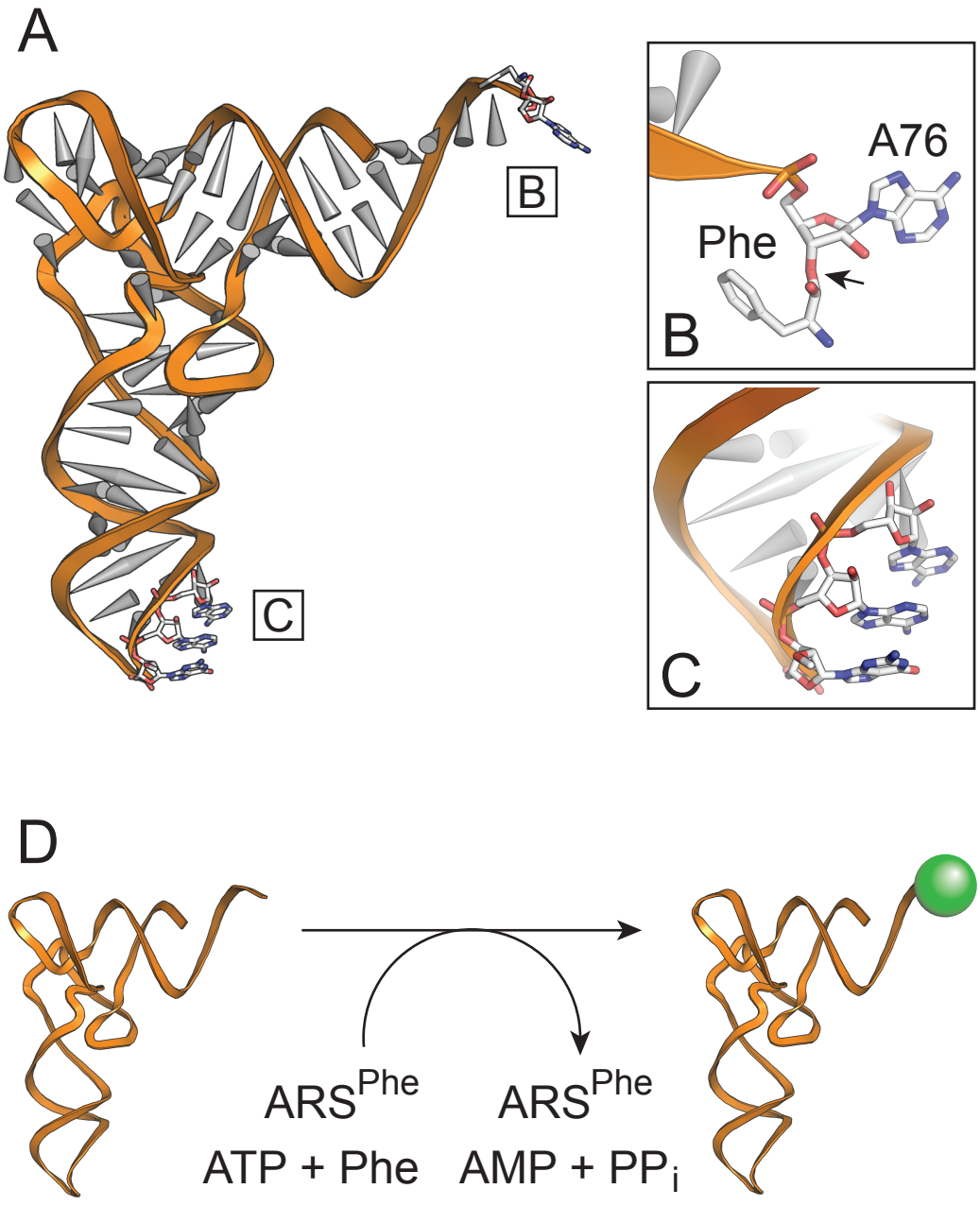
A
B
C
A76
Phe
B
C
D
ARS^Phe
ATP + Phe
ARS^Phe
AMP + PPi

Figure 6. Overview of Protein Synthesis

(A) Cartoon of the 30S and 50S ribosomal subunits showing the location of the A, P, and E tRNA binding sites. mRNA is bound to the 30S ribosome. (B-G) Initiation, elongation, and termination phases of protein synthesis are aided by translation elongation factors, some of which possess GTPase activity, indicated in red.

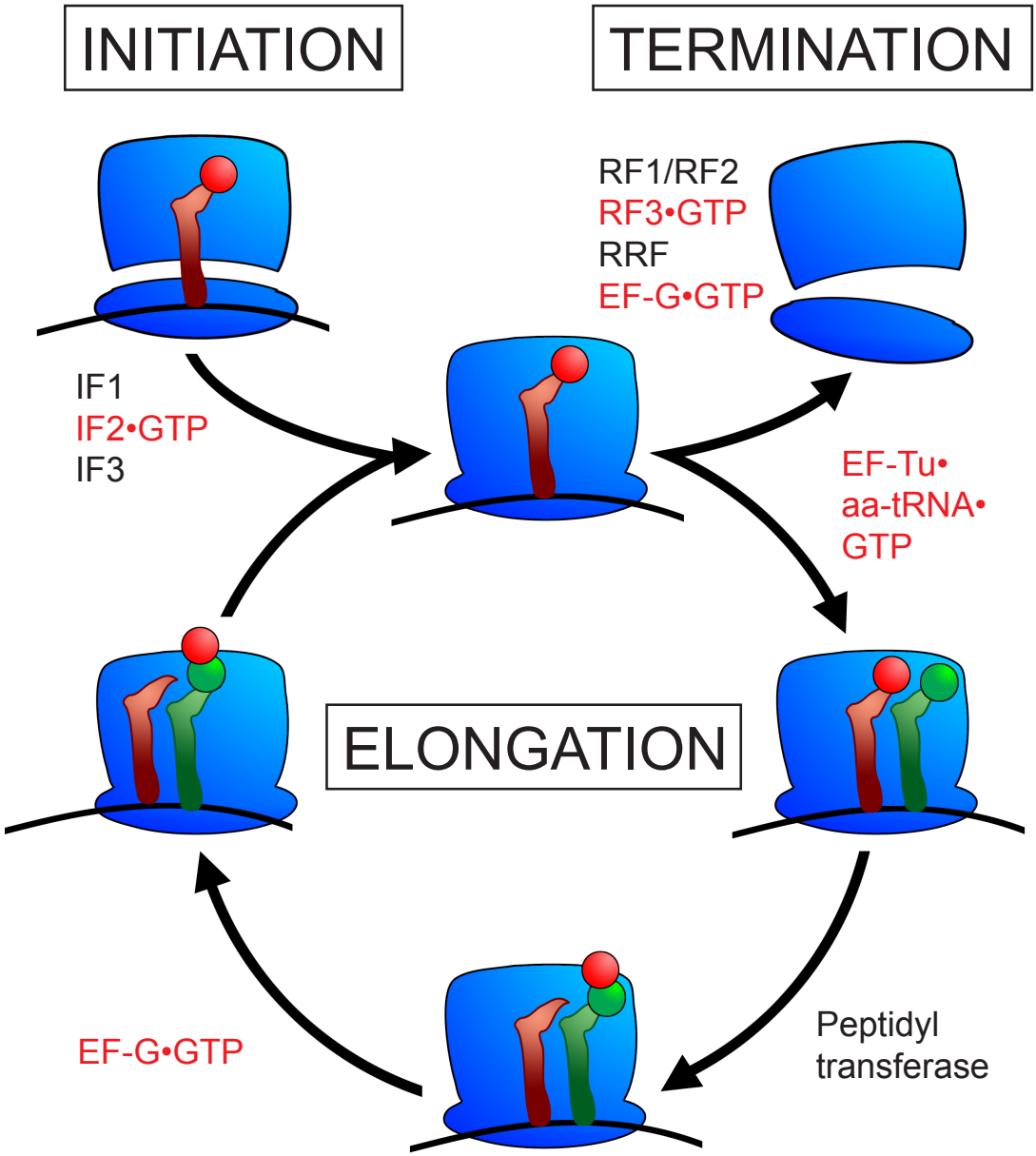
INITIATION
TERMINATION
RF1/RF2
RF3•GTP
RRF
EF-G•GTP
IF1
IF2•GTP
IF3
EF-Tu•
aa-tRNA•
GTP
ELONGATION
EF-G•GTP
Peptidyl
transferase

Figure 7. Elongation Cycle: Box Diagrams

The ribosome is shown in cartoon box diagrams. (A-C) Binding of aa-tRNA to the ribosomal A-site. (A) The ribosomal substrate for EF-Tu ternary complex contains a peptidyl-tRNA bound in the P-site, the A-site is vacant and the next codon to be decoded is presented on the 30S subunit. (B) Prior to GTPase activation, EF-Tu ternary complex is bound in the A/T transition state. (C) GTPase activation leads to the release of EF-Tu•GDP and accommodation of aa-tRNA into the A/A state. (D) The peptidyl transferase reaction transfers the peptidyl group from the P-site tRNA to the amino acid (*) attached to the A-site aa-tRNA. (E-F) Translocation. (E) Translocation occurs spontaneously on the 50S subunit, resulting in the hybrid P/E and A/P tRNA binding configuration. (F) Translocation on the 30S subunit is promoted by EFG•GTP. Following the completion of translocation, the peptidyl tRNA is once again bound in the P site and E-site tRNA is released.

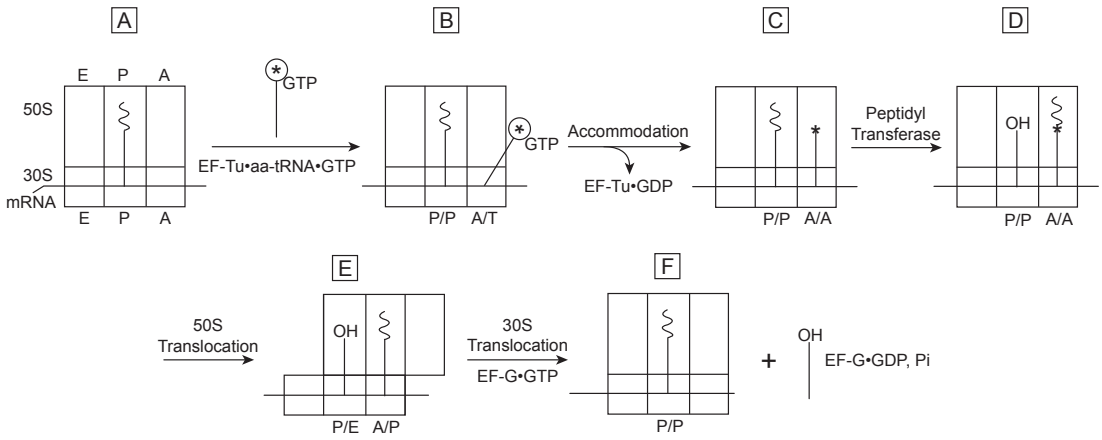
A
B
C
D
E
F
E P A
50S
30S
mRNA
E P A
GTP
EF-Tu•aa-tRNA•GTP
GTP
P/P A/T
Accommodation
EF-Tu•GDP
P/P A/A
Peptidyl
Transferase
OH
P/P A/A
50S
Translocation
OH
P/E A/P
30S
Translocation
EF-G•GTP
P/P
+
OH
EF-G•GDP, Pi

Figure 8. Structural Analogy between EF-Tu Ternary Complex and EF-G

(A) EF-Tu ternary complex and (B) EF-G are structurally analogous; domain numbering is indicated. The elbow of aa-tRNA and domain V of EF-G interact with the L11 stalk of the 50S ribosome (arrow heads). (C) Super-positioning of EF-Tu ternary complex (green) and EF-G (magenta).

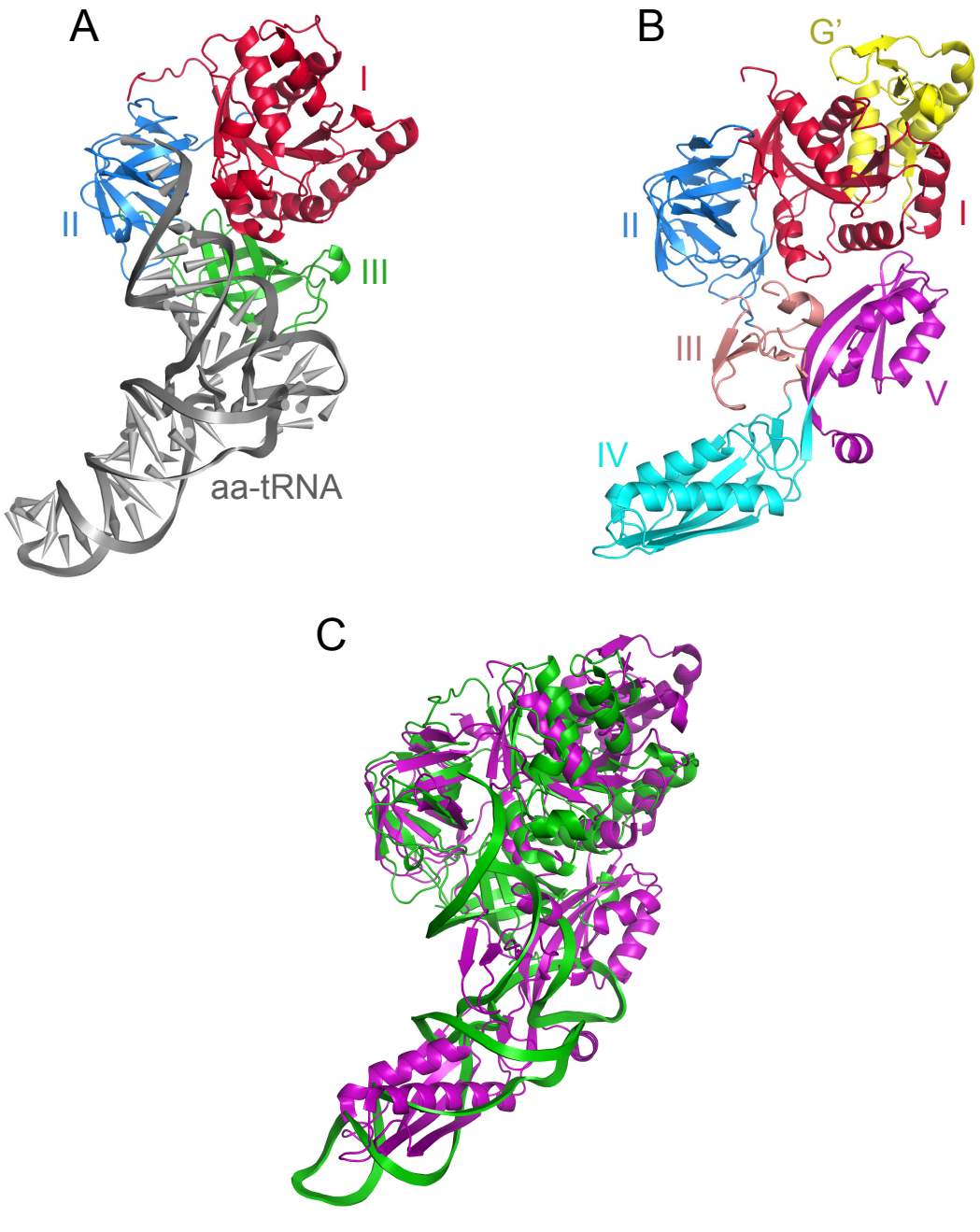
A
I
II
III
aa-tRNA
B
G'
II
I
III
V
IV
C

CHAPTER II: Testing the Role of the Sarcin-Ricin Loop in EF-G-Dependent GTP Hydrolysis

INTRODUCTION

This chapter contains results and discussion that have been previously published in Lancaster et al. (2008). Maklan EJ is responsible for the data and analysis presented in Figure 4C of that work. Portions of that work of particular relevance to this thesis are presented within this chapter.

During the course of protein synthesis the ribosome interacts with a family of conserved protein factor GTPases that assist the ribosome in all stages of translation. The initiation factor IF2 stimulates the binding of the initiator tRNA fMet-tRNA^{fMet} to the 30S subunit P-site (Mazumder et al. 1969). Elongation factors EF-Tu and -G catalyze the binding of A-site aa-tRNA and the translocation of mRNA and tRNAs through the ribosome (Wintermeyer et al. 2004). Release factor RF3 catalyzes the dissociation of release factors RF1 and RF2 from the ribosome following the termination of peptide synthesis (Freistroffer et al. 1997). The factors are stimulated by their interaction with the ribosome to hydrolyze a bound molecule of GTP.

The GTPase factors share a common ribosomal binding site. Cryo-EM reconstructions and X-ray diffraction structures place each of the factors near or in contact with two features of the large ribosomal subunit, the sarcin-ricin

loop (SRL) and the L11 stalk (Allen et al. 2005; Gao et al. 2009; Klaholz et al. 2004; Schmeing et al. 2009; Valle et al. 2003; Zhou et al. 2011). Collectively, these features are referred to as the GTPase associated center (GAC) (Beauclerk et al. 1985). The SRL is within helix 95 of the 23S rRNA (nucleotides 2653-2667) and the L11 stalk is composed of 23S rRNA helices 42, 43 and 44 (nucleotides 1051-1108). The SRL contains the largest universally conserved 23S rRNA sequences (Gutell et al. 1992). The secondary and tertiary structures of the L11 stalk are well conserved and contain a large proportion of invariant nucleotides (Cannone et al. 2002).

The SRL and L11 stalk are implicated in the process of factor binding and GTP hydrolysis (Moazed et al. 1988). Modification of the SRL by depurination of A2660 by ricin or cleavage of the G2661-A2662 phosophodiester bond by α-sarcin, are inhibitory to translation (Endo et al. 1987; Endo et al. 1982). The binding of various peptide antibiotics to the L11 stalk selectively inhibits or stimulates the GTPase activity of the factors (Egebjerg et al. 1989).

To study the role of the SRL in the GTPase activation of EF-G, SRL nucleotides 2653-2667 were replaced with a GAAA tetraloop hairpin in *E. coli* (ΔSRL). Expression of ΔSRL 23S rRNA resulted in a dominant-lethal phenotype. Affinity purification of ΔSRL ribosomes by means of an incorporated phage MS2 coat protein binding RNA helix inserted into helix 95

of 23S rRNA (Ali et al. 2006; Youngman et al. 2004) was employed to facilitate detailed *in vitro* biochemical analysis. Affinity-purified ΔSRL ribosomes were found to be inactive in the ribosome-dependent hydrolysis of GTP by EF-G, and the K_d for EF-G binding was increased significantly. The reactivity of ΔSRL 23S rRNA within domains II, V, and VI towards base-specific structural probes was unexpectedly altered, and ΔSRL ribosomes lack ribosomal protein L16.

RESULTS

Construction and purification of ΔSRL ribosomes

For complete details on the construction and purification of ΔSRL 50S subunits please refer to Lancaster et al (2008). In brief, 23S rRNA nucleotides 2653-2667 of the SRL were replaced with a GAAA tetraloop hairpin (Figure 9A) by site-directed mutagenesis (Kunkel 1985) within the expression plasmid pLK35.50S.MS2 (Ali et al. 2006). The transient expression of plasmid-derived ΔSRL 23S rRNA by *E. coli* resulted in a complete lack of growth, indicating the dominant-lethal phenotype (Figure 9B). To facilitate *in vitro* characterization, ΔSRL 50S ribosomes were affinity purified on a 5 mL GST-trap column (Amersham) that was pre-bound with MS2-GST fusion protein

(Lancaster et al. 2005). Presence of the mutation in ribosomes was confirmed by primer extension analysis of affinity-purified ΔSRL 23S rRNA (Figure 9C).

ΔSRL Ribosomes do not support EF-G-dependent activities

Affinity-purified ΔSRL ribosomes were found to be inactive in polyphenylalanine synthesis and EF-G-dependent translocation (data not shown). To explore these defects, the interaction between ΔSRL ribosomes and EF-G was tested in the translocationally uncoupled GTPase idling reaction (Rodnina et al. 1999). Wild-type ribosomes efficiently stimulated the hydrolysis of GTP by EF-G·GTP in contrast to ΔSRL ribosomes, which did not (Figure 10A). The addition of mRNA and tRNA is stimulatory for the idling reaction (Robertson et al. 1986). The activity of wild-type ribosomes in the EF-G idling reaction increased 2-fold when poly(U) mRNA and $tRNA^{Phe}$ were included in the reaction. There was no improvement in the activity of ΔSRL ribosomes under these conditions. These results indicate that ΔSRL ribosomes do not support a functional interaction with EF-G required for the hydrolysis of GTP.

To test the possibility that the lack of EF-G idling reaction was due to altered binding of EF-G·GTP to ΔSRL ribosomes, the K_d for EF-G binding was measured by monitoring the change in signal intensity of fluorescein-labeled

EF-G (D. Ermolenko, unpublished), derived from the method of Seo et al. (2004). The K_d for wild-type ribosomes binding of EF-G was found to be 26.5 nM +/- 3.3, compared to 1300 nM +/-98 for ΔSRL ribosomes (Fig 10B). This result indicates that replacement of the SRL with a GAAA tetraloop results in an EF-G binding defect.

Structural changes in the 23S rRNA and protein composition of ΔSRL 50S subunits

For complete details on the structural changes in the 23S rRNA of ΔSRL 50S subunits please refer to Lancaster et al (2008). In brief, the structure of ΔSRL 23S rRNA was studied by means of base-specific chemical probing. More than 40 bases of 23S rRNA derived from ΔSRL ribosomes displayed increased reactivity and two showed decreased reactivity compared to wild-type. Changes in reactivity were distributed throughout 23S rRNA domain II, V, and VI (Figure 11A-D). Due to the folding of rRNA, these nucleotides are located closely to one another and contain much of the functional core of the ribosome (Schuwirth et al. 2005). This region may be viewed as front and back layers of rRNA helices. The front layer is composed of 23S rRNA from domain V and VI and includes the SRL and H91 (Figure 11A, B). The back layer contains 23S rRNA from domain II, V, and VI and

includes H42, which leads directly the L11 stalk (Figure 11C, D). The front and back layers are connected by rRNA tertiary interactions (Figure 11E). The binding site for ribosomal protein L16 straddles both of these layers, and ΔSRL ribosomes were found to be specifically lacking protein L16, see Lancaster et al (2008).

Figure 9. Deletion of the SRL Confers a Dominant-Lethal Phenotype

(A) Wild-type (WT) sequence of 23S rRNA nucleotides 2650– 2670 and that of the SRL deletion mutant (ΔSRL), in which nucleotides 2653–2667 (the SRL) were replaced with a GAAA tetraloop. (B) *E. coli* strains that express either WT or ΔSRL MS2-tagged 50S subunits from plasmid, via a heat-inducible promoter, were grown at 30°C, spotted on plates, and incubated at 30°C or 42°C. (C) Primer-extension analysis of 23S rRNA from affinity-purified WT and ΔSRL 50S subunits probed with either D, dimethylsulfate, or K, kethoxal. Lanes A and G are sequencing lanes; (-) unmodified subunits. Reproduced from Lancaster et al (2008).

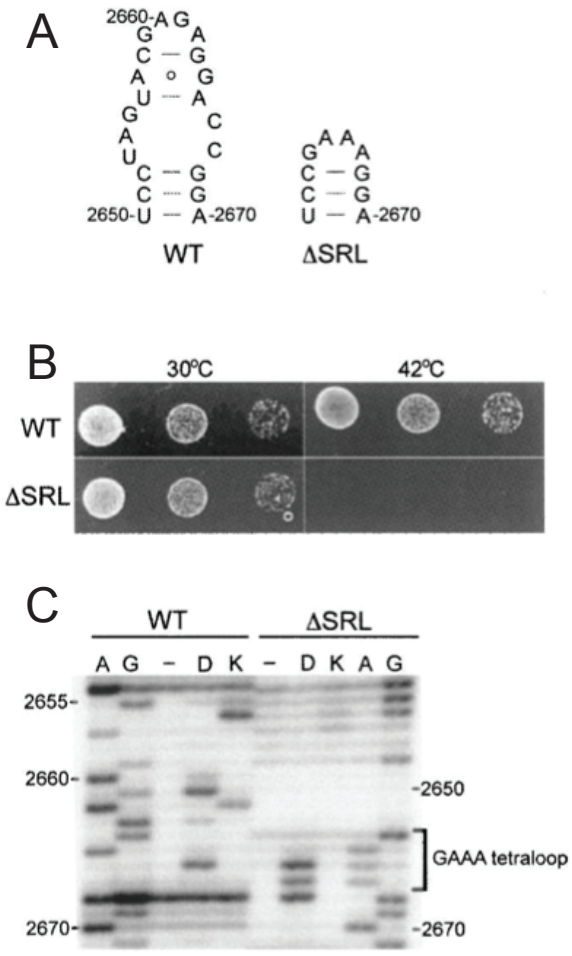
A
2660-A G
G A
C — G
A ° G
U — A
G C
A
U C
C — G
C — G
2650-U — A-2670
WT
G A A A
C — G
C — G
U — A-2670
ΔSRL
B
30°C
42°C
WT
ΔSRL
C
WT
ΔSRL
A G – D K – D K A G
2655-
2660-
2670-
-2650
GAAA tetraloop
-2670

Figure 10. ΔSRL 50S Subunits are Defective in Interaction with EF-G

(A) Ribosome-dependent EF-G•GTP hydrolysis. ΔSRL (△) or WT (□) vacant ribosomes (filled symbols) or those containing poly(U) mRNA and $tRNA^{Phe}$ (open symbols) were incubated in the presence of EF-G and [^{32}P]-γ-GTP. (B) EF-G binding. Quenching of fluorescein-labeled EF-G was measured with increasing concentrations of ΔSRL (△) or WT (□) ribosomal complexes containing mRNA and $tRNA^{fMet}$. Reproduced from Lancaster et al (2008).

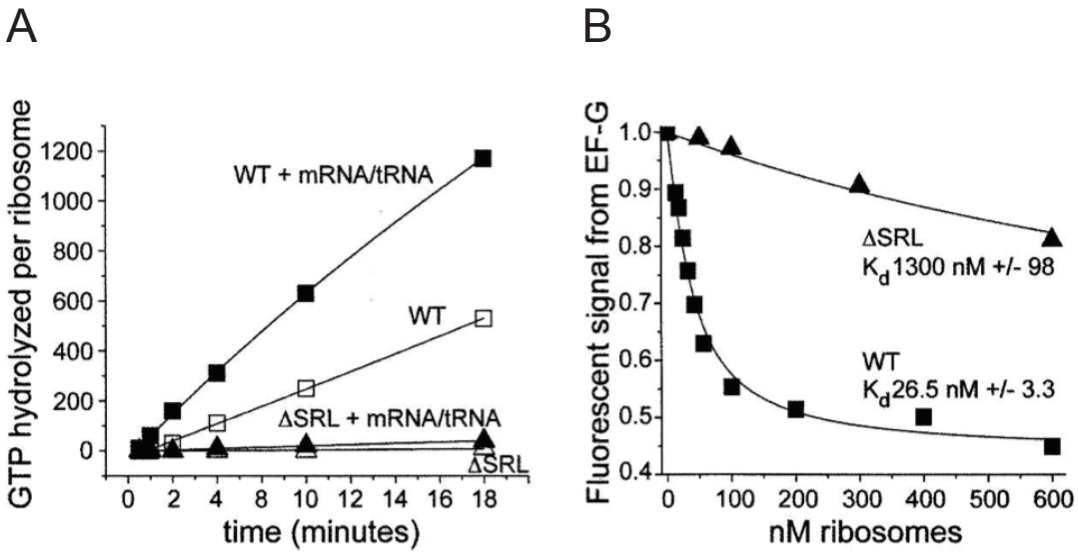
A
B
GTP hydrolyzed per ribosome
1200
1000
800
600
400
200
0
WT + mRNA/tRNA
WT
ΔSRL + mRNA/tRNA
ΔSRL
0 2 4 8 10 12 14 16 18
time (minutes)
Fluorescent signal from EF-G
1.0
0.9
0.8
0.7
0.6
0.5
0.4
ΔSRL
K_d1300 nM +/- 98
WT
K_d26.5 nM +/- 3.3
0 100 200 300 400 500 600
nM ribosomes

Figure 11. Disrupted Tertiary Interactions within ΔSRL 23S rRNA

Protected (orange) and enhanced (blue and pink) nucleotides; 23S rRNA (gray) helix numbers are indicated. (A) The front layer as seen in the 50S subunit crown view. (C) The corresponding back layer, with helix 95 (yellow) and the SRL (red) indicated. (B) and (D) are 180° rotations of (A) and (C). (E) Secondary structure of 23S rRNA showing the front (cyan) and back (pink) layers; lines indicate tertiary interactions within the front (blue) or back (magenta) layers or between layers (orange) that are disrupted in the ΔSRL 50S subunits. Reproduced from Lancaster et al (2008).

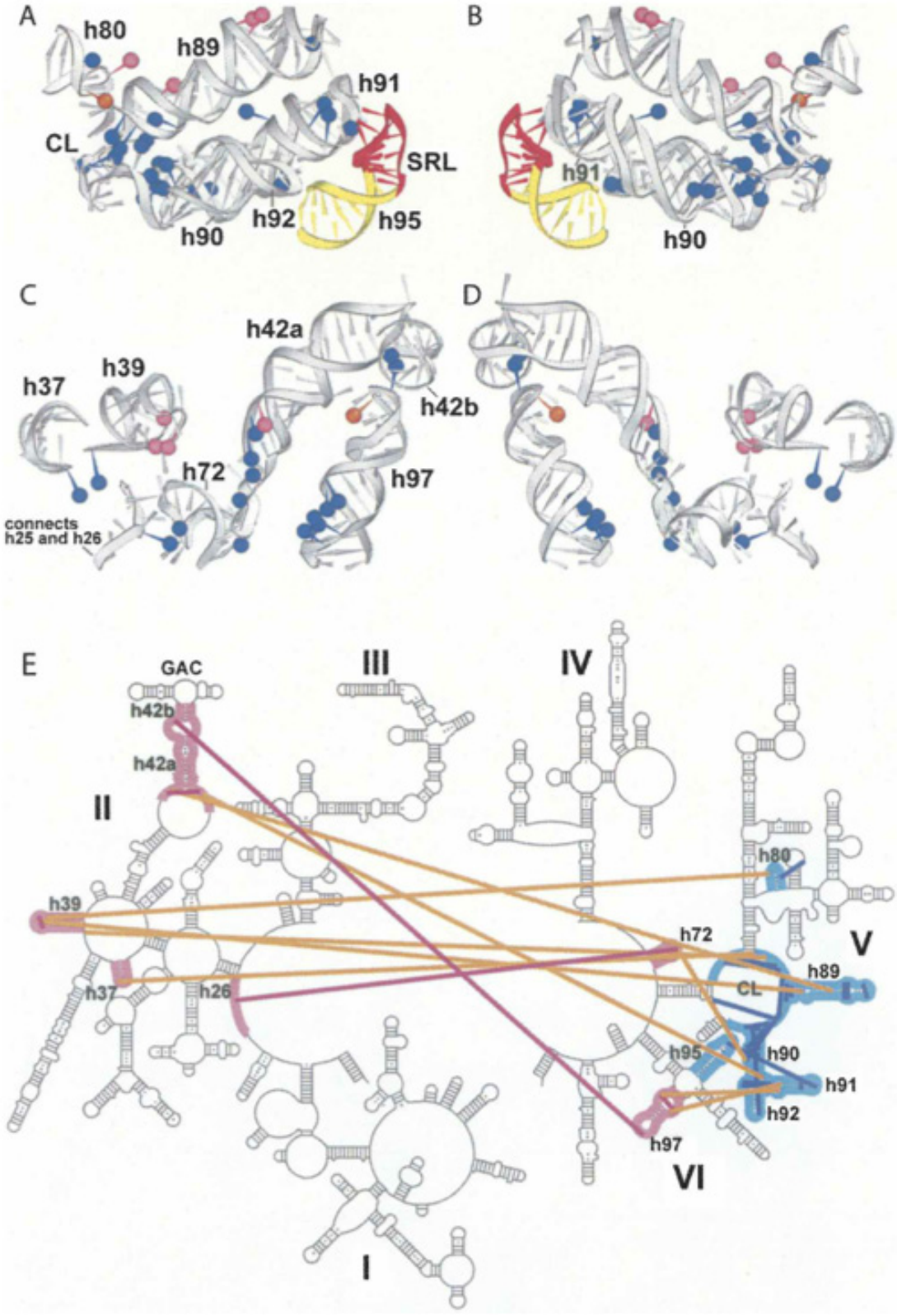
A
h80
h89
h91
CL
SRL
h92
h95
h90
B
h91
h90
C
h42a
h39
h37
h42b
h72
h97
connects
h25 and h26
D
E
GAC
III
IV
h42b
h42a
II
h80
h39
h72
V
h89
h37
h26
CL
h95
h90
h91
h92
h97
VI
I

DISCUSSION

Interaction between the GTPase translation factors and the ribosome is predicted to involve the sarcin-ricin loop within H95 of 23S rRNA. The sequence of this loop is universally conserved (Cannone et al. 2002) and is found in close proximity to the GTPase active G domain of EF-G (Agrawal et al. 1999; Gao et al. 2009; Moazed et al. 1988), EF-Tu (Moazed et al. 1988; Schmeing et al. 2009; Valle et al. 2003), IF2 (Allen et al. 2005), and RF3 (Klaholz et al. 2004). In keeping with the predicted importance of the SRL as a component of the GAC, affinity-purified ΔSRL ribosomes in which the 15-nucleotide SRL is replaced with a GAAA tetraloop are significantly altered in the binding of EF-G·GDPNP and do not support the hydrolysis of GTP. Additionally, the structure of ΔSRL 50S subunits was dramatically altered within the functional core, and protein L16 was absent.

We wished to know if the SRL was required for the catalytic activation of the GTPase activity of EF-G in the so-called EF-G idling reaction. Although this reaction is uncoupled from the events of authentic translocation, it serves as an effective benchmark of ribosomal activity (Rodnina et al. 1999). To this end we tested the GTPase activity of ribosomes containing affinity-purified ΔSRL 50S subunits. Vacant ΔSRL ribosomes, and those pre-bound by mRNA and tRNA, were found to be inactive in stimulating GTP hydrolysis by EF-G

(Figure 10A). Similarly, ΔSRL ribosomes failed to synthesize poly-phenylalanine peptides in an *in vitro* translation assay and failed to translocate in the presence of EF-G·GTP; for details see Lancaster et al (2008). These results may be interpreted in one of two ways: the ΔSRL mutation may inactivate the catalytic activation of EF-G's GTPase center, or ΔSRL ribosomes may be defective in the binding of EF-G.

To explore these possibilities, we determined the Kd for EF-G on ΔSRL ribosomes by following the quenching of fluorescein on labeled EF-G (Seo et al. 2004). Domain IV of EF-G is required for translocation (Savelsbergh et al. 2000). The presence of a fluorescein label on an engineered cysteine residue at position 591 within domain IV is an effective reporter of the ribosomal binding of EF-G (D. Ermolenko, unpublished). It is important to note that the specific mechanism underlying the binding associated quenching is not fully understood. Quenching may or may not depend on conformational changes within EF-G and the ribosomal subunits (Agrawal et al. 1999; Gao et al. 2009) or interaction between EF-G domain IV and the A site of the 30S subunit. Binding of EF-G was determined in the presence of GDPNP, a non-hydrolyzable analogue of GTP, which effectively stabilizes EF-G on the ribosome. The Kd for the binding of EF-G·GDPNP to ΔSRL ribosomes was approximately 50-fold greater than that of wild-type ribosomes (Figure 10B). We interpret these results as indicating that ΔSRL ribosomes are defective in

their binding of EF-G·GDPNP. Based on these results we may conclude that EF-G does not bind to ΔSRL ribosomes, a finding that fully explains the lack of EF-G-dependent GTP hydrolysis.

Replacement of the SRL with a GAAA tetraloop resulted in significant and unexpected changes in the reactivity of 23S rRNA, as well as the complete absence of ribosomal protein L16. The SRL is located within the subunit interface and its contact with the rest the 50S subunit is limited to a three-nucleotide interaction with the loop of helix 91 (H91). Chemical probing results indicate the disruption of multiple tertiary interactions that may be required for the proper assembly of the functional core of the 50S subunit. These interactions also highlight a potential for communication between the SRL and the L11 stalk, the two components of the GTPase-associated center. When the SRL was removed, altered levels of base reactivity were observed between H91 and H97, and H91 and H42, both of which lead directly to the L11 stalk. Of particular interest is the altered reactivity of C1049 located within kink-turn 42, a region proposed to generate dynamic flexibility within the L11 stalk rRNA (Razga et al. 2004; Razga et al. 2006). Nucleotides with altered reactivity also form the binding site for protein L16, explaining why ΔSRL ribosomes are devoid of this protein.

Following the publication of this work in 2008, Clementi et al (2010) published their findings on the role of SRL nucleotide A2660 of 23S rRNA.

A2660 is universally conserved (Cannone et al. 2002), and depurination at this location results in the inactivation of ribosomes in GTP hydrolysis (Endo et al. 1987). Clementi et al (2010) generated circularly permuted *T. aquaticus* 23S rRNA transcripts in which the 5' and 3' ends are moved to lie on either side of the SRL; thus, 45 nucleotides of the SRL are not present. Mutant ribosomes were assembled *in vitro*, and the missing segment of SRL rRNA was provided in *trans* as a chemically synthesized RNA fragments. By employing this technique, A2660 was determined to be critical for promoting EF-G-dependent GTP hydrolysis.

The specific requirement for A2660 was further investigated by the introduction of nucleoside analogs at that position (Clementi et al. 2010). Replacement of A2660 with purine, which lacks the exo-cyclic N6 amino group, effectively suppressed GTP hydrolysis. Activity was recovered by replacement with either inosine or N6,N6-di-methyladenosine. These last two analogs are distinctly different in structure from adenosine, but share a similar electron configuration allowing for participation in the aromatic π-electron system.

To exclude the possibility that altered GTP hydrolysis by circularly permuted ribosomes was due to a defect in the binding of EF-G·GTP, EF-G binding was measured by ultrafiltration (Clementi et al. 2010). Mutant ribosomes inactive in GTP hydrolysis (ΔSRL, A2660-purine, A2660-abasic)

bound similar levels of EF-G as wild-type ribosomes. Taking these results into consideration, we may reevaluate our own finding with ΔSRL ribosomes (Lancaster et al., 2008). It seems likely that ΔSRL ribosomes may in fact support an altered binding of EF-G, which supports neither the quenching of fluorescein nor GTPase activation. In this binding mode EF-G would be statically associated with the ribosome and incapable of further activity. This hypothesis may be tested by ultrafiltration or pelleting of ΔSRL-EF-G complexes.

METHODS

GTP hydrolysis was measured by combining 6.4 pmol ribosomes (either vacant or preassociated with 20 pmol tRNAPhe and 15 A260U/mL poly-U mRNA) and 6.4 pmol of EF-G in buffer B supplemented with 2 mM GTP and trace amounts of [γ-32P]-GTP (MP Biomedical, 800 Ci/mmol) in a total volume of 32 mL. The reaction was incubated at 37°C, and 4-mL aliquots were with- drawn at each time point and quenched in 4 mL of 60 mM acetic acid, then analyzed by thin layer chromatography (PEI cellulose) developed in 0.5 M KH2PO4.

For EF-G binding, ribosomal complexes containing mRNA and tRNAfMet were titrated from 0 to 600 nM in reactions that contained 20 nM EF-G-591-IAF, 0.5 mM GDPNP, 0.015% Nikkol, 1.6 mM DTT, 10 mM MgCl2, 100 mM NH4Cl, 50 mM Tris-HCl (pH 7.0), in a total volume of 30 mL, and incubated for 10 min at 37°C. Fluorescence spectra (500–600 nm) were acquired using a Cary Eclipse fluorescence spectrophotometer (Varian, Inc.) at 22°C with excitation at 485 nm, in a 10-mL cuvette (Starna Cells). The quench in fluorescent signal upon EF-G binding to the ribosome was normalized to that of EF-G alone; the Kd for EF-G binding was determined by fitting the data to the following equation:

*F*ratio =

$$1 - \Phi \left[\frac{(K_d + P_O + L_T) - \left\{ \sqrt{(K_d + P_O + L_T)^2 - (4P_O * L_T)} \right\}}{2P_O} \right]$$

(Roy 2004).

CHAPTER III: Functional Consequences of Truncation of a Conserved Loop in the L11 Stalk of 23S rRNA

ABSTRACT

The L11 stalk of the large ribosomal subunit is a component of the so-called GTPase-associated center (GAC), which is the interaction site for conserved translation factors with GTPase activity. The GAC has been proposed to regulate the ribosomal binding and inherent GTPase activity of two translation elongation factors, EF-Tu and EF-G, which assist ribosomes in the selection of cognate aminoacyl-tRNA (aa-tRNA), and translocation of mRNA and tRNA, respectively. The L11 stalk is composed of 23S rRNA helices 42-44 and is bound by ribosomal proteins L10 and L11. The elbow of aa-tRNA in the EF-Tu ternary complex and domain V of EF-G individually contact 23S rRNA loop 43 (L43) in the L11 stalk. To examine the role of L43 in GTPase activation, selection and binding of aa-tRNAs, and translocation, we replaced the 9-nucleotide L43 with a GAAA tetraloop (ΔL43). Affinity-purified ΔL43 ribosomes support EF-dependent poly-phenylalanine synthesis, but misincorporate near-cognate aa-tRNA with increased frequency and translocate at a slower rate. L11-depleted ΔL43 ribosomes are inactive in EF-G-dependent translocation but not EF-Tu-dependent aa-tRNA binding. Based on inspection of thirty-nine ribosome crystal structures, we observe that the position of the L11 stalk correlates with the presence of bound translation factors, and suggest that the L11 stalk contributes to translational fidelity by influencing activation of the GTPase of EF-Tu.

INTRODUCTION

The elongation phase of protein synthesis depends on two universally conserved translation elongation factor (EF) GTPases that work sequentially with the ribosome during aminoacyl-tRNA (aa-tRNA) selection and translocation. EF-Tu delivers aa-tRNA to the vacant ribosomal A site in a ternary complex (TC) of EF-Tu·GTP·aa-tRNA. EF-G stimulates translocation of mRNA by one codon together with coupled movement of deacylated P-site and peptidyl A-site tRNAs, vacating the A site in preparation for the next round of aa-tRNA selection (Spirin 1985). Elongation depends on the coordinated activation of each factor's inherent GTPase activity. The EFs share structural homology (Nissen et al. 1995) and both factors contact two conserved features of the large ribosomal subunit (50S): the L11 stalk (nucleotides 1051-1108) and the sarcin-ricin loop (SRL, nucleotides 2653-2667) (Moazed et al. 1988; Munishkin et al. 1997). Collectively, the factor-binding site is referred to as the GTPase associated center (GAC) (Beauclerk et al. 1985).

The L11 stalk and SRL are proposed to regulate EF binding and GTPase activation. The stalk cannot be directly involved in GTPase activation because it is located more than 45 Å from the GTP-binding G domains of the factors, which instead contact the SRL (Gao et al. 2009; Schmeing et al.

2009). Mutation of the SRL (Clementi et al. 2010; Lancaster et al. 2008) or treatment with ribotoxins (Endo et al. 1987; Endo et al. 1982) abolishes GTPase activation. In contrast to the SRL, whose position shows remarkably little variation between all of the structures (Gao et al. 2009; Selmer et al. 2006; Voorhees et al. 2010), the L11 stalk occupies a range of positions in different ribosome crystal structures and cryo-EM reconstructions {Schuwirth, 2005; Valle, 2003}. Positional changes of the stalk have been suggested to perturb the properties of the factor-binding site, altering its binding specificity for EF-Tu or EF-G (Frank et al. 2005; Sergiev et al. 2005; Valle et al. 2003).

The L11 stalk consists of fifty-eight nucleotides, which encompass helices 42, 43, and 44 of 23S rRNA (Schmidt et al. 1981) (Figure 12A). The stalk rRNA adopts a compact three-dimensional fold that is maintained by rRNA tertiary interactions and the binding of 50S ribosomal protein L11 (Xing et al. 1995) (Figure 12A). The C-terminal domain of protein L11 binds to H43 and its mobile N-terminal domain has been implicated in the activity of EF-G before and after GTP hydrolysis (Agrawal et al. 2001; Harms et al. 2008; Kavran et al. 2007). Ribosomal protein L10 binds to the three-way junction formed by H42, H43, and H44 (Figure 12A), and is itself the binding site of an essential tetrameric complex of ribosomal proteins (L7/L12)4 that has been implicated in the recruitment and release of the elongation factors (Diaconu et al. 2005; Wahl et al. 2002). A recent study showed that deletion of the entire

stalk rRNA, including the binding sites for proteins L11 and the L10(L7/L12)6 complex from *in vitro* transcribed and reconstituted *T. aquaticus* ribosomes, abolished *in vitro* poly(Phe) synthesis, but not ribosome-dependent EF-G·GTP hydrolysis (Clementi et al. 2010). This result is consistent with the conclusion that the L11 stalk is required for protein translation, but is not directly involved in the GTPase activation of EF-G.

EF-Tu ternary complex and EF-G interact with a set of conserved nucleotides within 23S rRNA loops 43 and 44 (L43, L44) of the L11 stalk (Moazed et al. 1988). The elbow of aa-tRNA within the EF-Tu-TC contacts U1066 and A1067 of L43 when bound to the ribosome in the pre-accommodation A/T state (Schmeing et al. 2009; Valle et al. 2002; Voorhees et al. 2010) (Figure 12A). Domain V of EF-G, which is structurally analogous to the tRNA elbow, also contacts A1067, and L44 at A1095 (Gao et al. 2009) (Figure 12A). In addition, binding of the peptide antibiotic thiostrepton protects A1067 and A1095 from chemical modification (Figure 12A) (Egebjerg et al. 1989). Thiostrepton inhibits productive binding of EF-Tu-TC to the ribosome, (Gonzalez et al. 2007), and blocks release of EF-G·GDP following GTP hydrolysis (Rodnina et al. 1999). Mutational studies have shown that transversion of A1067 to uracil impairs interaction between the ribosome and the elongation factors, with a greater effect on EF-Tu (Saarma et al. 1997),

and confers thiostrepton resistance but does not diminish *in-vitro* poly(Phe) synthesis (Thompson et al. 1988).

As a key point of contact between the elongation factors and the 50S subunit, L43 is predicted to be critically important. In this study, we directly test the role of L43 in the function of EF-Tu and EF-G during the elongation cycle of protein synthesis. We replaced the endogenous L43 sequence (nucleotides 1065-1073) with a GAAA tetraloop (ΔL43), a minimum RNA-loop structure predicted to preserve the overall architecture of the L11 stalk while removing the L43 nucleotides contacted by aa-tRNA, EF-G, and thiostrepton (Figure 12B). Expression of ΔL43 23S rRNA results in a dominant-lethal phenotype in *E. coli*. *In vivo* assembled affinity-purified ΔL43 ribosomes are active in poly(Phe) synthesis but select aa-tRNA with reduced accuracy. A fraction of ΔL43 ribosomes are missing protein L11. We show that the dissociation of protein L11 from ΔL43 ribosomes results in the inactivation of EF-G, but not EF-Tu, suggesting that the presence of protein L11 is able to rescue the effects of loss of the rRNA tertiary interactions caused by deletion of L43. Based on inspection of thirty-nine different ribosome crystal structures, we observe that the position of the L11 stalk correlates with the presence of bound translation factors, and suggest that the L11 stalk contributes to translational fidelity by influencing activation of the GTPase of EF-Tu.

RESULTS

The ΔL43 mutation confers a dominant-lethal phenotype

Nine nucleotides of *E. coli* 23S rRNA L43 (1065-1073) (Figure 12A) were replaced with a GAAA tetraloop hairpin (ΔL43) (Figure 12B) in the plasmid pLK35.50S.MS2, derived from *E. coli*, which contains the phage MS2 coat protein binding site inserted into helix 98 of 23S rRNA to facilitate affinity purification of mutant ribosomes (Ali et al. 2006; Youngman et al. 2004). The tetraloop motif is a ubiquitous feature in ribosomal and other structured RNAs (Woese et al. 1990), and in the context of a CG closing base pair is predicted to be highly stable (Antao et al. 1992). Inspection of the X-ray structure of the *E. coli* ribosome (Schuwirth et al. 2005; Wimberly et al. 1999) suggested that the tetraloop would replace L43 with minimal distortion of H43 and the rest of the L11-stalk rRNA. Expression of ΔL43 23S rRNA was induced by growth at 42˚C. *E. coli* cells containing the pLK35.ΔL43.MS2 plasmid failed to grow at 42˚C, indicating a dominant-lethal phenotype (Figure 12C). Affinity purification of ΔL43 50S subunits was carried out as described in (Lancaster et al. 2008). Affinity-purified 50S subunits were found to be >90% free of wild-type 50S contamination (Appendix), as determined by primer extension (Lancaster et al. 2005; Sigmund et al. 1988).

ΔL43 ribosomes are thiostrepton-resistant and active in translation elongation

The dominant-lethal phenotype of ΔL43 expression suggests that L43 plays an essential role in protein synthesis. We tested the *in vitro* translational capability of ΔL43 ribosomes in the poly(Phe) assay (Traub et al. 1981), which depends on the activities of both EF-Tu and EF-G. Because thiostrepton binds to L43 (Schmidt et al. 1981) and mutation of nucleotides within the loop confer thiostrepton resistance (Thompson et al. 1988), we anticipated that the ΔL43 mutation would confer thiostrepton-resistance. ΔL43 ribosomes were found to be active in poly(Phe) synthesis and, unlike wild-type ribosomes, were not inhibited by 10 μM thiostrepton (Figure 13A). ΔL43 ribosomes generated fewer poly(Phe) peptides over the time-course than did wild-type; however, the t1/2 of the reactions were similar, suggesting that only a sub-population of ΔL43 ribosomes is fully active.

To test the possibility that depletion of one or more ribosomal proteins from purified ΔL43 subunits is responsible for inactivation, the protein compositions of wild-type and ΔL43 50S subunit preparations were compared by two-dimensional gel electrophoresis (Figure 13B), and quantified by densitometric scanning (Figure 13C). To varying degrees, preparations of

ΔL43 subunits were specifically depleted of the stalk-associated ribosomal protein L11 (Figure 13B, boxed region and lower left). The extent of L11 depletion correlated with increased exposure to high-salt washing during purification (Figure 13C). I estimate that two 0.1M salt washes (LSW) removes approximately 0.3 equivalents of protein L11 per ΔL43 50S, and two 0.5M salt washes (HSW) results in loss of between 0.5 and 0.7 equivalents of L11. No significant changes in the levels of the other stalk-associated proteins L10 and L7/12, or any other 50S proteins were detected. We were unable to restore L11 to L11-depleted ΔL43 (ΔL43/L11-) subunits by reconstitution with purified L11 protein (data not shown). In the experiments described below, we compare the activities of low and high salt-washed ΔL43 preparations.

ΔL43 ribosomes associate with wild-type 30S subunits

To test the possibility that reduced association of ribosomal subunits is responsible for their inactivation in poly(Phe) synthesis, we characterized the sedimentation of ΔL43 50S subunits through a sucrose gradient in the presence and absence of wild-type 30S subunits. ΔL43 50S subunits sediment ahead of wild-type 50S subunits (Fig 14A). In the presence of excess wild-type 30S subunits, ΔL43 subunits were no longer resolved into a 50S peak (Figure 14B). A new peak consistent with the association of

ribosomal subunits was again found to sediment ahead of the wild-type 70S ribosome peak. These results indicate that ΔL43 50S subunits support the association of ribosomal subunits and suggest that the ΔL43 mutation results in a more compact and hydrodynamic 50S structure.

ΔL43 ribosomes are active in P-site tRNA binding and peptidyl transferase

P-site tRNA binding and peptidyl transferase were tested by nitrocellulose filter binding and reaction with puromycin. Wild-type and ΔL43 50S ribosomes stimulated the binding of [35S]-fMet-tRNAfMet to 30S-mRNA complexes and exhibited similar reactivity towards puromycin (Figure 14C). These results show that the ΔL43 mutation does not affect the 50S core functions of P-site tRNA binding or peptidyl transferase.

ΔL43 ribosomes require protein L11 for EF-G-dependent activities

Vacant ribosomes stimulate EF-G-dependent GTP hydrolysis that is uncoupled from translocation - the so-called "idling" GTPase reaction (Arai et al. 1974). This reaction involves binding of EF-G·GTP, ribosome-dependent activation of its GTPase, and release of EF-G·GDP. All preparations of ΔL43

ribosomes were active to some extent in the idling reaction (Figure 15A), indicating that L43 is not essential for any steps of the reaction. It has been shown that wild-type ribosomes depleted of protein L11, or those isolated from an *E. coli* strain lacking endogenous protein L11 have reduced activity in the idling reaction (Stark et al. 1980). Since HSW ΔL43 ribosomes show less activity than LSW ΔL43 ribosomes, it suggests that the observed defect may be due to loss of protein L11. To distinguish the contribution of L11 from that of L43, we compared the activities of ΔL43 to that of ΔL11 ribosomes in the idling reaction. LSW ΔL43 ribosomes were more active than ΔL11 ribosomes, indicating that protein L11 contributes more to the reaction than does L43 (Figure 15A). In contrast, ΔL11 ribosomes were more active than HSW ΔL43 ribosomes. This result indicates that although neither L43 nor protein L11 is strictly required for ribosome activity in the idling reaction, loss of both stalk components confers a strong defect (Figure 15A).

To determine if reduced activity in the GTPase idling reaction was due to deficient EF-G binding, we pelleted EF-G-ribosome complexes through a sucrose cushion, dissolved the pellets, and monitored the amount of ribosome-bound EF-G by SDS PAGE. EF-G was bound stably on ribosomal complexes containing mRNA and P-site tRNAfMet using either the non-hydrolyzable GTP analogue GDPNP, or GTP and the antibiotic fusidic acid (GTP/FA). Deacylated P-site tRNA binds equally well to ΔL43 and wild-type

ribosomes (Figure 14C). LSW and HSW ΔL43 ribosomes bound about 2-fold less EF-G·GTP/FA than wild-type, and 10-20 fold less EFG·GDPNP (Figure 15B). Because ΔL43 ribosome preparations contain a low level of wild-type ribosomes, we cannot exclude the possibility that the observed binding with GDPNP is due to wild-type background. As observed for the GTPase idling reaction, EF-G binding to ΔL43 ribosomes was reduced in proportion to increased salt washing. In contrast, ΔL11 ribosomes bound more EF-G than did wild-type ribosomes, indicating that the absence of protein L11 in the context of wild-type L43 may contribute to the stability of EF-G binding (Figure 15B). These results indicate that the ΔL43 mutation reduces EF-G binding, and has a greater effect when EF-G is in its GTP-bound conformation.

The rate of EF-G-dependent translocation was determined by monitoring the quenching of fluorescein dye conjugated to the 3' end of mRNA in a stopped-flow kinetics assay (Studer et al. 2003). Pre-translocation ribosome complexes containing mRNA, P-site tRNAMet, and A-site Phe-tRNAPhe were rapidly mixed with a 10-fold excess of EF-G·GTP. To control for the small fraction of non-MS2-tagged wild-type ribosomes present in each sample, experiments were conducted in the presence and absence of thiostrepton (Figure 16A-C). Apparent rate constants were determined by fitting the averaged time traces to a double-exponential equation, as previously described (Ermolenko et al. 2011; Munro et al. 2010; Peske et al.

2004; Shi et al. 2009) (Table 1). Translocation by wild-type and MS2-tagged wild-type (MS2-WT) ribosomes (data not shown) was undetectable in the presence of 10 μM thiostrepton, whereas ΔL43 ribosomes were unaffected. The percentage of translocationally active ribosomes was determined by comparing the observed total change in fluorescent signal to that of MS2-WT translocation. LSW and HSW ΔL43 ribosomes were 68% and 15% active, respectively. The rate of translocation by ΔL43 ribosomes was 2 fold slower than wild-type, and again correlated negatively with increased salt washing. Translocation by ΔL11 ribosomes in the presence of thiostrepton occurred with slow single rate kinetics, suggesting that the drug inhibits certain translocation pathways (Figure 16C). These results indicate that ΔL43 ribosomes support translocation, but are inactivated by salt washing.

ΔL43 ribosomes have increased error frequency in aa-tRNA selection

We next characterized the impact of the ΔL43 mutation on the activity of EF-Tu. EF-Tu performs two roles: binding of aa-tRNA to the A site and aiding the ribosome in the accurate selection of cognate aa-tRNA. EF-Tu-dependent binding of [14C]Phe-tRNAPhe to the A site was tested under saturating conditions. Ribosomes were bound with a short, defined mRNA, and tRNAfMet was non-enzymatically loaded into the P site. Complexes were

mixed with either excess EF-Tu·GTP·[14C]Phe-tRNAPhe, or [14C]Phe-tRNAPhe alone (Figure 17A). HSW ΔL43 ribosomes containing 0.5 equivalents of L11 were fully saturated with [14C]Phe-tRNAPhe in the presence of EF-Tu, and wild-type and ΔL43 ribosomes bound similarly low levels of [14C]Phe-tRNAPhe when EF-Tu was omitted from the reaction (Figure 17A). This result indicates that neither the ΔL43 mutation nor depletion of protein L11 from ΔL43 ribosomes impairs the activity of EF-Tu in ribosomal binding of aa-tRNA.

The error rate of *in vivo* aa-tRNA selection by wild-type ribosomes is estimated to be on the order of 1x10**-3**-1x10**-4** (Loftfield, 1963). The accuracy of aa-tRNA selection was tested in a modified poly(Phe) assay containing a complete set of cellular tRNAs and amino acids as well as [14C]Phe and [3H]Leu (Bartetzko and Nierhaus, 1988). The tRNALeu isoacceptor bearing the anticodon UAA is a near-cognate for tRNAPhe as it differs only in the wobble position. Selection errors were determined by quantification of the relative amounts of [3H]Leu and [14C]Phe incorporated into doubly-labeled peptides. We used a polymix buffer containing spermine, spermidine, and a low concentration of Mg2+ that supports *in vitro* translation with error rates approaching those of *in vivo* synthesis (Gromadski et al. 2004). Although HSW ΔL43 ribosomes were less active, peptides generated by both LSW and HSW ΔL43 ribosomes contained proportionally nearly 4-fold more [3H]Leu

than did peptides generated by wild-type ribosomes. This corresponds to error rates of 7x10-3 and 1.8x10-3 for ΔL43 and wild-type ribosomes, respectively (Figure 17B). The error rate of ΔL11 ribosomes was intermediate between those of wild-type and ΔL43. These results indicate that both the ΔL43 mutation and depletion of protein L11 impair the accurate selection of aa-tRNA. However, as our previous results indicate that ΔL43 ribosomes are dependent on protein L11 for EF-G-dependent translocation, we may conclude that only ΔL43 ribosomes containing protein L11 are translationally active. Therefore, the increased error rate observed for ΔL43 translation must be due to the ΔL43 mutation alone and not L11 depletion.

Figure 12. Secondary Structure of the L11 Stalk and the ΔL43 mutation

The L11 stalk is formed by 23S rRNA nucleotides 1051-1108. (A) Folding of the stalk-rRNA is enforced by the binding of ribosomal proteins L10 (black outline) and L11 (grey outline) as well as tertiary interactions formed between L43 and H44, T1: G1071(G1091:C1100), T2: C1072(C1092:G1099). Nucleotides contacted by EF-G and thiostrepton (filled circles); nucleotides contacted by EF-Tu ternary complex (filled triangles). (B) The replacement of L43 (nucleotides 1065-1073) with GAAA (ΔL43) removes nucleotides contacted by EF-G, EF-Tu, and thiostrepton. (C) *E. coli.* cells expressing ΔL43 23S rRNA fail to grow at 42˚ C.

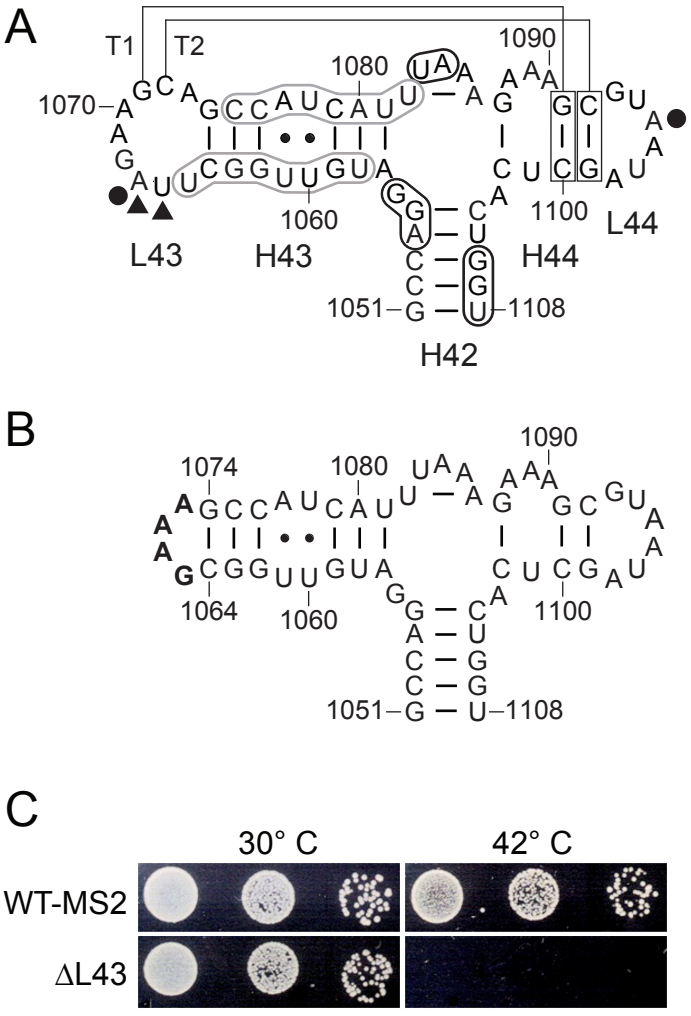
A
T1
T2
1090
1080
1070
1060
1100
L43
H43
H44
L44
H42
1051
1108
B
1074
1090
1080
1064
1060
1100
1051
1108
C
30° C
42° C
WT-MS2
ΔL43

Figure 13. ΔL43 Ribosomes are Active in poly(Phe) Synthesis but Contain Less Ribosomal Protein L11

(A) Time-course of poly(U) mRNA directed synthesis of poly-phenylalanine, WT (◯) but not ΔL43 ribosomes (△) are strongly inhibited by 10 uM thiostrepton (filled symbols). (B) Two-dimensional gel electrophoresis of ΔL43 50S proteins. The boxed region contains L11 stalk proteins, which are expanded and labeled in lower left (L9 is not a stalk protein); (*) marks the multimeric non-ribosomal MS2-GST fusion protein. (C) Quantification of bound protein L11 to salt-washed ΔL43 50S subunits normalized to identically prepared WT subunits.

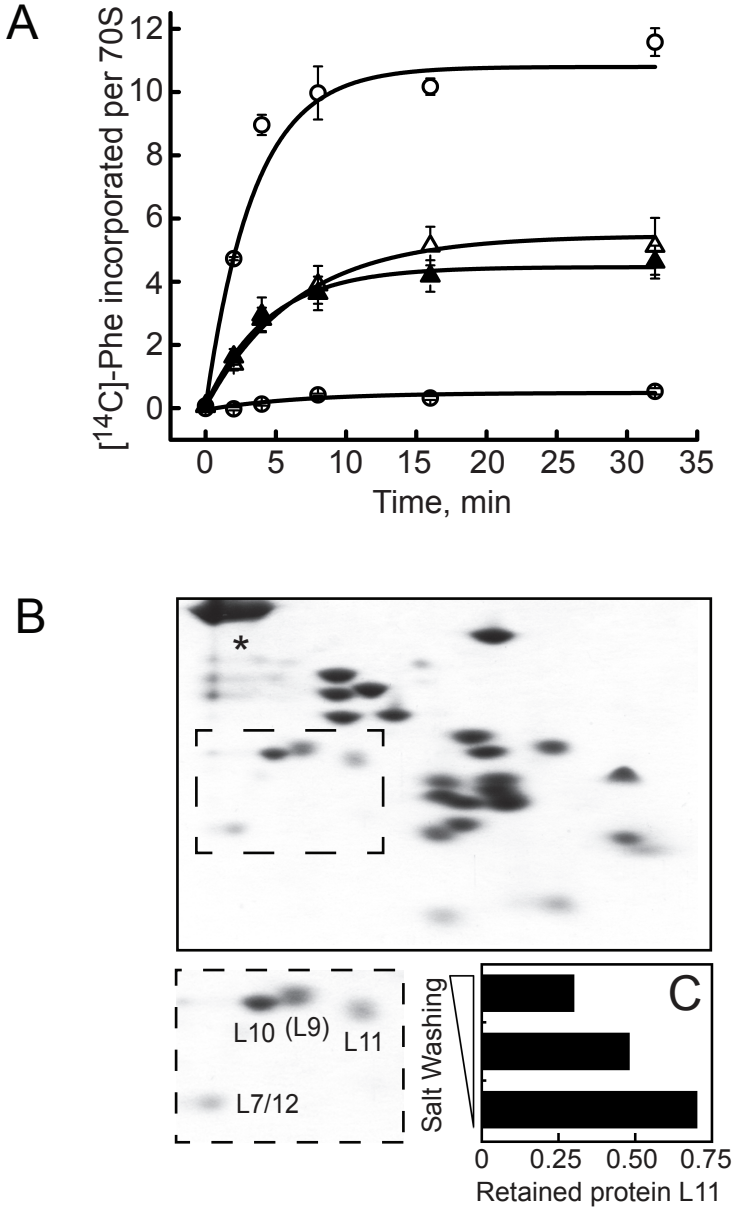
A
[14C]-Phe incorporated per 70S
0
2
4
6
8
10
12
0
5
10
15
20
25
30
35
Time, min
B
*
L10 (L9)
L11
L7/12
C
Salt Washing
0
0.25
0.50
0.75
Retained protein L11

Figure 14. Subunit Association of ΔL43 Ribosomes and P-site tRNA Binding

Sucrose density-gradient sedimentation of MS2-WT and ΔL43 ribosomes in the absence (A) or presence (B) of excess wild-type 30S subunits. Arrows indicate the position of the 30S subunits, 50S subunits, and 70S ribosomes. (C) Binding of [35S]-fMet-tRNAfMet (grey bars) and puromycin reactivity (white bars) was equally stimulated by addition of ΔL43 or WT 50S subunits.

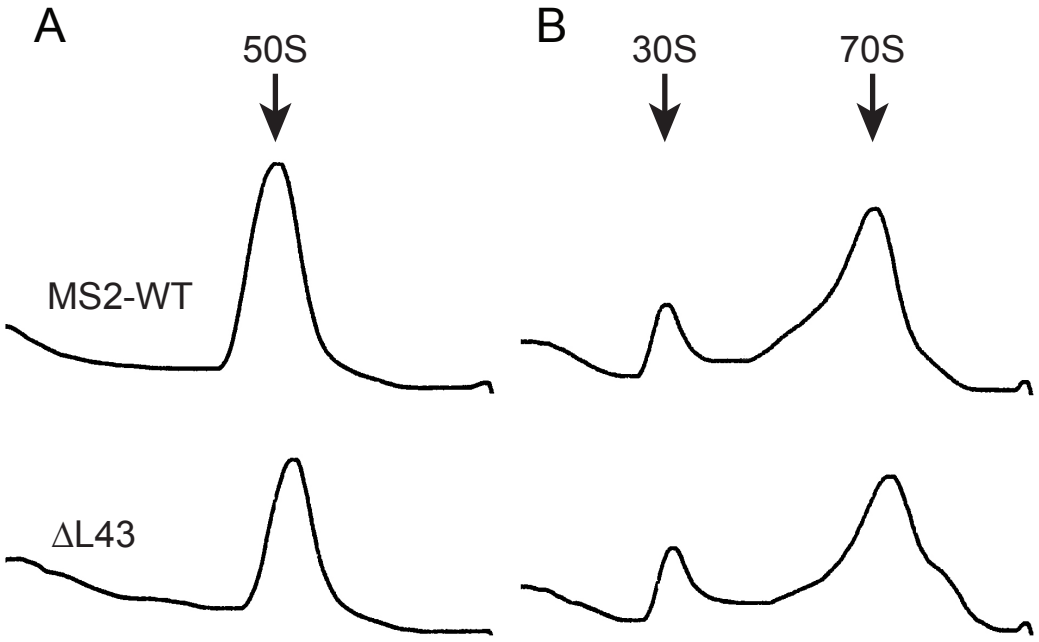
A
50S
MS2-WT
ΔL43
B
30S
70S

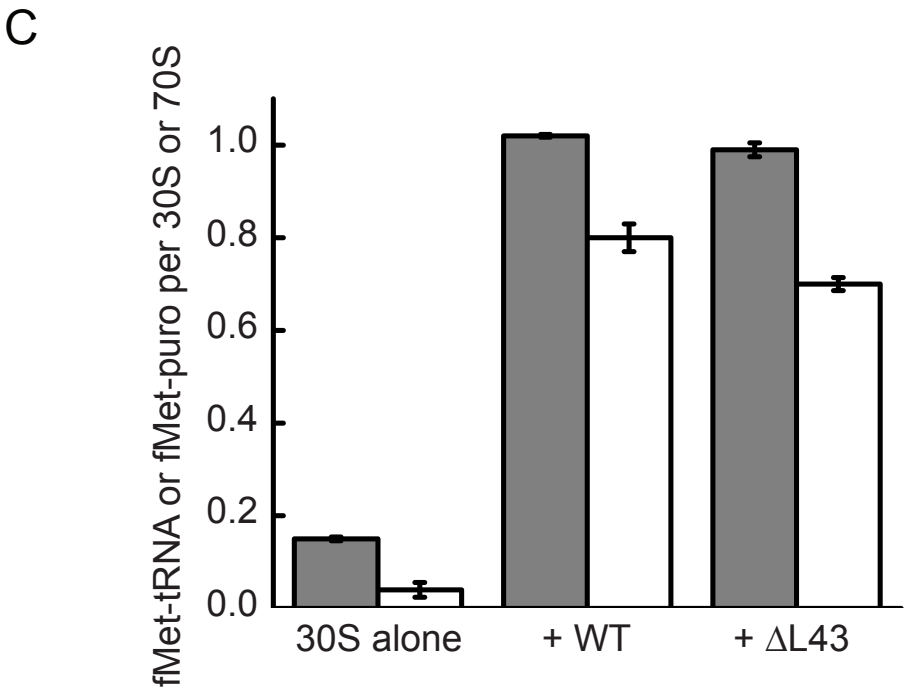
C
fMet-tRNA or fMet-puro per 30S or 70S
1.0
0.8
0.6
0.4
0.2
0.0
30S alone
+ WT
+ ΔL43

Figure 15. EF-G-Dependent GTPase Idling Reaction and EF-G Binding

(A) GTPase idling reaction with 0.2 μM 70S, 0.04 μM EF-G, and 5 μM [32P] GTP. (B) Ribosome-EF-G complexes were pelleted through a 1M sucrose cushion in the presence of either GDPNP or GTP/FA. The EF-G band was quantified from Coomassie-blue stained gels and normalized to that of WT ribosomes with GDPNP.

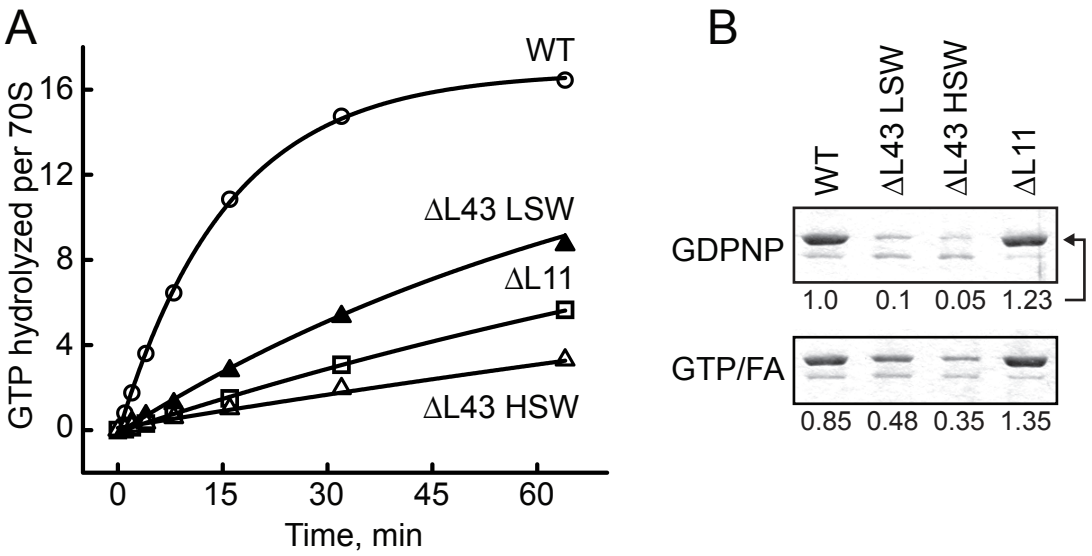
A
GTP hydrolyzed per 70S
16
12
8
4
0
0
15
30
45
60
Time, min
WT
ΔL43 LSW
ΔL11
ΔL43 HSW
B
WT
ΔL43 LSW
ΔL43 HSW
ΔL11
GDPNP
1.0
0.1
0.05
1.23
GTP/FA
0.85
0.48
0.35
1.35

Figure 16. ΔL43 Ribosomes are Partially Active in Translocation

Fluorescent stopped flow analysis of translocation. Ribosomes were assembled into pre-translocation complexes containing 3'-fluorescein labeled mRNA, tRNAMet and N-Ac-Met-Phe-tRNAPhe in the P and A site respectively. Rapid mixing with EF-G·GTP was carried out in the absence or presence of 10 μM thiostrepton (+Ts). Fluorescence change is in arbitrary units and the initial value has been set to 1.0. (A) MS2-wild-type (MS2-WT) and wild-type (WT), (B) ΔL43 HSW and LSW, (C) ΔL11.

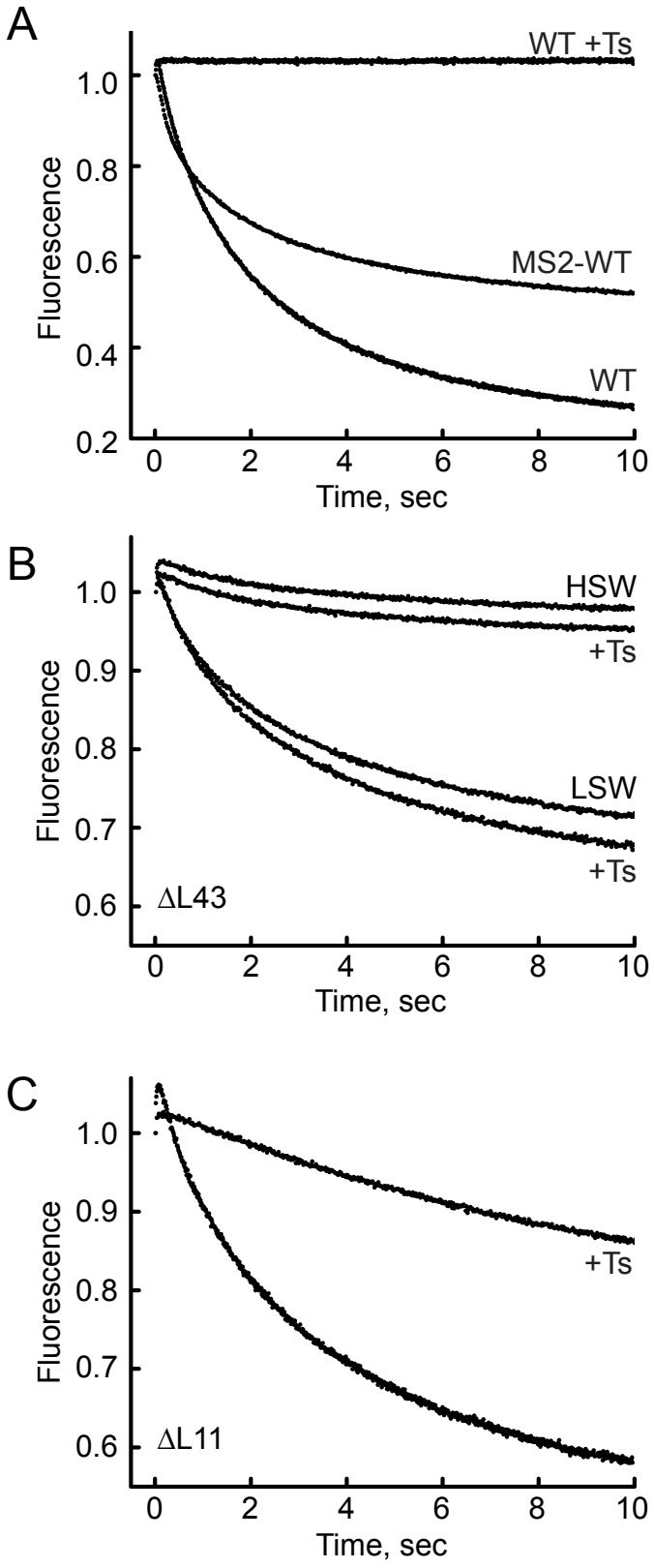
A
WT +Ts
MS2-WT
WT
Fluorescence
1.0
0.8
0.6
0.4
0.2
0
2
4
6
8
10
Time, sec
B
HSW
+Ts
LSW
+Ts
ΔL43
Fluorescence
1.0
0.9
0.8
0.7
0.6
0
2
4
6
8
10
Time, sec
C
+Ts
ΔL11
Fluorescence
1.0
0.9
0.8
0.7
0.6
0
2
4
6
8
10
Time, sec

Table 1. Translocation Kinetics

Ribosomes	#	ΔA_T [a]	Extent [b]	k_1 (s^{-1})	k_2 (s^{-1})	$A_1 / (A_1 + A_2)$	k_{av} (s^{-1})
WT	7	0.776 ± 0.021	1.522 ± 0.041	1.192 ± 0.033	0.287 ± 0.004	0.371 ± 0.007	0.623 ± 0.011
WT + Ts	4	-0.004 ± 0.015	0	-	-	-	-
MS2-WT	8	0.510 ± 0.077	1.001 ± 0.151	1.917 ± 0.128	0.272 ± 0.026	0.402 ± 0.017	0.931 ± 0.032
ΔL43 LSW	9	0.387 ± 0.082	0.758 ± 0.161	1.013 ± 0.186	0.162 ± 0.020	0.142 ± 0.006	0.399 ± 0.066
ΔL43 LSW + Ts	8	0.391 ± 0.028	0.766 ± 0.028	1.298 ± 0.188	0.219 ± 0.016	0.282 ± 0.022	0.520 ± 0.039
ΔL43 HSW	7	0.077 ± 0.012	0.150 ± 0.023	0.938 ± 0.442	0.159 ± 0.034	0.368 ± 0.131	0.408 ± 0.117
ΔL43 HSW + Ts	9	0.077 ± 0.026	0.152 ± 0.051	0.866 ± 0.476	0.153 ± 0.050	0.385 ± 0.127	0.394 ± 0.147
ΔL11	7	0.550 ± 0.066	1.078 ± 0.129	1.245 ± 0.158	0.219 ± 0.010	0.252 ± 0.009	0.477 ± 0.042
ΔL11 + Ts	5	0.296 ± 0.007	0.581 ± 0.015	0.086 ± 0.007	-	1	-

The rate constants of EF-G-dependent translocation were extracted from multiple time traces (Fig. 4) and fit to single- or double-exponential equations. #, number of time traces. [a] ΔAT is the total change in signal amplitude at 10 sec. [b] Extent of reaction based on ΔA_T at the endpoint. k_1 and k_2 are the fast and slow rate constants of translocation. $A_1 / (A_1 + A_2)$ is the relative amplitude change for the fast phase of translocation. k_{av} is the weighted average rate of translocation, calculated by $k_{av} = (k_1A_1 + k_2A_2) / (A_1 + A_2)$. WT, wild-type, MS2-WT, MS2-tagged wild-type; LSW, low salt washed; HSW, high salt washed; Ts, thiostrepton.

Figure 17. ΔL43 Ribosomes are Active in A-site aa-tRNA Binding, but Select aa-tRNA with Reduced Accuracy

(A) EF-Tu dependent A-site tRNA binding of [14C]-Phe-tRNAPhe to WT and HSW ΔL43 ribosomes (0.5 equivalents of L11) pre-bound with mRNA and P-site fMet-tRNAfMet was measured by filter binding, black bars with EF-Tu, white without. (B) End-point analysis of poly(U) mRNA translation in high-fidelity polymix buffer in the presence of cognate [14C]Phe-tRNAPhe and near-cognate [3H]Leu-tRNALeu.

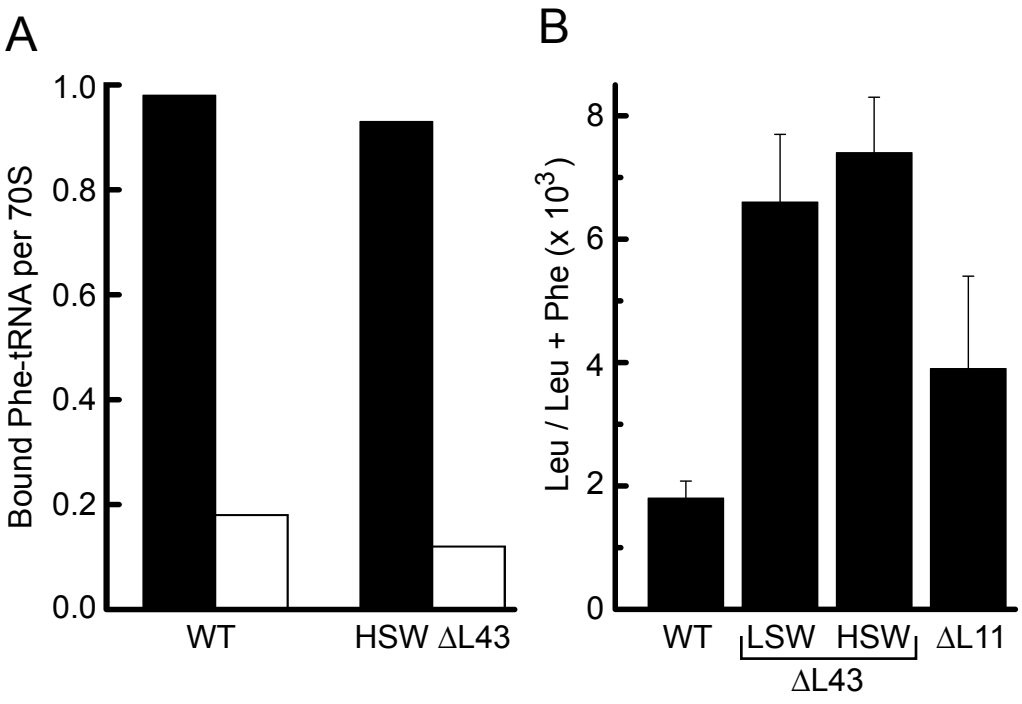
A
Bound Phe-tRNA per 70S
1.0
0.8
0.6
0.4
0.2
0.0
WT
HSW ΔL43
B
Leu / Leu + Phe (x 10^3)
8
6
4
2
0
WT
LSW
HSW
ΔL43
ΔL11

DISCUSSION

These studies provide the first analysis of the highly conserved loop 43 of 23S rRNA in the EF-Tu- and EF-G-dependent elongation functions of protein synthesis using natively assembled, affinity-purified ribosomes. *In vivo* expression of ΔL43 50S subunits results in a dominant-lethal growth phenotype in *E. coli* (Figure 12C). We conclusively demonstrate that L43 is not required for elongation factor-dependent poly(Phe) synthesis (Figure 13A). Extensively salt-washed ΔL43 ribosomes are depleted of protein L11 (Figure 13B), but support subunit association (Figure 14B) and P-site tRNA binding and peptidyl transferase (Figure 14C). ΔL43 ribosomes are defective in the EF-G GTPase idling reaction (Figure 15A), binding of EF-G·GDPNP (Figure 15B), and EF-G-dependent translocation (Figure 16B). The ΔL43 mutation does not impair EF-Tu-dependent binding of aa-tRNA (Figure 17A); however, the error rate of aa-tRNA selection is increased (Figure 17B).

Loop 43 of 23S rRNA forms the predominant contacts between the 50S subunit and the elongation factors (Figure 12A) (Gao et al. 2009; Moazed et al. 1988; Schmeing et al. 2009). In spite of the presumed role of L43 as a key feature of the "GTPase-associated center" and the dominant-lethal phenotype of the ΔL43 mutation, affinity-purified ΔL43 ribosomes in which the 9-

nucleotide loop 43 is replaced by a GAAA tetraloop retain substantial activity in *in vitro* translation.

Activity of EF-G but not EF-Tu is sensitive to L11 stalk-rRNA structure

We show that protein L11 is specifically depleted from ΔL43 subunits by exposure to high ionic strength conditions during affinity purification (Figure 13B). The activity of ΔL43 ribosomes in poly(Phe) synthesis (Figure 13A), the EF-G GTPase idling reaction (Figure 15A), EF-G binding (Figure 15B), and translocation (Figure 16B), all correlate negatively with increased salt washing and the correspondingly reduced L11 content. In contrast, L11-depleted ΔL43 ribosomes (ΔL43/L11-) efficiently bind A-site aa-tRNA under EF-Tu dependent conditions (Figure 17A). We conclude that the ΔL43 mutation results in an acquired dependency on the normally non-essential ribosomal protein L11 in EF-G-dependent reactions.

Much is known about the structure of the rRNA and protein components of the L11 stalk (Wimberly et al., 1999)(Yusupov et al., 2001) (Schuwirth et al., 2005). The C-terminal domain of protein L11 makes extensive contact with helix 43 and makes a single hydrogen bond to the phosphate backbone of U1065 in loop 43 (Figure 12A). In the ΔL43 mutant (Figure 12B), this binding site is entirely intact except for the identity of the

nucleobase at position 1065, a change that is not expected to dramatically alter the stability of L11 binding. Our inability to reconstitute ΔL43/L11- ribosomes with added L11 suggests that the conformation of the stalk rRNA becomes altered following dissociation of the protein.

The tertiary structure of the stalk rRNA is stabilized by the binding of protein L11 (Blyn et al. 2000) and by tertiary base triples formed between bases G1071, C1072 and helix 44 (Figure 12A). Mutation of C1072 to U, which eliminates these tertiary contacts reduces binding of L11 to a transcribed fragment of stalk-RNA by 10-fold (Conn et al. 1998). Substitution of L43 by GAAA eliminates both tertiary base triples by removal of G1071 and C1072 (Figure 12B). Depletion of L11 from these ribosomes would likely further destabilize the conformation of the stalk. During *in vivo* ribosome assembly, L11 is incorporated into ΔL43 ribosomes (Figure 2), where it appears to be capable of maintaining proper tertiary folding of the stalk rRNA, as indicated by the high activity of LSW ΔL43 ribosomes. However, protein L10 is not depleted from HSW ΔL43 50S subunits, indicating that alteration of the stalk rRNA conformation does not propagate to the L10 binding site located within the junction of H42, H43, and H44 (Figure 12A). Thus, folding of the stalk rRNA into its active conformation requires stabilization by L43-H44 tertiary interactions or binding of protein L11.

The activity of EF-G on ΔL43/L11- ribosomes may be blocked at one or more of the steps of EF-G·GTP binding, GTPase activation, translocation or release of EF-G·GDP. *In vitro*-transcribed and reconstituted *T. aquaticus* ribosomes in which nucleotides 1034-1122 of the L11 stalk are replaced by a BamH1 cloning sequence (ΔGAC), are reported to have a reduced rate of turnover in EF-G-dependent GTP hydrolysis and are inactive in poly(Phe) synthesis (Clementi et al. 2010). Because our ΔL43/L11- ribosomes are inactive in translocation (Figure 16B), we may infer that ΔGAC ribosomes, although active in EF-G-dependent GTP hydrolysis are in fact translocationally inactive. Therefore ΔL43/L11- ribosomes, like their ΔGAC counterparts, are likely impaired in their functional interaction with EF-G specifically at a step following GTP hydrolysis but preceding translocation. This single round GTP hydrolysis would not have been detected by our EF-G idling assay.

Altered translocation activity by ΔL43 ribosomes may be explained by reduced EF-G binding. In the presence of GDPNP, which mimics the GTP bound conformation, EF-G binding by ΔL43 ribosomes was ten- to twenty-fold lower than that of wild-type, however, binding was markedly improved when the release of EF-G·GDP was blocked by fusidic acid (Figure 15B). Conformational changes in EF-G and the ribosome following GTP hydrolysis lead to increased contact between the factor and both ribosomal subunits

(Agrawal et al. 1999) and brace EF-G domain V between 23S rRNA of L11 stalk, SRL and L89 (Gao et al. 2009; Harms et al. 2008). These contacts are predicted to stabilize binding of EF-G so that domain IV may induce translocation upon its interaction with the 30S A-site (Agrawal et al. 1999; Savelsbergh et al. 2000); as observed for the related molecule eEF2 (Taylor et al. 2007). It is likely that these conformational rearrangements are perturbed in ΔL43 ribosomes by altered contacts between EF-G and L43. The improved binding of EF-G in the presence of fusidic acid indicates that EF-G·GDP is stabilized on ΔL43 ribosomes by contacts formed between the post GTP-hydrolysis conformation of EF-G and the ribosome (Gao et al. 2009). The structure of the L11 rRNA is altered in translocationally inactive ΔL43/L11- ribosomes, suggesting that interaction between EF-G domain V and the rRNA of the L11 stalk is necessary for the coupling of GTP hydrolysis to translocation.

METHODS

Buffer A is 50 mM Tris-HCl (pH 7.6), 100 mM NH4Cl, 5 mM β-mercaptoethanol (BME). Buffer B is 50 mM Tris-HCl (pH 7.6) 70 mM NH4Cl, 30 mM KCl, 1 mM DTT. Buffer C is 10 mM HEPES-KOH, 100 mM NH4Cl, 1 mM DTT. All buffers contain MgCl2 at the concentration indicated; for example, buffer A(7) contains 7 mM MgCl2.

GTP and GDPNP were purchased from Sigma. [γ-32P]-GTP (800 Ci/mmol) from MP Biomedical; [14C]-Phe (496 mCi/mmol) from Perkin Elmer; [3H]-Leu (166 Ci/mmol) from ICN; thiostrepton from Calbiochem; and fusidic acid from Alexis Biochemicals. tRNAfMet and tRNAPhe (Sigma) were aminoacylated, extracted, and purified as described (Lancaster et al. 2005; Moazed et al. 1989). DNA oligonucleotides were synthesized by IDT. T7 RNA polymerase was provided by J. Zhu.

The m36g32 mRNA (Cate et al. 1999) was transcribed *in vitro* by T7 RNA polymerase (Milligan et al. 1987) from a synthetic template made from the following DNA oligonucleotides. Promoter strand (T7-21): 5'-TTC TAA TAC GAC TCA CTA TAG; template strand (T7-m36g32): 3'-AAG ATT ATG CTG AGT GAT ATC CCG TTC CTC CAT TTT TAC AAA TTT GCA TTT AGA

TGA. A 1.5 mL transcription reaction containing 35 pmol of gel-purified T7-m36g32 annealed to 25 pmol T7-21 in 40 mM HEPES-KOH (pH 7.6), 16 mM MgCl2, 12.5 mM NaCl, 1 mM spermidine, 15 mM DTT, 3 mM NTPs, and T7 RNA polymerase was incubated at 37˚C for 3 hours. The mRNA transcript was precipitated and purified on a 10% polyacrylamide gel (yield: 16.8 nmoles).

EF-G with a C-terminal 6His tag (Wilson and Noller, 1998) was expressed for 4 hours following induction with IPTG (1 mM final concentration) in a 1 liter culture of *E. coli* strain BL21 in LB containing kanamycin (30 μg/mL), grown to A600 = 0.6 at 37˚C. Cells were harvested by centrifugation and resuspended in lysis buffer (50 mM HEPES-KOH (pH 7.6), 60 mM NH4Cl, 7 mM MgCl, 15 mM imidazole, 5% glycerol w/v) and passed twice through a French press. The lysate was cleared by centrifugation at 15,000 rpm for 20 min in a JA20 rotor and loaded onto a column containing 2 mL equilibrated Ni-NTA agarose resin (Qiagen). The resin was washed 3X with 5 mL lysis buffer, 3X with 5 mL lysis buffer containing 500 mM KCl, and eluted 6X with 2 mL lysis buffer containing 250 mM imidazole. Fractions 1-4 were pooled and dialyzed (Spectra/Por 3 MWCO = 3,500 D) into 50 mM HEPES-KOH (pH 7.6), 60 mM NH4Cl, 7 mM MgCl, 10% glycerol. EF-G concentration was determined by the molar extinction coefficient E6(HIS)-EF-

G = 61,435 M-1cm-1; aliquots were flash frozen in liquid nitrogen and stored at -80˚C.

Wild-type ribosomes were prepared from strain MRE600 (Moazed et al. 1989). The ΔL11 strain FTP6027 (Bouakaz et al. 2006) was provided by S. Sanyal, Uppsala University. 50S and 30S subunits were purified from sucrose gradients as described in (Powers et al. 1991) with the following modifications. Crude ribosomes were pelleted twice in 25 mM Tris-HCl (pH 7.6), 10 mM MgCl, 5 mM BME, and either 100 mM (low salt) or 500 mM (high salt) NH4Cl. Pellets were resuspended in low salt buffer and dissociated into subunits by adjusting the Mg2+ concentration to 1 mM by dilution with Mg**2+** free buffer.

Construction of the ΔL43 mutant and affinity purification of mutant ribosomes

The ΔL43 mutation was generated by replacing 23S rRNA nucleotides 1065-1073 with GAAA by site-directed mutagenesis (Kunkel 1985) of plasmid pLK35.50S.MS2 as described (Ali et al. 2006) using the mutagenic oligo: 5'-CAGACAGCCAGGATGTTGGC**GAAA**GCCATCATTTAAAGAAAGCGTA.
MS2-tagged ribosomes were expressed in *E. coli* and affinity-purified on GST-sepharose essentially as described in (Lancaster et al. 2008). Prior to affinity-

purification 70S ribosomes were washed in either high- or low-salt buffer as described above.

In vitro assays

30S subunits were heat-activated for 10 min at 42˚C in buffer containing 20 mM MgCl2. 50S subunits were then added followed by incubation at 37˚C for a minimum of 10 min.

Poly(U)-directed poly(Phe) synthesis was measured as described in (Lancaster et al. 2005) with the following modification. The reaction mixture [containing 8 pmol of 70S (1.25X 50S) in 20 mM Tris-HCl (pH 7.6), 10 mM Mg(OAc)2, 50 mM NH4Cl, 1 mM ATP, 0.5 mM GTP, 5 mM phosphoenolpyruvate, 20 μg/mL pyruvate kinase (Roche), 1375 pmol Phe, 660 pmol [14C]-Phe, 20 pmol *E. coli* tRNAPhe, 1 μl S-100 enzymes (Traub et al. 1981), 1 mM DTT, 3.6 mM BME, and either 2% DMSO or 2% DMSO plus 10 μM thiostrepton in a total volume of 36 μl] was incubated at 37˚C for 10 min and then moved to ice. The reaction was initiated at 37˚C with 4 μL of poly(U) RNA (2.4 mg/mL). At the indicated times 5 μl samples were spotted onto paper filters (Whatman) and placed into ice-cold 10% TCA (2 mL/filter).

50S ribosomes proteins were extracted and analyzed by two-dimensional gel electrophoresis as described in (Lancaster et al. 2008) with the following modification. To reduce disulfide cross-links 2.7 μl of thioglycolic acid per mL running buffer was added to the upper buffer chamber during electrophoresis in the second dimension.

P-site tRNA binding and puromycin reactivity were determined as in (Lancaster et al. 2008). For A-site tRNA binding, 70S-mRNA-fMet-tRNAfMet complexes were prepared by adding 9.75 pmol of m36g32 mRNA and 13 pmol fMet-tRNAfMet to 6.5 pmol 70S ribosomes (1.5X 50S) or 6.5 pmol 30S subunit alone in a total volume of 65 μL in buffer B(20) and incubated at 37˚C for 20 min. Ternary complex was prepared by incubating 5 μM 6(His)-EF-Tu (Boon et al. 1992) with 1 mM GTP, 5 mM phosphoenolpyruvate, and 20 μg/mL pyruvate kinase in buffer B(20) at 37˚C for 15 min; [14C]-Phe-tRNAPhe was then added and incubated for an additional 5 min. Before use, the Mg2+ concentration was adjusted to 7 mM by addition of buffer B(0). 11.37 pmol of ternary complex or an equivalent mixture lacking EF-Tu was added to the ribosomes and incubated at 37˚C for 5 min. 10 μL of the reaction were spotted onto a nitrocellulose HA filter (Millipore), and washed 3X with 5 mL of ice-cold buffer B(7). Filters were dried in a 70˚C oven for 20 min, combined with scintillation cocktail and counted.

GTPase idling was measured by thin-layer chromatography as described in (Rodnina et al. 1999).

Translocation was measured as described in Studer (2003). Pre-translocation complexes were assembled by sequentially binding 65 pmol 3'-fluorescein-labeled mRNA (provided by D. Ermolenko), 105 pmol tRNAMet, and 105 pmol N-Ac-Phe-tRNA to 70 pmol ribosomes (1.25X 50S) in buffer C(20). Ribosome complexes were diluted to 7 mM Mg2+ using a buffer C(0) mixture containing 1 mM GTP and either 2% DMSO or 10 μM thiostrepton dissolved in 100% DMSO (final concentration DMSO 2%) as indicated. Translocation was initiated by rapid mixing with 6(HIS)-EF-G·GTP using an Applied Photophysics stopped-flow fluorimeter. Final concentrations after mixing were: 35 nM ribosomes, 500 nM 6HIS-EF-G, 1 mM GTP, 2% DMSO or 10 μM thiostrepton. The fluorescein dye was excited at 494 nm and fluorescence emission detected using a 515 nm long-pass filter. All stopped-flow experiments were done at room temperature. Time traces were analyzed using Pro-Data-Viewer software (Applied Photophysics). A baseline curve representing slow photoquenching in the absence of translocation was subtracted from each data set.

For EF-G binding, ribosomes complexes were assembled by combining 10 pmoles of ribosomes (1.33X 50S) with 20 pmol m36g32 mRNA and 15 pmol tRNAfMet in buffer A(20). The Mg2+ concentration was adjusted to 10 mM with buffer A(0) before addition of an EF-G mixture in buffer A(10) containing 10 pmoles EF-G and either 500 mM GDPNP or 500 mM GTP and 500 mM fusidic acid. Following a 5 minute incubation at 37˚C the ribosome-EF-G complexes were layered on top of a 200 μL 1M sucrose cushion in buffer A(10) containing either 500 mM GDPNP or 500 mM GTP and 500 mM fusidic acid. Pelleting was achieved by spinning for 45 minutes at 100K rpm in a TLA-100 rotor. The sucrose cushion was aspirated away and the pellet resuspended directly in SDS loading buffer and run on a 12% polyacrylamide gel. Gels were stained with Coomassie blue and analyzed with ImageQuant software. Each gel included a serial dilution of EF-G, which served as a loading control to determine EF-G retention efficiency.

The incorporation of [3H]-Leu by ribosomes programmed with poly(U) mRNA was measured as described in (Bartetzko et al. 1988) with the following modifications. Ribosome complexes were prepared by associating 25 pmol 30S subunits with 30 pmol 50S subunits followed by addition of a mixture containing 0.05 mg poly(U) mRNA, 100 pmol tRNAPhe 25 mM Tris-HCl (pH 7.5), 4.8 mM HEPES-KOH (pH 7.6), 100 mM NH4Cl, 20 mM MgOAc,

4 mM BME in a final volume of 20 μL. After 20 min incubation at 37˚C the volume was increased to 125 μL by addition of 105 μL of a mixture containing 13 mM HEPES-KOH (pH 7.6), 100 mM NH4CL, 3.33 mM Mg(OAc)2, 1 mM BME, 0.714 mM spermine and 0.5 mM spermidine. tRNAs were charged by combining 75 μL of energy mixture (48 mM HEPES-KOH (pH 7.6), 861 mM NH4CL, 4 mM BME, 3.5 mM spermine, 2.3 mM spermidine, 10 mM ATP, 1 mM GTP, 50 mM phosphoenolpyruvate) with 320 μL of tRNA and amino acid mixture (27 mM HEPES-KOH (pH 7.6), 2 mM Mg(OAc)2, 1.5 mM BME, 70 nmol [14C]-Phe (13 cpm/pmol), 20 nmol [3H]-Leu (13,500 cpm/pmol), 10 A260 units bulk tRNA from *E. coli* (Roche), 15 μg pyruvate kinase), and 30 μL S-100 enzymes, followed by a 5 min incubation at 37˚C. The reaction was initiated at 37 ˚C by combining the charging mixture and ribosome complex. 80 μL samples were withdrawn and stopped by mixing with 1.4 mL 10% TCA. Samples were incubated for 10 min at 95˚C then moved to ice; precipitates were collected on GC/F glass filters (Whatman) and washed 2X with 15 mL room temperature 5% TCA containing 0.5% w/v cold Phe and Leu amino acids, and twice with 2.5 mL 100% ethanol. Filters were dried and counted as above.

CHAPTER IV: Structural Dynamics within the L11 stalk

INTRODUCTION

The ribosome is a complex molecular machine composed of catalytic rRNAs and protein components. Structured rRNAs account for two-thirds the total mass of the ribosome. The overall biological function of the ribosome in protein synthesis is dependent on ribosome structure as defined by the specific folding of the three rRNAs. Unlike DNA, RNA exploits an expanded variety of folding motifs due to additional hydrogen-bonding capability. These include, but are not limited to, simple and complex helices formed by complementary base-pairing, non Watson-Crick base-pairing, hairpins, tetraloops, kink-turns, and pseudoknots, all of which are present in the structure of the rRNAs, for a review see (Moore 1999). Specific folding patterns of structured RNAs form the basis for functional centers of catalysis as well as small molecule, ion, and protein binding sites. Changes in RNA structure lend themselves to the formation of multiple regulatory states that may have differing properties of catalysis and ligand binding. A complete understanding of ribosome biology is dependent not only on knowing the secondary and tertiary folding of a single ribosome complex. Instead, it is necessary to understand the range of structures and conformations accessible to the rRNAs as observed in a large number of diverse structures.

Techniques for inferring structural dynamics

Traditionally, ribosome structure has been deduced by biochemical techniques relying on use of chemical agents serving as molecular probes. In brief, these techniques rely on covalent modification or cleavage of rRNAs by specific base-selective and non-specific agents. Base-selective agents target individual nucleotides reporting on interactions such as hydrogen-bonding and solvent accessibility. Non-selective techniques such as hydroxyl radical probing and selective 2' hydroxyl acylation analyzed by primer extension (SHAPE) target the RNA backbone and provide information on solvent accessibility, local nucleotide dynamics, and flexibility. Antibiotics may be used to stall specific reactions, allowing for before and after comparisons. Dynamics with ribosome structure may be determined by analysis of single ribosomes or by the comparison of related structures along a common reaction pathway.

Ribosome dynamics may also be determined by visualization of ribosomes by cryo-electron microscopy (cryo-EM) and X-ray diffraction crystallography. These methods produce structural models of ribosomes and their associated ligands at resolutions permitting analysis of fine and gross conformational rearrangements. Dynamics may be inferred by the comparison of related structures along a common reaction pathway. In this manner,

frame-by-frame snap-shots of the ribosome lead to cartoons of function. Cryo-EM reconstructions have been used to identify numerous inter- and intra-subunit changes in ribosome structure. Most dramatic are independent rotations of the small ribosomal subunit body and head, and changes in the position of the L11 and L1 stalks, which are induced by binding of ribosomal ligands. True atomic resolution structures are produced by X-ray crystallography. Diffraction between 3.0 and 5.5 Å resolution allows for direct visualization of phosphate and protein backbones as well as nucleotide bases and amino-acid side chains. Crystallographic approaches have been used to study the process of peptide bond formation (Korostelev et al. 2006; Selmer et al. 2006), GTP hydrolysis (Voorhees et al. 2010), and the selection of aa-tRNA (Schmeing et al. 2011).

Despite the challenges associated with the determination of ribosome structure, research over the past fifteen years has yielded a wealth of important structures. To date, approximately forty high-resolution X-ray diffraction structures of the ribosome, in isolation, bound by tRNAs, elongation factors, and translation factors, have been solved. Using available ribosome structures, changes in the position of the mobile L11 stalk of the 50S subunit associated with the binding of translation, elongation, and termination factors have been systematically analyzed. Correlations between the position of the stalk and factor binding suggest that the stalk may play a direct role in

regulating the GTPase activation of EF-Tu and EF-G. These findings suggest a role for the L11 stalk as a component of the aa-tRNA selection mechanism and explain the reduced accuracy of ΔL43 ribosomes.

RESULTS

We have made use of high-resolution X-ray crystal structures of ribosome functional complexes to systematically assess the change in position of the L11 stalk by measuring the distance between the 5' phosphates of A1067 in L43, and two stationary elements of 23S rRNA: A2660 in the SRL and C2475 in loop 89 (L89). Stalk displacement relative to the SRL is equivalent to vertical widening or narrowing of the factor-binding site, and displacement relative to L89 reports lateral movement of the stalk in relationship to the body of the 50S subunit.

Analysis of 39 ribosome crystal structures shows that the positions of the L11 stalk cluster in three locations. We designate these positions as distal (Figure 18A, 1-9), medial (Figure 18A, 10-34), and proximal (Figure 18A, 35-39) (Table 2). Representative structures of each state are shown in Fig 18B (Gao et al. 2009; Jenner et al. 2010; Schmeing et al. 2009). The positions of the L11 stalk correlate with the binding state of the ribosome (Table 2). The stalk occupies the distal and medial positions in vacant, RRF, and tRNA-bound ribosomes. The medial position is also occupied when ribosomes are bound with the translation factors EF-G, RF1, RF2, and RF3. The proximal position correlates uniquely with binding of the EF-Tu ternary complex, in either its pre- (Voorhees et al. 2010) or post-GTP-hydrolysis state (Schmeing

et al. 2009), and containing either cognate (Schmeing et al. 2009) or near-cognate aa-tRNA (Schmeing et al. 2011).

Figure 18. The L11 Stalk Assumes Three Conformations that Correlate with the Functional State of the Ribosome

(A) The position of the L11 stalk was determined in thirty-nine X-ray crystal structures by measuring displacements observed between the 5' phosphate of A1067, L89 (C2475/P) and the SRL (A2660/P). Error bars show the average location and standard deviation within each state. Numbering corresponds to Table 2, overlaying points have been averaged for clarity, (filled symbols) bound by a translation factor. (B) distal (green), medial (magenta), and proximal (blue) positions of the L11 stalk and their relationship to L89 and the SRL, spheres indicate phosphate atoms utilized in the analysis. Inset: overview of the 50S ribosome, L11 stalk, L89 and SRL in red.

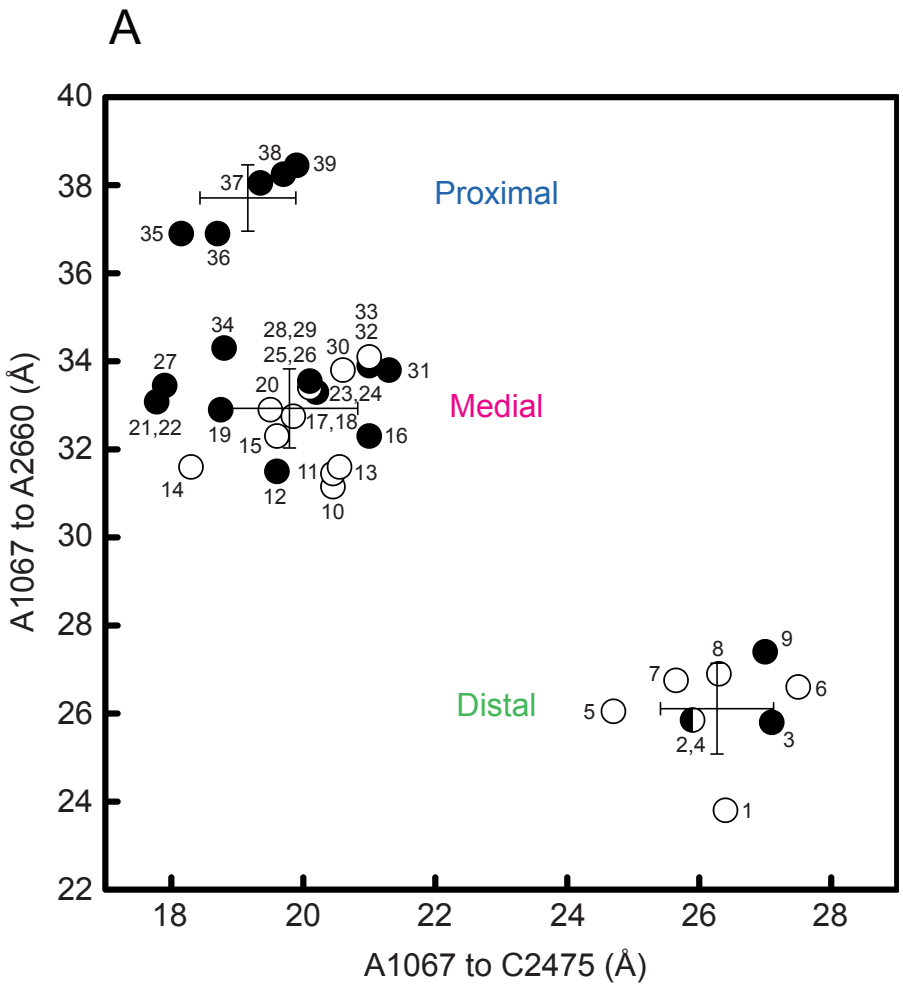
A
A1067 to A2660 (Å)
A1067 to C2475 (Å)
Proximal
Medial
Distal
40
38
36
34
32
30
28
26
24
22
18
20
22
24
26
28
38
39
37
35
36
34
28,29
33
32
25,26
30
31
27
20
23,24
21,22
19
17,18
16
15
14
11
13
12
10
8
9
7
6
5
2,4
3
1

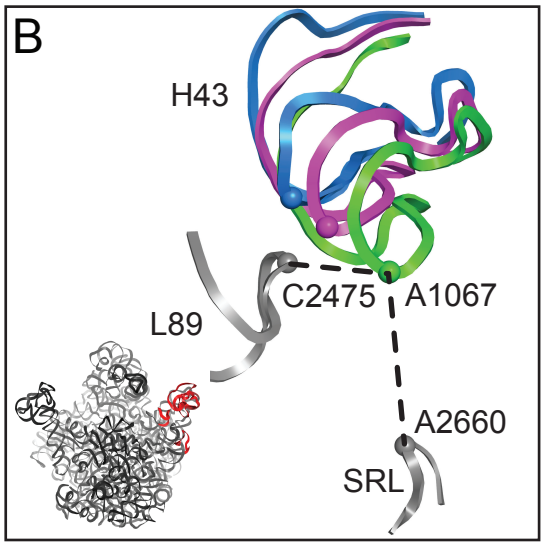
B
H43
C2475
A1067
L89
A2660
SRL

Table 2. L11 Stalk Position Relative to the SRL and L89

The distance between the 5' phosphates of A1067 within loop 43 and A2660 of the SRL and C2475 of L89 were measured in 39 X-ray diffraction structures of ribosomes. Measurements were averaged for crystals of *T. thermophilus* ribosomes containing 2 similarly structured ribosomes per asymmetric unit. Crystals of *E. coli* ribosomes containing 2 dissimilar ribosomes per asymmetric unit are treated separately (rbs I and rbs II). Abbreviations used: ASL = anticodon stem-loop, kirro = kirromycin, Tth = *T. thermophilus*, Eco = *E. coli*.

Table 2. L11 Stalk Position Relative to the SRL and L89

#	Ligands	Reference	Organism	PDB	A1067 to A2660 (Å)	A1067 to C2475 (Å)
1	tRNA: P, E	Korostelev et al. 2006	Tth	1VSA	23.80	26.40
2	RRF, gentamycin (rbs II)	Borovinskaya et al. 2007	Eco	2QBK	25.80	25.90
3	RRF (rbs II)	Borovinskaya et al. 2007	Eco	2QBG	25.80	27.10
4	gentamycin (rbs II)	Borovinskaya et al. 2007	Eco	2QBC	25.90	25.90
5	tRNA: P, E	Jenner et al. 2010	Tth	3I9E	26.05	24.70
6	tRNA: A, P, E	Jenner et al. 2010	Tth	3I8F	26.75	25.65
7	Vacant (rbs II)	Schuwirth et al. 2005	Eco	2AWB	26.90	26.30
8	Neomycin (rbs II)	Borovinskaya et al. 2007	Eco	2QAO	26.60	27.50
9	RRF, paromomycin (rbs II)	Borovinskaya et al. 2007	Eco	2Z4N	27.40	27.00
10	ASL: A, P	Zhang et al. 2009	Eco	3I2O	31.15	20.45
11	ASL: P	Zhang et al. 2009	Eco	3I1R	31.45	20.45
12	RF3·GDPNP	Zhou et al. 2011	Tth	3SGF	31.50	19.60
13	Vacant	Zhang et al. 2009	Eco	3I1P	31.60	20.55
14	tRNA: P	Dunkle et al. 2011	Eco	3R8T	31.60	18.30
15	Vacant (rbs I)	Schuwirth et al. 2005	Eco	2AW4	32.30	19.60
16	RRF, tRNA: Hybrid P	Dunkle et al. 2011	Eco	3R8S	32.30	21.00
17	gentamycin (rbs I)	Borovinskaya et al. 2007	Eco	2QBA	32.70	19.90
18	neomycin (rbs I)	Borovinskaya et al. 2007	Eco	2QAM	32.80	19.80
19	EF-G·GDP/FA	Gao et al. 2009	Tth	2WRJ	32.90	18.75
20	tRNA: A, P, E	Yusupov et al. 2006	Tth	2HGQ	32.90	19.50

#	Ligands	Reference	Organism	PDB	A1067 to A2660 (Å)	A1067 to C2475 (Å)
21	RF2, tRNA: P	Jin et al. 2010	Tth	2X9S	33.05	17.70
22	RF2	Weixlbaumer et al. 2008	Tth	2WH2	33.10	17.85
23	RRF, gentamycin (rbs I)	Borovinskaya et al. 2007	Eco	2QBI	33.30	20.10
24	RRF, paromomycin (rbs I)	Borovinskaya et al. 2007	Eco	2Z4L	33.30	20.30
25	tRNA: P, E	Yusupova et al. 2006	Tth	2HGU	33.40	20.00
26	tRNA: A, P	Yusupova et al. 2006	Tth	2HGJ	33.40	20.20
27	RF2, tRNA: P	Korostelev et al. 2008	Tth	3F1F	33.45	17.90
28	RRF Split (rbs I)	Borovinskaya et al. 2007	Eco	2QBE	33.50	20.10
29	RF3·GDPCP, tRNA: P	Jin et al. 2011	Tth	3ZVP	33.60	20.10
30	tRNA: A, P	Jenner et al. 2005	Tth	1YL3	33.80	20.60
31	RF1, tRNA: P	Petry et al. 2006	Tth	2B66	33.80	21.30
32	RF2 tRNA: P	Petry et al. 2005	Tth	2B9N	33.90	21.00
33	tRNA: P	Petry et al. 2005	Tth	2B9P	34.10	21.00
34	RF1, tRNA: P	Laurberg et al. 2008	Tth	3D5B	34.30	18.80
35	EF-Tu·(GTP/kirro)·Cognate	Schmeing et al. 2009	Tth	2WRO	36.90	18.15
36	EF-Tu·GDPNP·Cognate	Voorhees et al. 2010	Tth	2XQE	36.90	18.70
37	EF-Tu·(GTP/kirro)·Cognate	Schmeing et al. 2011	Tth	2Y11	38.05	19.35
38	EF-Tu·(GTP/kirro)·Near-	Schmeing et al. 2011	Tth	2Y0V	38.25	19.70
39	EF-Tu·(GTP/kirro)·Near-	Schmeing et al. 2011	Tth	2Y0Z	38.45	19.90

DISCUSSION

Although clearly discrete states, we consider the distal and medial states to be freely interchangeable because vacant and tRNA bound ribosomes are found in both states. *E. coli* ribosomes within a single crystal have a propensity to occupy both states (Schuwirth et al. 2005) (Borovinskaya et al. 2007), a fact that may depend upon rotation of the 30S subunit head towards to E site. Additionally, *E. coli* ribosomes with rotated (ratcheted) 30S subunits bound by tRNA anticodon stem-loops (Zhang, et al., 2009) or full length tRNAPhe in the hybrid P/E conformation and RRF (Dunkle, et al., 2011), results in the medial state, suggesting that 30S subunit rotation may also be linked to the stalk position.

Regulation of GTP hydrolysis by the L11 stalk

Unlike EF-G, which hydrolyzes GTP rapidly upon binding to the ribosome (Savelsbergh et al. 2003), the GTPase activation of EF-Tu only occurs following codon-anticodon pairing, a process that is directly linked to the fidelity of aminoacyl-tRNA selection. Aminoacyl-tRNAs are selected by a kinetic discrimination mechanism in which the GTPase rate of EF-Tu in ternary complexes containing cognate aa-tRNAs is preferentially accelerated

by several orders of magnitude (Pape et al. 1999; Rodnina et al. 2005). The mechanism underlying this acceleration is not fully understood. Correlation between the position of the L11 stalk and elongation factor binding led us to ask if the L11 stalk could serve as a selective mechanism in the binding of each factor.

Steric clash between L43 of the L11 stalk and the aa-tRNA elbow or EF-G domain V may regulate the binding of elongation factors. Aminoacyl-tRNA bound by EF-Tu interacts with the 70S ribosome in four regions: three on the 30S subunit and exclusively through L43 with the 50S subunit (Schmeing et al. 2009). The conformation of the EF-Tu ternary complex as observed on the ribosome (Figure 19A,D) (Schmeing et al. 2009; Schmeing et al. 2011; Voorhees et al. 2010) is incompatible with the distal (Figure 19B) and medial (Figure 19C) conformations of the L11 stalk due to steric clash between L43 and the aa-tRNA elbow. In contrast to EF-Tu ternary complex, EF-G makes numerous contacts with both the 30S and 50S subunits. The G domain, domains III and V contact the 50S subunit around the GAC. Domain V is positioned between the L11 stalk and 23S rRNA H89. Domains II, III, and IV interact with the 30S subunit. The conformation of EF-G as observed on the ribosome (Figure 20A) (Gao et al. 2009) is incompatible with the distal conformation of the L11 stalk due to steric clash (Figure 20B). This clashing is

avoided in the medial (Figure 20C) and proximal (Figure 20D) conformations; however, in the latter domain V makes no contact with the L11 stalk.

A model for the GTPase activation of EF-Tu

In ribosome structures determined thus far, the L11 stalk exists in the proximal conformation only when bound by EF-Tu ternary complex. Since the position of the L11 stalk prior to interaction with EF-Tu is likely medial or distal, the orientation of the ternary complex, must be different during initial binding and codon sampling. Fitting the structure of the isolated ternary complex (Nissen et al. 1995) to the structure of a medial-state ribosome (Korostelev et al. 2008), while maintaining contact between the aa-tRNA elbow and L43, and the anticodon stem-loop and mRNA (Figure 21A), moves the G domain of EF-Tu away from the SRL by 4Å (Figure 21D). Contact between the G domain and the SRL is not established unless the stalk is proximal (Figure 21B). If contact between the G domain of EF-Tu with the SRL is required for activation of its GTPase (Chan et al. 2004; Hausner et al. 1987; Voorhees et al. 2010) this suggests a mechanism for how the L11 stalk could play a role in the accuracy of aa-tRNA selection by limiting activation of the GTPase activity of EF-Tu.

We propose that movement of the aa-tRNA associated with ribosomal binding is directly responsible for displacement of the stalk to the proximal state, which permits productive binding of EF-Tu to the SRL. In this model, the stalk serves as a physical barrier that opposes access of EF-Tu ternary complex to the GTPase-activating SRL. When cognate ternary complex is bound, concerted rearrangements within the ribosome (Ogle et al. 2001; Ogle et al. 2002), aa-tRNA (Valle et al. 2002; Valle et al. 2003), and EF-Tu (Schmeing et al. 2009), stabilize the binding and allow for the aa-tRNA elbow to displace the stalk into the proximal position (Figure 21B), creating contact between the G domain and the SRL (Figure 21BE). Near- and non-cognate aa-tRNAs may erroneously trigger GTP hydrolysis following the temporary and thermodynamically unfavorable excursion of the stalk to the proximal position, or in the presence of aminoglycoside antibiotics, which promote errors in aa-tRNA selection by stabilization of tRNA interaction with 16S rRNA (Carter et al. 2000).

Our findings on the relationship between the position of the L11 stalk, binding of tRNA and translation factors, and GTP hydrolysis, differ in several key aspects from previous models. Additionally, this work is the first encompassing not only EF-Tu and EF-G, but also RF1, RF2, RF3 and RRF. Somewhat conflicting two- and three-state models governing stalk dynamics in relationship to the activity of elongation factors have been proposed based

on cryo-EM reconstructions of ribosome complexes, in which the stalk is described as moving towards and away from the body of the 50S subunit, assuming 'open', 'closed', and intermediate positions (Frank et al. 2005; Sergiev et al. 2005; Valle et al. 2003). Additional models incorporate movement occurring in the N-terminal domain of protein L11 (Agrawal et al. 2001; Kavran et al. 2007; Lee et al. 2007; Wimberly et al. 1999), which appears to stabilize EF-G binding (Harms et al. 2008).

Sergiev et al (2005) propose that the L11 stalk produces specificity in the factor-binding site for EF-Tu and EF-G by alternating between 'open' and 'closed' conformations, respectively. GTP hydrolysis is additionally predicted to shift the position of the stalk and thereby establish contact with the factor and prepare the ribosome for the binding of the next factor (Sergiev et al. 2005). In agreement with this model we find that EF-G and EF-Tu interact with alternating conformations of the stalk (Figure 18A, compare points 19 and 35-39). However, we find no evidence for the coupling of GTP hydrolysis to inter-conformational stalk transitions as EF-Tu·GDPCP and EF-Tu·GDP/kirromycin are both bound to the proximal stalk (Figure 18A, compare points 36 and 35,37-39). In contrast to their model, we propose that the L11 stalk makes continuous contact with the aa-tRNA elbow within ternary complex and domain V of EF-G both before and after GTP hydrolysis.

Alternate two- (Valle et al. 2003) and three-state (Frank et al. 2005) models specifically relate to the GTPase activation of EF-Tu, and propose that EF-Tu binding to the 'open' state induces a transition directly to a GTPase active 'closed' state, or proceeds through an intermediate 'half-closed' GTPase active state. These models are in closest agreement with our findings, although we may exclude the possibility of a 'half-closed' GTPase active state because EF-Tu is only found bound to proximal state ribosomes (Figure 7A points 35-39).

Specific effects of the ΔL43 mutation

The GAAA tetraloop substitution was modeled by replacing L43 nucleotides in the X-ray structures of T. thermophilus ribosomes bound by EF-G and EF-Tu with the atomic coordinates of the GAAA tetraloop from 16S rRNA H40 (nucleotides 1163-1174) (Gao et al. 2009; Schmeing et al. 2009). The modeled tetraloop nucleotides do not clash with other positions in the stalk-rRNA or interfere with the binding sites of proteins L11 or L10 (Figure 22A). As predicted, the modeled tetraloop lacks necessary length and suitable hydrogen bonding patterns required to form tertiary interactions with H44 (Figure 22A). Our modeling indicates that the ΔL43 mutation shortens H43 by 4.2Å as measured along its helical axis, which serves to artificially widen the

factor-binding site formed between the stalk and the SRL. This shortened helix no longer contacts the aa-tRNA (Figure 22B) or EF-G domain V (Figure 22C).

Increased error frequency of ΔL43 ribosomes

Our proposed mechanism for the GTPase activation of EF-Tu could account for the increased error frequency and translocation defect of ΔL43 and ΔL43/L11- ribosomes, respectively. Contact between the aa-tRNA and L11 stalk in the medial position creates a ~4 Å gap between the SRL and GTPase center of EF-Tu. The enlarged factor-binding site of ΔL43 or ΔL43/L11- ribosomes would increase the likelihood for the G domain of EF-Tu in the near-cognate tRNALeu ternary complex to contact the SRL, leading to activation of its GTPase. The mechanism underlying the increased error frequency of ΔL43 ribosomes would therefore be analogous to that proposed for tRNATrp variants in which their misincorporation is attributed to increased flexibility or stability of their anticodon arms (Schmeing et al. 2011). ΔL43 ribosomes translate with an error rate similar to that of ribosomes harboring mutations in the small ribosomal proteins S4 or S5 (RAM mutants) (Allen et al. 1991; Andersson et al. 1983), which are defective in the initial selection of aa-tRNA leading to acceleration of GTP hydrolysis (Zaher et al. 2010). The

approximately four-fold increase in tRNALeu incorporation by ΔL43 ribosomes (Figure 17B) likely represents a significantly larger defect in initial aa-tRNA screening capacity as the burden of selection is shifted onto the proofreading apparatus of the ribosome.

We may speculate that the L11 stalk could have functioned as an early proofreading mechanism in ancestral ribosomes before the evolution of EF-Tu and thermodynamic separation by GTP hydrolysis of the first and second steps of tRNA selection. Serving as an adaptor molecule between amino-acids and mRNA, the tRNA is the most important and likely most ancient of the ribosomal ligands. The interaction between the 50S subunit and tRNA occurs entirely along an RNA interface between 23S rRNA L43 of the L11 stalk and the aa-tRNA elbow. Access of aa-tRNA to the ribosomal A site would depend on displacement of the stalk towards the 50S subunit and bending within the aa-tRNA body, events that are thermodynamically linked to the stability of tRNA interactions within the 30S subunit. Evolution of EF-Tu would occur within this established framework, co-opting these conformational rearrangements and coupling them to the activation of GTP hydrolysis via the SRL.

Inactivation of ΔL43/L11- ribosomes in translocation

In the post-GTPase state, domain V of EF-G makes three contacts with the 50S subunit: the SRL, L11 stalk, and H89 (Figure 23) (Gao et al. 2009). EF-G mutants lacking domain V are active in GTP hydrolysis and translocation, but are not released from the ribosome (Savelsbergh et al. 2000). Deletion of the SRL alters the binding conformation of EF-G preventing GTPase activation and translocation (Clementi et al. 2010; Lancaster et al. 2008). ΔL43/L11**-** ribosomes support a different binding configuration of EF-G, which facilitates GTP hydrolysis but not translocation or release. These findings indicate that all three contacts between the ribosome and domain V are necessary for the stable binding of EF-G, leading to translocation. Therefore, it is likely that the altered stalk structure of ΔL43/L11**-** ribosomes would not stabilize the binding of EF-G domain V to the ribosome.

The C-terminal domain of protein L11, which binds to H43, stabilizes a tertiary structure of the ΔL43 L11 stalk rRNA. Therefore, when L11 is present, a three-point contact between EF-G domain V, the L11 stalk, SRL, and H89 is maintained. In the absence L11 and the tertiary structure of the stalk rRNA, EF-G domain V would be braced on the ribosome by only two contact points, which may be insufficient for the coupling of GTP hydrolysis to translocation.

Figure 19. The Distal and Medial Positions of the L11 Stalk Clash with aa-tRNA in EF-Tu Ternary Complex

(A) (Left) Overview of the 50S ribosome indicating major features, central protuberance (CP), L11, and L1 stalks; and (right) the orientation of EF-Tu ternary complex (EF-Tu, light blue; aa-tRNA, yellow) bound to the ribosome (Schmeing et al. 2009) with proximal (blue) L11 stalk. (B, C) Clash (red) between the aa-tRNA elbow and the distal (B) or medial (C) position of the L11 stalk is resolved when the stalk is proximal (D).

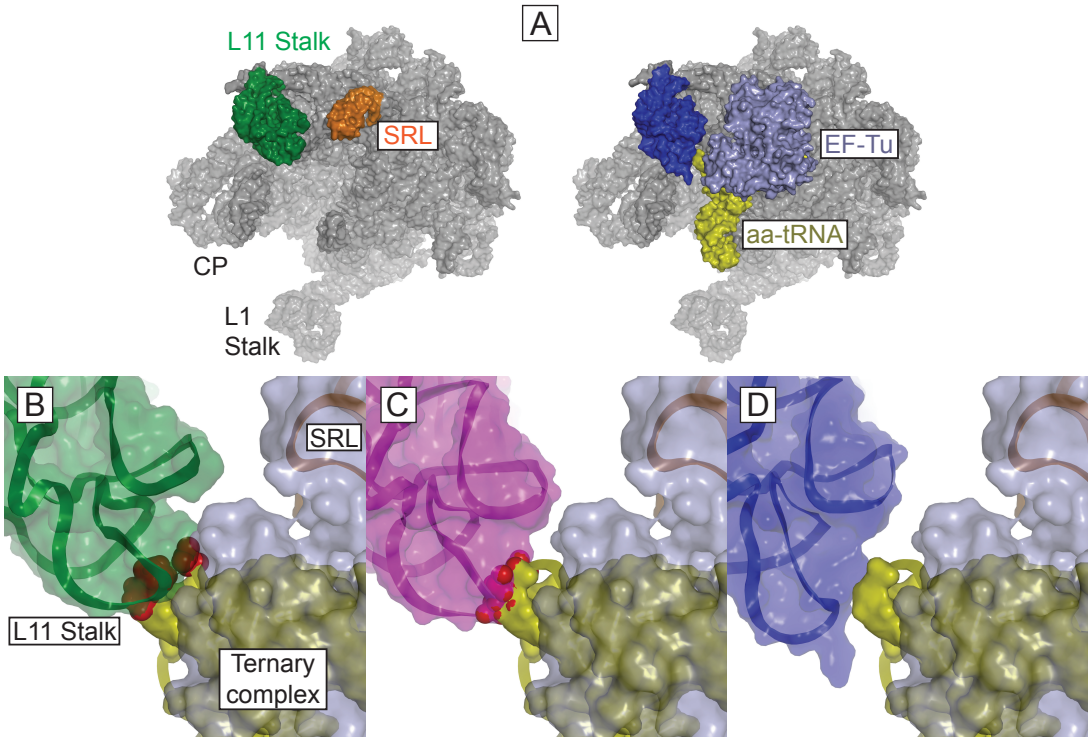
A
L11 Stalk
SRL
CP
L1
Stalk
EF-Tu
aa-tRNA
B
SRL
L11 Stalk
Ternary
complex
C
D

Figure 20. The Distal and Medial Positions of the L11 Stalk Clash with EF-G

(A) Overview of the 50S ribosome indicating major features, central protuberance (CP), L11 and L1 stalks. (B) Orientation of EF-G (cyan) bound to the ribosome (Schmeing et al. 2009) with the L11 stalk in the medial position (magenta). (C) Clash (red) between EF-G domain V (cyan) and the distal position of the stalk (green) is resolved when the stalk is in the medial position (D, magenta). For clarity the other domains of EF-G have been colored grey. (E) Contact between EF-G domain V and the stalk does not occur when the stalk is proximal (blue).

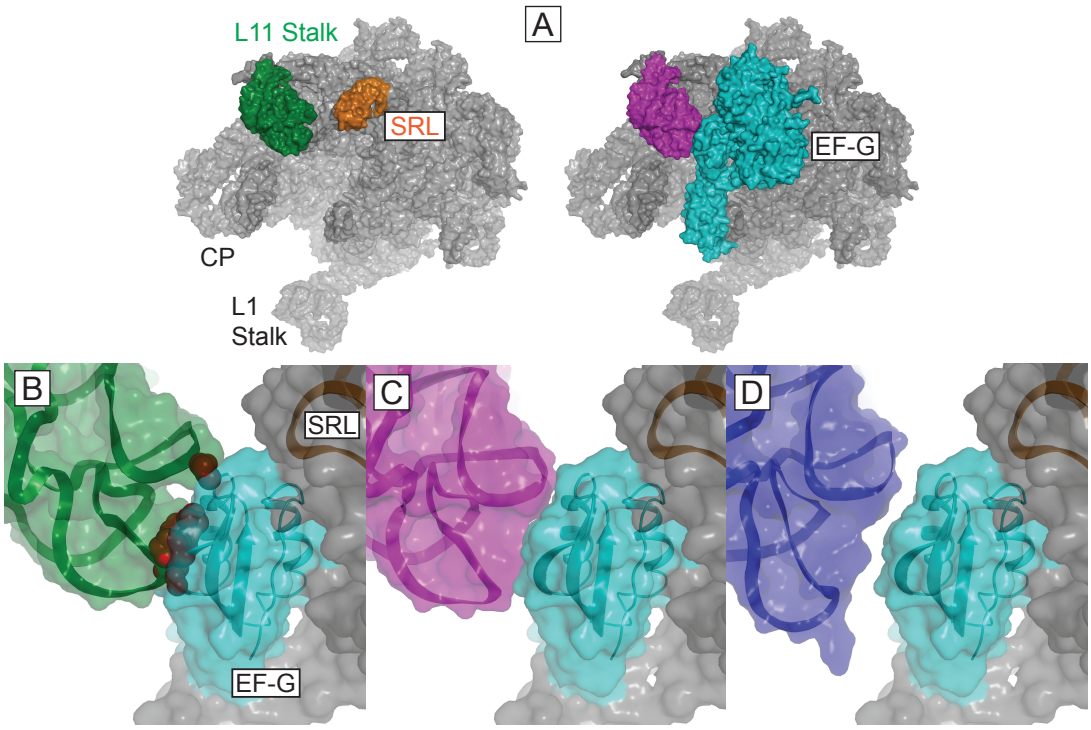
A
L11 Stalk
SRL
CP
L1
Stalk
EF-G
B
SRL
EF-G
C
D

Figure 21. The ΔL43 Mutation Shortens H43 and Abolishes Normal L43 Contacts with aa-tRNA and EF-G.

(A) H43 and H44 of the L11 stalk (grey), WT L43 (red), ΔL43 (grey), bound by the C-terminal domain of protein L11 (blue). The ΔL43 mutation removes nucleotides contacted by EF-Tu and EF-G as well as G1071 and C1072, which form tertiary interactions (yellow) with H44. (B) ΔL43 model in the proximal position (grey) interacting with aminoacyl-tRNA (purple), WT L43 (red). (C) ΔL43 model in the medial position (colored as in B) interacting with EF-G (cyan).

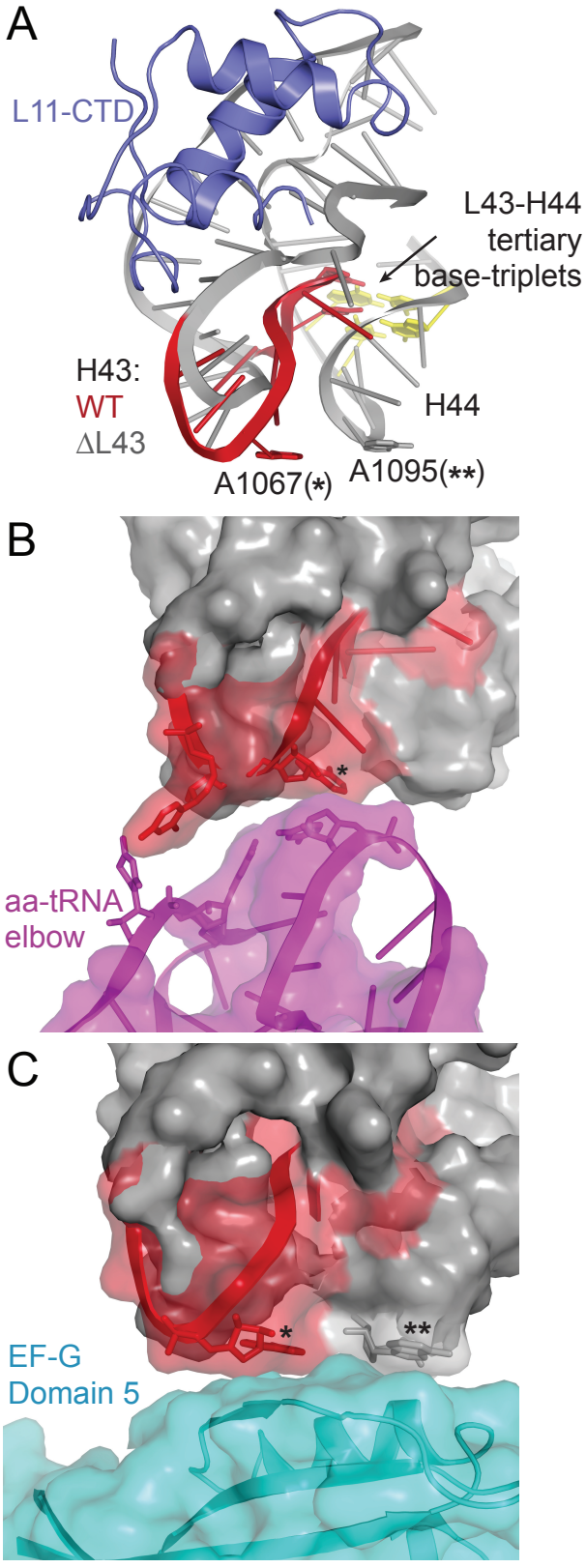
A
L11-CTD
L43-H44
tertiary
base-triplets
H43:
WT
ΔL43
H44
A1067(*)
A1095(**)
B
*
aa-tRNA
elbow
C
*
**
EF-G
Domain 5

Figure 22. EF-G Domain V Contacts the SRL, L11 Stalk, and H89

(A-B) Domain V of EF-G•GDP bound to the ribosome in the post translocation state contacts the L11 stalk, SRL and H89 of the 50S subunit. L11 stalk (magenta), H89 (blue), SRL (orange), EF-G (grey cartooon), domain V (green). (B) colored as in A, rotated 180˚ around the vertical axis.

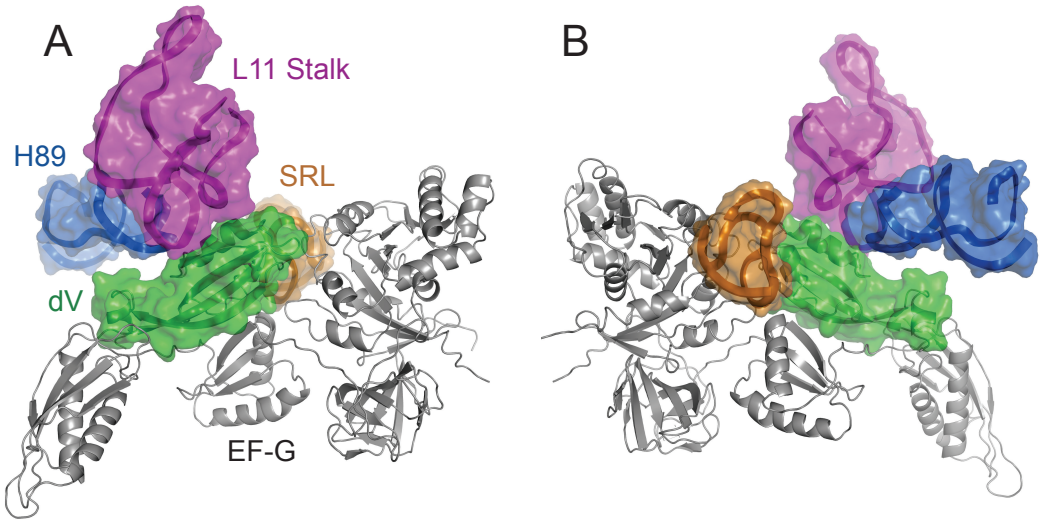
A
L11 Stalk
H89
SRL
dV
EF-G
B

CHAPTER V: Extended Truncations within the L11 Stalk of 23S rRNA

INTRODUCTION

In addition to the replacement of 23S rRNA loop 43 with a GAAA tetraloop (ΔL43) two larger truncations within the rRNA of the L11 stalk (Figure 23A) were generated and characterized. The same methodology as presented in chapter III was used to replace 23S rRNA helix 43 (ΔH43, nucleotides 1060-1078, Figure 23B) and helices 42-44 (ΔGAC, nucleotides 1043-1112, Figure 23C) with GAAA tetraloops. Collectively, ΔL43, ΔH43, and ΔGAC mutations are referred to as the L11 stalk mutants.

RESULTS

ΔH43 and ΔGAC mutations confer a dominant-lethal phenotype

The expression of ΔH43 or ΔGAC 23S rRNA by *E. coli* resulted in dominant-lethal growth phenotypes (Figure 23D). MS2-tagged ΔH43 and ΔGAC 50S ribosomal subunits were affinity purified from *E. coli* cells and characterized by biochemical assays. MS2 affinity-purified subunits were found to be greater than 95% free of wild-type 50S contamination, as determined by primer extension (Appendix C).

Altered protein content of mutant ribosomes

The protein content of ΔH43 and ΔGAC ribosomes was characterized by two-dimensional gel electrophoresis of extracted 50S ribosomal proteins. In comparison to wild-type 50S subunits (Figure 24A), ΔH43 subunits were found to completely lack ribosomal protein L11 and were partially depleted of protein L10 and the associated L7/12 complex (Figure 24B). Proteins L11, L10, and L7/12 of the L11 stalk were completely absent from ΔGAC ribosomes in addition to protein L16 (Figure 24C). The altered protein content of mutant ribosomes is consistent with the known 23S rRNA binding locations of the proteins (Figure 24A). The N-terminal domain of L11 binds to H43, which is absent in ΔH43 ribosomes (Figure 23B). L10 binds to the three-way junction formed by H42, H43, and H44, which are absent in ΔGAC ribosomes (Figure 23C). The loss of protein L16 from ΔGAC ribosomes was unexpected but not unprecedented. This protein was also absent from ribosomes in which the SRL was replaced with a GAAA tetraloop (Chapter II) (Lancaster et al. 2008).

P- and A-site tRNA binding

P- and A-site tRNA binding to ΔH43 and ΔGAC ribosomes were measured by filter binding. The L11 stalk mutants became fully saturated with P-site N-Ac-[3H]-Phe-tRNAPhe under non-enzymatic binding conditions when programmed with the defined mRNA m36g32 and incubated with excess tRNA in a buffer containing 20 mM Mg2+ (Figure 25A). Reaction with puromycin confirmed P-site placement (data not shown). The binding of A-site tRNA was measured under EF-Tu-dependent conditions in the presence and absence of EF-Tu. When EF-Tu was included in the reaction, ΔH43 and ΔGAC ribosomes reacted with EF-Tu ternary complex and became saturated with [3H]-Phe-tRNAPhe (Figure 25B). ΔGAC ribosomes were less reactive and were approximately 50% saturated with tRNA under identical conditions (Figure 25B). Neither wild-type nor the L11 stalk mutants bound a significant amount of tRNA when EF-Tu was omitted from the reaction (Figure 25B). These results indicate that the L11 stalk mutants are active in the non-enzymatic binding of P-site tRNA, and that ΔH43 but not ΔGAC ribosomes are fully active in their interaction with EF-Tu ternary complex.

Idling GTPase reaction by L11 stalk mutants

Functional interaction between EF-G and ΔH43 and ΔGAC ribosomes was tested in the GTPase idling reaction (Arai et al. 1974; Rodnina et al. 1997). The activity of ΔH43 and ΔGAC ribosomes was greatly reduced but measurable. Unlike wild-type and ΔL43 ribosomes, the activity of these mutant ribosomes rapidly reached a plateau (Figure 26A). These results suggest that truncation of H43 interferes with the release of EF-G·GDP from the ribosome but does not inhibit GTPase activation.

ΔH43 ribosomes are active in translation and are thiostrepton resistant, but not ΔGAC ribosomes

The *in vitro* translational capability of ΔH43 and ΔGAC ribosomes was tested in the poly(Phe) assay (Traub et al. 1981). Based on the thiostrepton resistance of ΔL43 ribosomes (Chapter III, Figure 11A, and 15B), we reasoned that ΔH43 and ΔGAC ribosomes would be resistant as well. Thiostrepton was included in the reaction to prevent translation from occurring on the small fraction of wild-type ribosomes that contaminate MS2-tagged affinity-purified ribosomes. ΔH43 ribosomes were found to be partially active in poly(Phe) synthesis and were unaffected by 10 μM thiostrepton (Figure

26C). ΔH43 ribosomes synthesized approximately 5-fold less poly(Phe) peptides than did wild-type over the same time period. As observed for ΔL43 ribosomes, the t1/2 for the reaction was comparable between wild-type and ΔH43 ribosomes. This suggests that the reduced translational activity of ΔH43 ribosomes is due to the presence of a subpopulation of inactive ribosomes. ΔGAC ribosomes did not produce detectable quantities of poly(Phe) peptides (Figure 26D), suggesting that the complete removal of the L11 stalk rRNA inactivates ribosomes in poly(Phe) synthesis. These results indicate that a sub-population of ΔH43 ribosomes, but not ΔGAC ribosomes, are active in *in vitro* translation elongation.

Figure 23. Secondary Structures of ΔH43 and ΔGAC Ribosomes

The L11 stalk is formed by 23S rRNA nucleotides 1051-1108 and is a projection of helix 42. (A) Folding of the stalk-rRNA is enforced by the binding of ribosomal proteins L10 (black outline) and L11 (grey outline) as well as tertiary interactions formed between L43 and H44, T1: G1071(G1091:C1100), T2: C1072(C1092:G1099). Nucleotides contacted by EF-G and thiostrepton (filled circles); nucleotides contacted by EF-Tu ternary complex (filled triangles). (B) The replacement of H43 (nucleotides 1060-1078) with GAAA (ΔH43) removes nucleotides contacted by EF-G, EF-Tu, and thiostrepton, and the majority of the L11 binding site. (C) The partial replacement H42, and total removal of H43 and H44 (nucleotides 1043-1112) with GAAA (ΔGAC) removes the entire L11 stalk. (D) *E. coli.* cells expressing ΔH43 or ΔGAC 23S rRNA fail to grow at 42˚ C.

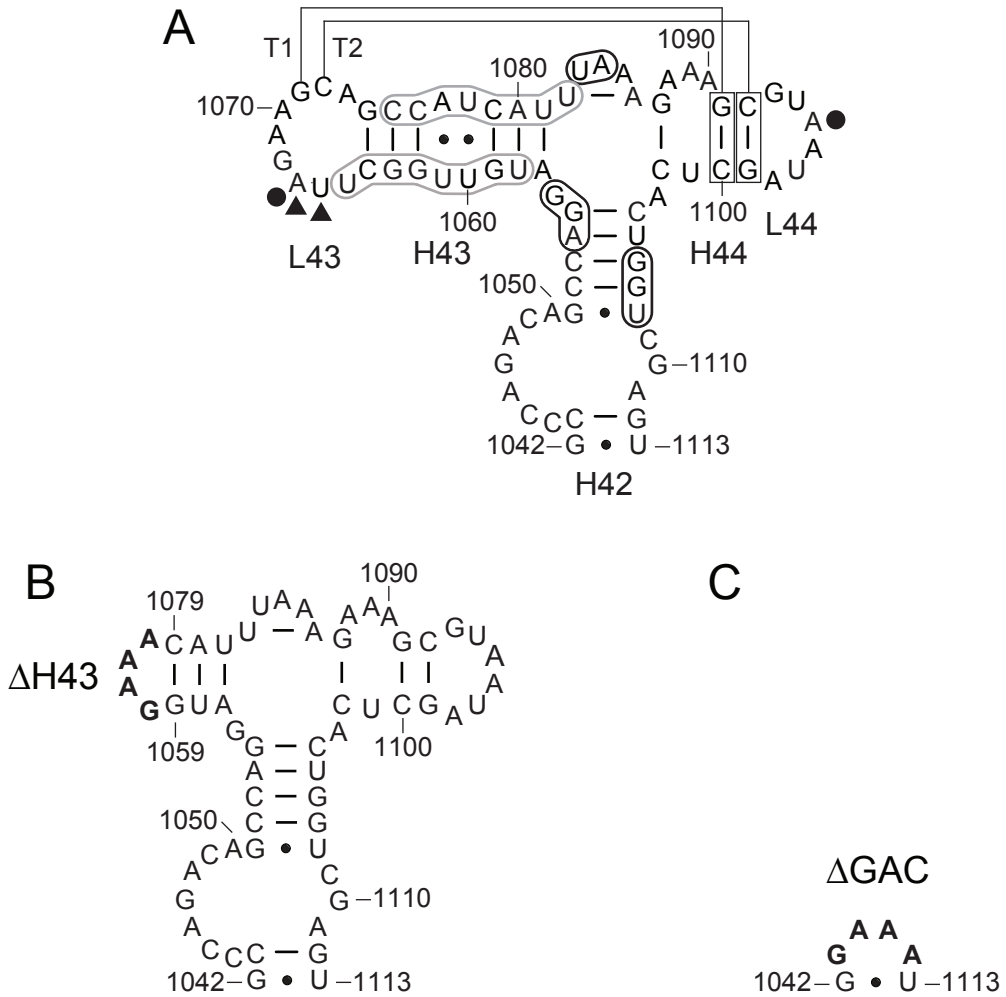
A
T1
T2
1090
1080
1070
1060
1100
L43
H43
H44
L44
1050
1042
1113
1110
H42
B
ΔH43
1079
1059
C
ΔGAC
D
30° C
42° C
WT-MS2
ΔH43
ΔGAC

Figure 24. ΔH43 and ΔGAC 50S Subunits are Missing L11 Stalk Associated Proteins

Two-dimensional gel electrophoresis of (A) MS2-WT, (B) ΔH43 and (C) ΔGAC 50S proteins. The boxed region in A contains proteins of the L11 stalk, which are expanded and labeled in upper right of that panel (L9 is not a stalk protein). Additional 50S proteins absent from ΔGAC subunits are indicated in C.

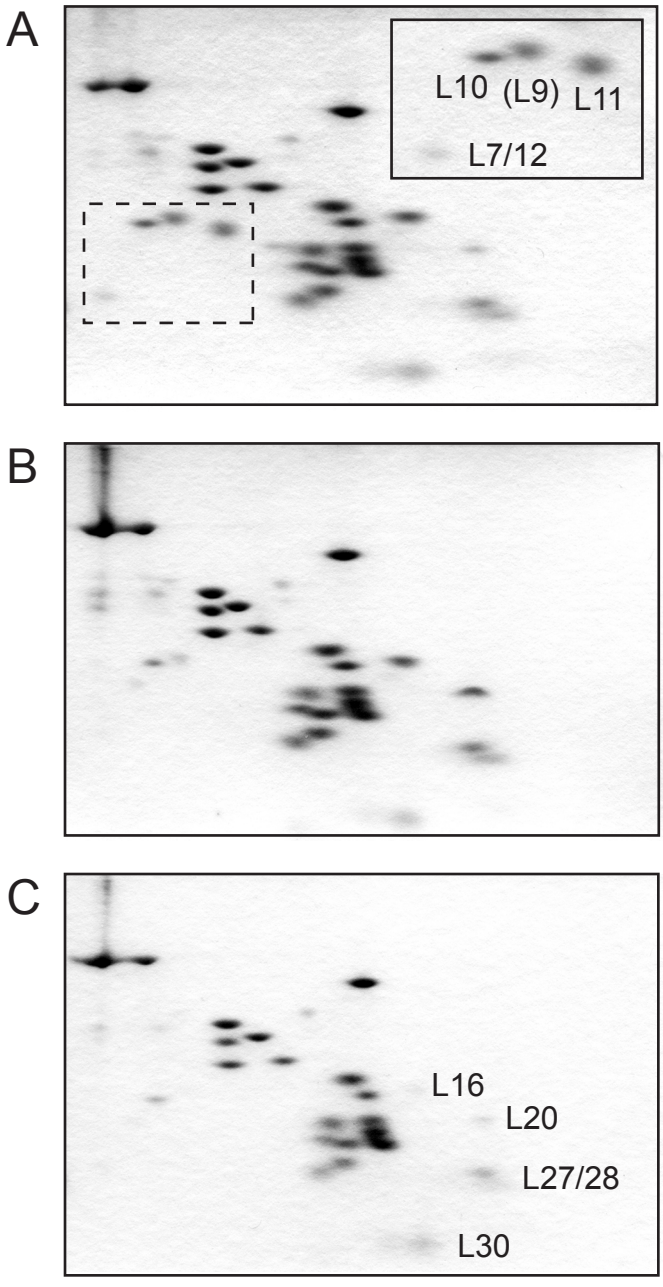
A
L10
(L9)
L11
L7/12
B
C
L16
L20
L27/28
L30

Figure 25. A- and P-Site tRNA Binding to L11 Stalk Mutants

P- and A-site tRNA binding was measured by filter binding. (A) P-site binding, the L11 stalk mutants programed with m291 mRNA become fully saturated with N-Ac-[3H]-tRNAPhe. (B) A-site tRNA binding of [3H]-Phe-tRNAPhe to complexes containing P-site tRNAfMet, in the presence (black bars), or absence (white bars) of EF-Tu.

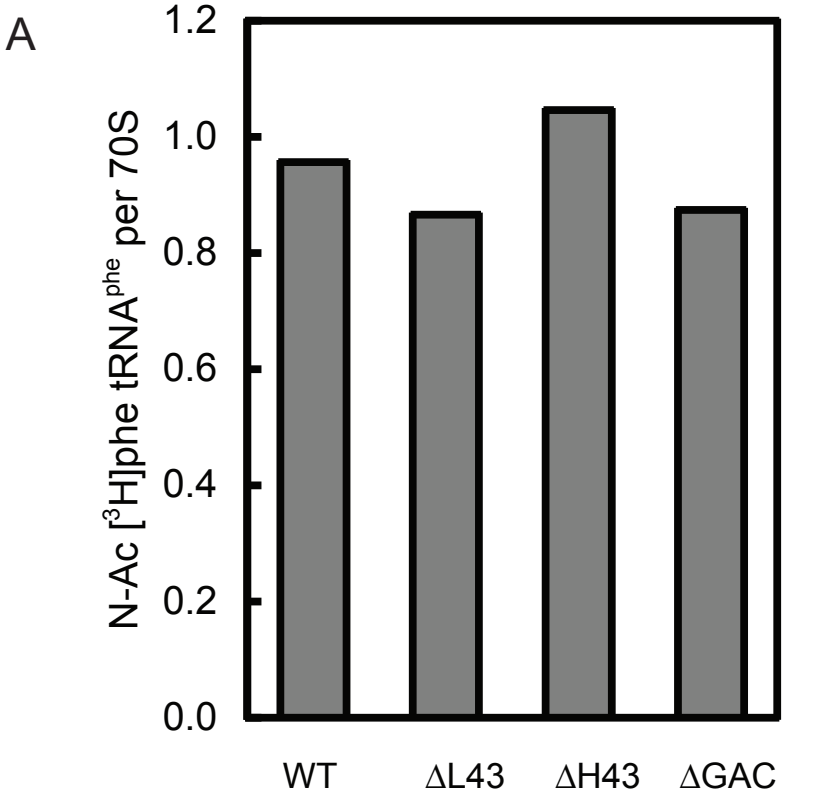
A
1.2
1.0
0.8
0.6
0.4
0.2
0.0
N-Ac [3H]phe tRNAphe per 70S
WT
ΔL43
ΔH43
ΔGAC

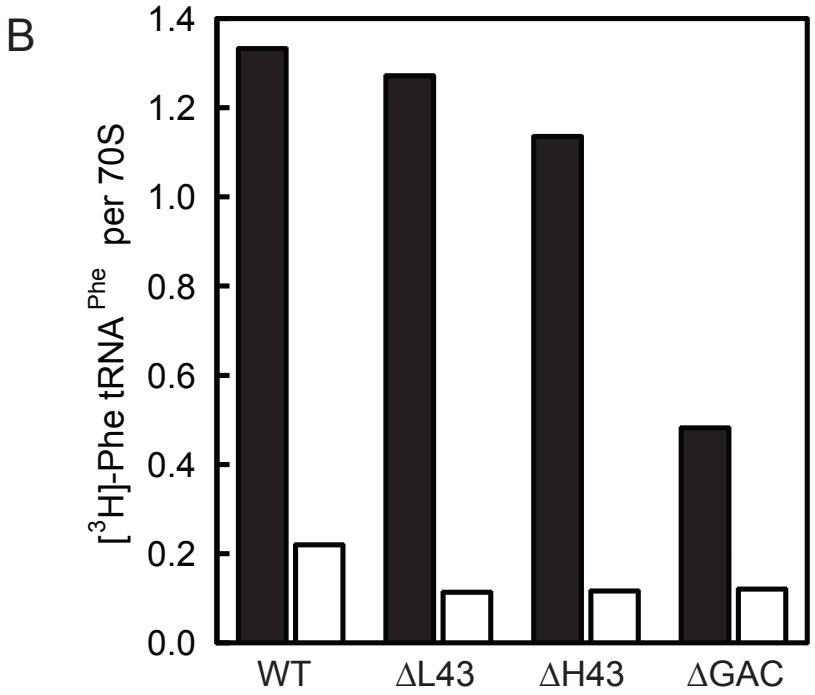
B
1.4
1.2
1.0
0.8
0.6
0.4
0.2
0.0
[3H]-Phe tRNAPhe per 70S
WT
ΔL43
ΔH43
ΔGAC

Figure 26. ΔH43 but not ΔGAC Ribosomes are active in GTPase idling and poly(Phe) Synthesis

(A) GTPase idling reaction with 0.25 μM EF-G, 20 μM [32P]-GTP and 0.2 μM WT (○, left axis), ΔL43 (△), ΔH43 (▽), and ΔGAC (□) ribosomes (stalk mutants right axis) The data points for ΔH43 and ΔGAC ribosomes overlay upon one another. Time course of *in vitro* translation of poly(U) mRNA into poly(Phe) peptides. WT (B) but not ΔH43 (C) ribosomes are inhibited by 10 μM thiostrepton (filled symbols). Synthesis by ΔGAC (D) ribosomes was undetectable.

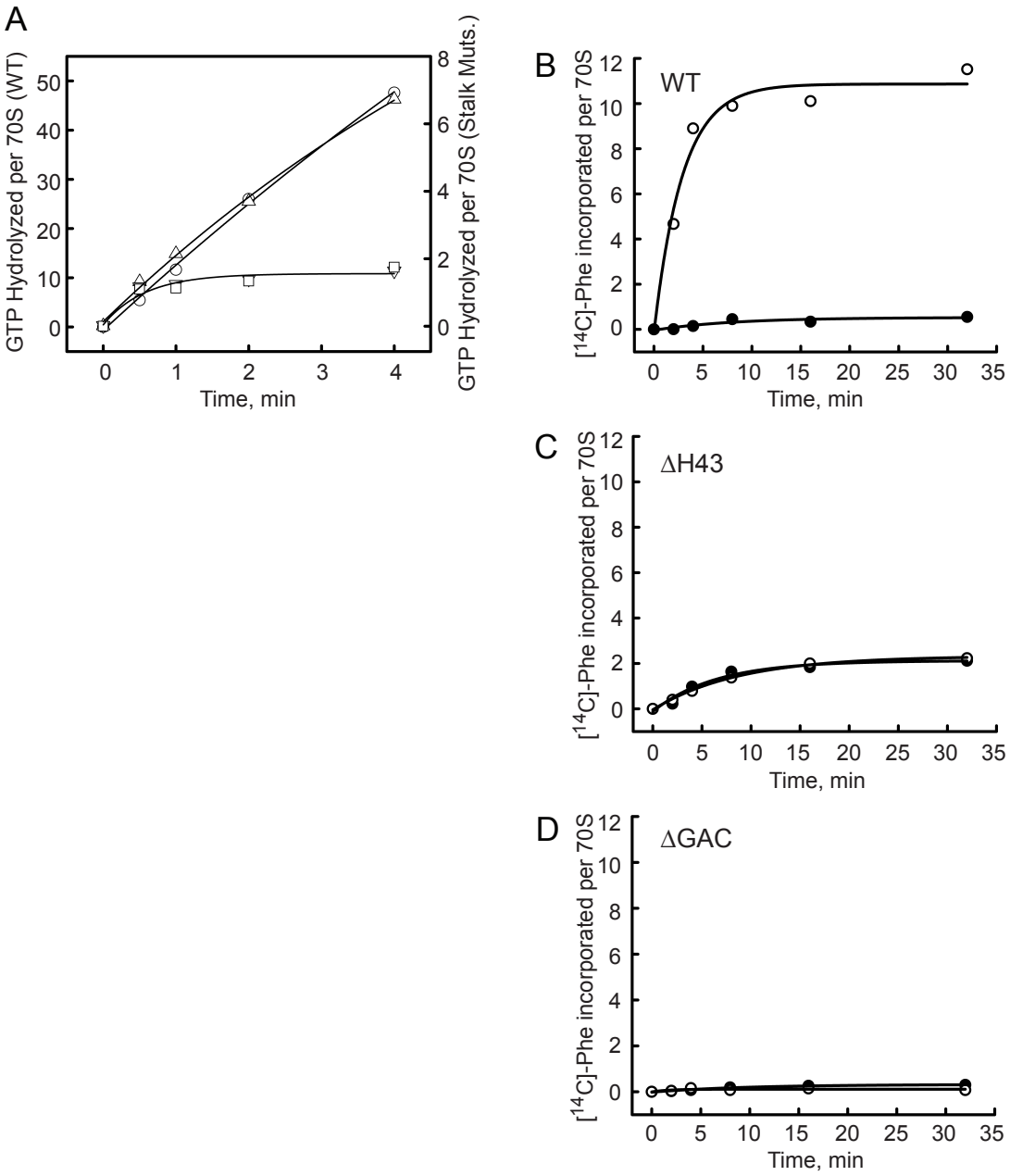
A
GTP Hydrolyzed per 70S (WT)
GTP Hydrolyzed per 70S (Stalk Muts.)
Time, min
B
WT
[14C]-Phe incorporated per 70S
Time, min
C
ΔH43
[14C]-Phe incorporated per 70S
Time, min
D
ΔGAC
[14C]-Phe incorporated per 70S
Time, min

DISCUSSION

Two additional mutations within the L11 stalk of the 50S ribosomal subunit have been characterized in the EF-Tu- and EF-G-dependent reactions of protein synthesis. The *in vivo* expression of ΔH43 or ΔGAC 23S rRNAs by *E. coli* resulted in dominant-lethal phenotypes (Figure 23D). Affinity-purified mutant subunits were depleted of ribosomal proteins (Figure 24B-C) known to bind to nucleotides within the L11 stalk rRNA that were removed by the GAAA tetraloop substitutions (Figure 23B-C). Additionally, ΔGAC ribosomes were missing protein L16 (Figure 24C). ΔH43 and ΔGAC ribosomes were active in P- and A-site tRNA binding (Figure 25A-B). ΔH43 and ΔGAC ribosomes support limited EF-G-dependent GTP hydrolysis (Figure 25A), but only ΔH43 ribosomes were active in poly(Phe) synthesis (Figure 25B).

Inactivation of ΔH43 ribosomes by dissociation of L10

Ribosomal proteins L10 and the L7/12 complex are required for the EF-G-dependent reactions of protein synthesis. The strict requirement for L10 is likely two-fold. First, L10 binds to the three-way junction of H42, H43, and H44 within the L11 stalk and stabilizes the folding of the L11 rRNA (Iben et al.

2008). Secondly, L10 forms the entire binding site for the L7/12 complex (Diaconu et al. 2005), which controls the release of inorganic phosphate following EF-G-dependent GTP hydrolysis (Mohr et al. 2002; Savelsbergh et al. 2005; Wahl et al. 2002). ΔH43 ribosomes are partially depleted of proteins L10 and L7/12 (Figure 24B). The depletion of L10 may be explained by the proximity of the L10 binding site to the H43 truncation. Therefore, the loss of L7/12 is a direct result of L10 depletion (Figure 23B). ΔH43 ribosomes were partially active in poly(Phe) synthesis, indicating that only ΔH43 ribosomes containing both L10 and L7/12 are active.

GTPase idling and translation elongation are unrelated reactions

The GTPase idling reaction is treated as the standard benchmark assay for interaction between EF-G and the ribosome. It is assumed that ribosomes defective in GTPase idling should be similarly impaired in their interaction with EF-G during the translocation reaction of the elongation cycle. ΔH43 and ΔGAC ribosomes are impaired approximately 50-fold in GTPase idling compared to wild-type ribosomes (Figure 26A). The results were consistent with approximately 2 rounds of GTP hydrolysis per ribosome. It is difficult to rationalize why these ribosomes would support only 2 rounds of hydrolysis. It is likely that errors in the concentration of GTP lead to a slight

overestimation of hydrolysis activity. Therefore, it is possible that ΔH43 and ΔGAC ribosomes support a single round of hydrolysis and are defective in the release of EF-G•GDP.

Surprisingly, ΔH43 ribosomes support poly(Phe) synthesis with only a 5-fold defect compared to wild-type ribosomes (Figure 26B). This activity was not inhibited by 10 μM thiostrepton, which rules out the possibility of contamination by wild-type ribosomes. This finding provides the first evidence that the reaction pathway by which EF-G•GTP interacts with vacant ribosomes is fundamentally different from that occurring between EF-G•GTP and ribosomes engaged in protein synthesis.

There are three fundamental differences between GTPase idling and translocation reactions: presence of peptidyl-A- and deacyl-P-site tRNAs on the ribosome, coupling of GTP hydrolysis to translocation, and conformational changes in the ribosomal subunits and EF-G related to translocation. Any one of these in isolation or in combination may be sufficient to explain the gained ability for ΔH43 ribosomes to release EF-G•GDP following translocation. Although EF-G does not directly interact with P-site tRNA, the presence of a deacylated-tRNA in the P site stimulates the idling reaction by approximately 2-fold. Stimulation is likely due to rotation of the 30S subunit to a conformation favoring the binding of EF-G due to the P-site tRNA assuming the hybrid P/E conformation (Ermolenko et al. 2007). The coupling of GTP hydrolysis to

conformational changes in EF-G and the ribosome coinciding with translocation may be sufficient to mechanically propel EF-G•GDP from the ribosome.

Is the L11 stalk required for the release of EF-G following translocation?

The contribution of the entire L11 stalk and its associated proteins in the process of translation has been learned from analysis of ΔGAC ribosomes. This mutant subunits support the non-enzymatic binding of P-site tRNA and EF-Tu-dependent binding of A-site aa-tRNA (Figure 25). Activity in A-site tRNA binding indicates that ΔGAC ribosomes bind to EF-Tu ternary complex and stimulate the GTPase activity of EF-Tu, which is required for the release of the factor and tRNA accommodation. Although inactive in poly(Phe) synthesis, ΔGAC ribosomes do apparently support a single round EF-G-dependent GTP hydrolysis (Figure 26A).

A tertiary pathway between the L11 stalk and SRL mediated by L16

Protein L16 of the large ribosomal subunit is required for ribosomal activity. Ribosomes depleted of L16 by treatment with LiCl are impaired in the reactions of peptidyl transferase (Moore et al. 1975), peptidyl-tRNA hydrolysis

(Tate et al. 1983), and EF-Tu-independent binding of aa-tRNA (Kazemie 1976). The role of L16 in these reactions is attributed to a large conformational change in 23S rRNA induced by binding of the protein, indicating that L16 is required for the architectural arrangement of the large ribosomal subunit (Teraoka et al. 1978).

L16 binds to 23S rRNA between the L11 stalk and the SRL, the two components of the GAC of the large ribosomal subunit. Domains II, V, and IV of 23S rRNA fold into two separate layers that constitute the L16 binding site (Lancaster et al. 2008; Schuwirth et al. 2005). The front layer is composed of 23S rRNA domains V and VI and encompasses the peptidyl transferase center and the SRL. The back layer is constructed from domains II, V, and VI, and includes H42 of the L11 stalk. The two layers are connected to one another through rRNA tertiary interactions that are likely stabilized by the presence of L16 (Lancaster et al. 2008). Therefore, L16 binds to a central region of 23S rRNA that directly connects the two components of the GAC.

The assembly of L16 onto the 50S subunit is disrupted by mutation of the L11 stalk or the SRL. *In vivo* assembled and affinity-purified ΔGAC 50S subunits showed a clear absence of L10, L11, and the L7/12 complex, as well as L16 (Figure 24C). Absence of L10, L11, and the L7/12 complex is easily explained by the total removal of their 23S rRNA binding sites (Figure 23A). However, the closest approach between L16 and the site of the ΔGAC

mutation is 25Å, and the distance is greater between the L16 binding site and the ΔGAC mutation. Therefore, the loss of L16 must be an indirect effect of the ΔGAC mutation.

H42 at the base of the L11 stalk is indirectly connected to the L16 binding site through tertiary interactions with H97 and protein L6 (Schuwirth et al. 2005). The specific interactions change depending on the position of the L11 stalk relative to the body of the 50S subunit (Table 3). Tertiary rRNA interactions between H42 and H97 are distributed between 23S rRNA nucleotides G2751 and C2752 of H97 and C1049, A1050, G1051, and C1052 of H42, of which the latter are absent in the ΔGAC mutant. Contacts were also identified between nucleotides A1048, A1111, G1112, and U1113 and protein L6. The L11 stalk is therefore directly linked to H97 and protein L6, and indirectly linked to the L16 binding site, which is in turn indirectly linked to the SRL. These tertiary interactions are functional, as demonstrated by mutagenesis (Miyoshi et al. 2008) and their disruption is sufficient to destabilize the L16 binding site, indicating that the ribosome maintains a delicate interaction between the L11 stalk and the SRL, which is mediated through the L16 binding site.

These findings with ΔGAC ribosomes are similar to those of mutant ribosomes in which the SRL was replaced with a GAAA tetraloop (ΔSRL), which were also found to lack L16 (Lancaster et al. 2008). This result was

attributed to disruption of tertiary contacts formed between the SRL and H91, which indirectly connects the SRL to the L16 binding site. These results indicate that the L16 binding site may be disrupted from either the SRL containing front layer, or the L11 stalk containing back layer. Therefore, L16 is positioned between two important components of the 50S subunit GAC and may be involved in communications between the L11 stalk and the SRL.

Changes in base reactivity for ΔSRL ribosomes attributed to loss of L16 were similar to another ribosomal mutant in which a G-C base pair was inserted into H42 at positions 1030 and 1124 (InsC1030/G1124) (Lancaster et al. 2008; Sergiev et al. 2005). The expression of InsC1030/G1124 ribosomes was lethal and streptavidin affinity-purified mutant ribosomes were defective in EF-G-dependent translocation but not EF-Tu dependent aa-tRNA binding (Sergiev et al. 2005). Inferring from the high degree of overlap in base reactivity changes resulting from the ΔSRL and InsC1030/G1124 mutations, it is likely that InsC1030/G1124 ribosomes are also lacking protein L16 (Lancaster et al. 2008). However, the authors of that work did not report on the protein content of their mutant ribosomes (Sergiev et al. 2005).

The InsC1030/G1124 mutation shifts the location and orientation of nucleotides C1049, A1050, and G1051, disrupting their ability to form tertiary interactions with H97. This base pair insertion is predicted to cause a 3.3 Å displacement along the H42 axis and a 33˚ rotation initiating at the site of

insertion. The displacement and rotation occur at the base of H42 and would therefore affect the H42 nucleotides involved in forming tertiary interactions with H97. We may therefore predict that the phenotype of InsC1030/G1124 ribosomes and the reported disruption of nucleotides composing the L16 binding site by Sergiev et al (2005) are due indirectly to altered rRNA tertiary contacts that support folding of 23S rRNA and are not caused by altered interactions between mutant ribosome and EF-G as predicted by the authors of that work.

Table 3. Tertiary Interactions Between H42 and H97, and H42 and L6

Frequency of hydrogen-bonding pairs between 23S rRNA H42 of the L11 stalk and 23S rRNA H97 or between H42 and protein L6. Avg = Average frequency of hydrogen-bond pair per ribosome structure. Avg # H-bonds per rbs = average total number of hydrogen-bonds between H42 and H97 and H42 and L6 per ribosomes. Five ribosome structures were analyzed for each position of the L11 stalk. PDB accession codes: DISTAL (2AWB, 1VSA, 3I9E, 3I8F, 2QAO), MEDIAL (3SGF, 1YL3, 3D5B, 2HGQ, 2WRJ), PROXIMAL (2WRO, 2XQE, 2Y11, 2Y0V, 2Y0Z). Hydrogen-bonding pairs were determined in Pymol (Delano Scientific).

Table 3. Tertiary Interactions Between H42 and H97, and H42 and L6

DISTAL				MEDIAL				PROXIMAL			
Avg	H42		H97	Avg	H42		H97	Avg	H42		H97
2.0	C1049	-	G2751	2.2	C1049	-	G2751	0.6	C1049	-	G2751
0.6	A1050	-	G2751	1.0	G1051	-	C2752	0.6	G1051	-	C2752
0.6	A1050	-	C2752	0.6	A1050	-	G2751	0.4	A1050	-	G2751
0.4	G1051	-	C2752	0.2	A1050	-	C2752	0.2	A1050	-	C2752
0.2	G1051	-	G2751	0.2	G1051	-	G2751	0.2	C1052	-	C2752
0.2	C1109	-	G2751								
0.4	G1112	-	L6	0.2	U1113	-	L6				
0.4	U1113	-	L6								
0.2	A1048	-	L6								
0.2	A1111	-	L6								
Average # H-bonds per rbs = 5.2				Average # H-bonds per rbs = 4.4				Average # H-bonds per rbs = 2.0			

METHODS

Construction and affinity purification of ΔH43 and ΔGAC ribosomes

The 23S rRNA mutations were generated by site-directed mutagenesis (Kunkel 1985) of plasmid pLK35.50S.MS2 as described in CHAPTER III using mutagenic oligos:

ΔH43, 23S rRNA nucleotides 1060-1078 → GAAA

5’

GAAGGCCCAGACAGCCAGGATG**GAAA**CATTTAAAGAAAGCGTAATAGCT

ΔGAC, 23S rRNA nucleotides 1043-1112 → GAAA

5’

AAGTGGGAAACGATGTGGGAAGGC**GAAA**GTCGGCCTGCGCGGAAGATG

TA

MS2-tagged ribosomes were expressed in *E. coli* and affinity-purified on GST-sepharose essentially as described in CHAPTER III.

50S ribosomal proteins were analyzed by two-dimensional gel electrophoresis as described in CHAPTER III.

For P-site binding 17.5 pmoles of 30S and 17.5 pmoles of 50S ribosomal subunits were associated and combined with 25 pmoles of m36g32

mRNA and 25 pmoles of N-Ac-[14C]-Phe-tRNAPhe in 50 mM Tris-Hcl (pH 7.5), 100 mM NH4Cl, 20 mM MgCl2, 5 mM ß-ME and incubated at 37˚ for 20 min. Samples were split into two even portions and reacted with puromycin (1 mM final) or spotted onto a Whatman filter and washed 3X with 5 mL of the same buffer. Filters were dried and placed into scintillation fluid and counted.

For A-site binding 20 pmoles of 30S and 30 pmoles of 50S ribosomal subunits were associated and combined with 40 pmole m291 mRNA and 50 pmoles of tRNAfMet. Samples were split into portions containing 7 pmoles of 70S and combined with 7 pmoles of [3H]-Phe-tRNAPhe in buffer containing 20 mM MgCl2, or diluted with Mg2+ free buffer to a final concentration of 7 mM Mg2+ and combined with 7 pmoles [3H]-Phe-tRNAPhe ternary complex. Ternary complex was prepared by incubating 70 pmoles of affinity-purified EF-Tu (provided by L. Lancaster) with 1 mM GTP, 5 mM PEP, and 20 mg/mL pyruvate kinase in 50 mM Tris-Hcl (pH 7.5), 100 mM NH4Cl, 7 mM MgCl2, 1 mM DTT at 37˚C for 15 min. To this mix 35 pmoles of [3H]-Phe-tRNAPhe was added and incubated for an additional 5 min. Samples were incubated at 37˚C for 5 min and then transferred to ice. Filter-binding was performed as above. GTPase idling and stopped-flow translocation assays were performed as in CHAPTER III.

APPENDICES

APPENDIX A: Database of Ribosome X-ray Diffraction Structures

The Database of Ribosome X-ray Diffraction Structures (DXDS) includes currently available X-ray diffraction structures of 30S, 50S, and 70S ribosomes.

DXDS is provided electronically (Excel, Microsoft Office) on the DVD accompanying this work.

Database of Ribosome X-ray Diffraction Structures

50S and 30S PDB entries (protein databank, www.pdb.org). Author, first author of reference work; Year, publication year; Source, organism from which ribosomes are derived; Subunits, 30S and 50S subunits or 70S ribosomes numbered according to reference; Space Group, crystal space group of diffracting crystal; Res, structure resolution in Å; tRNA, bound tRNA ligands; Factors/Antibiotics, identify of bound factors and antibiotics.

Abbreviations used, Source: Tth = T. thermophilus, Eco = E. coli, Dra = D. radiodurans, Sce = S. cerevisiae.

tRNA: fMet = tRNAfMet, Phe = tRNAPhe, Gln = tRNAGln, aa-Phe = Phe-tRNAPhe, Phe-NH = Phe-NH-tRNAPhe, ASL = anticodon stem-loop.

Antibiotics: Neo = neomycin, Gent = gentamycin, Paro = paromomycin, Micro = micrococcin, Nosi = nosiheptide, Thio = thiostrepton, Kirro = kirromycin, Vio = viomycin, Capr = capreomycin.

Other: TC = ternary complex.

Database of Ribosome X-ray Diffraction Structures

#	50S PBD	30S PDB	Author	Year	Source	Subunits	Space Group	Res (Å)	tRNA	Factors / Antibiotics
1	1GIY	1GIX	Yusupov, M.M.	2001	Tth	70S	I 422	5.5	A, P, E	
2	1YL3	1YL4	Jenner, L.B.	2005	Tth	70S	I 422	5.5	A, P: fMet	
3	2B9N	2B9M	Petry, S.	2005	Tth	70S	P 4_32_12	6.76	P: Phe	RF1, Post-hydrolysis
4	2B9P	2B9O	Petry, S.	2005	Tth	70S	P 4_32_12	6.46	P: Phe	
5	2B66	2B64	Petry, S.	2005	Tth	70S	P 4_32_12	5.9	P: Phe	RF1, Post-hydrolysis
6	2AW4	2AVY	Schuwirth, B.S.	2005	Eco	70S 1	P 4_32_12	3.5	Vacant	
7	2AWB	2AW7	Schuwirth, B.S.	2005	Eco	70S 2	P 4_32_12	3.5	Vacant	
8	1VSA	2OW8	Korostelev, A.	2006	Tth	70S	I 422	3.7	P: Phe, E	
9	2HGQ	2HGP	Yusupova, G.	2006	Tth	70S	I 422	5.5		
10	2HGJ	2HGI	Yusupova, G.	2006	Tth	70S	I 422	5	A: Phe, P: Phe	
11	2HGU	2HGR	Yusupova, G.	2006	Tth	70S	I 422	4.51	P, fMet, E, Phe	
12	2QBE	2QBD	Borovinskaya, M.A.	2007	Eco	70S (rbs I)	P $2_12_12_1$	3.3		RRF Split
13	2QAM	2QAL	Borovinskaya, M.A.	2007	Eco	70S (rbs I)	P $2_12_12_1$	3.21		Neo

#	50S PBD	30S PDB	Author	Year	Source	Subunits	Space Group	Res (Å)	tRNA	Factors / Antibiotics
14	2QBA	2QB9	Borovinskaya, M.A.	2007	Eco	70S (rbs I)	P $2_12_12_1$	3.54		Gent
15	2QBI	2QBH	Borovinskaya, M.A.	2007	Eco	70S (rbs I)	P $2_12_12_1$	4		RRF / Gent
16	2Z4L	2Z4K	Borovinskaya, M.A.	2007	Eco	70S (rbs I)	P $2_12_12_1$	4.45		RRF / Paro
17	2QBG	2QBF	Borovinskaya, M.A.	2007	Eco	70S (rbs II)	P $2_12_12_1$	3.3		RRF Unsplit
18	2QAO	2QAN	Borovinskaya, M.A.	2007	Eco	70S (rbs II)	P $2_12_12_1$	3.21		Neo
19	2QBC	2QBB	Borovinskaya, M.A.	2007	Eco	70S (rbs II)	P $2_12_12_1$	3.54		Gent
20	2QBK	2QBJ	Borovinskaya, M.A.	2007	Eco	70S (rbs II)	P $2_12_12_1$	4		RRF / Gent
21	2Z4N	2Z4M	Borovinskaya, M.A.	2007	Eco	70S (rbs II)	P $2_12_12_1$	4.45		RRF / Paro
22	2V47	2V46	Weixlbaumer, A.	2007	Tth	70S 1	P $2_12_12_1$	3.5	A: fMet, P: ASL-Phe	
23	2V49	2V48	Weixlbaumer, A.	2007	Tth	70S 2	P $2_12_12_1$	3.5	A: fMet, P: ASL-Phe	RRF
24	2ZJQ	-	Harms, J.M.	2008	Dra	50S	I 222	3.3		Micro

#	50S PBD	30S PDB	Author	Year	Source	Subunits	Space Group	Res (Å)	tRNA	Factors / Antibiotics
25	2ZJP	-	Harms, J.M.	2008	Dra	50S	I 222	3.7		Nosi
26	3CF5	-	Harms, J.M.	2008	Dra	50S	I 222	3.3		Thio
27	2ZJR	-	Harms, J.M.	2008	Dra	50S	I 222	2.91		Vacant
28	2ZJP	-	Harms, J.M.	2008	Dra	50S	I 222	3.7		Nosi
29	2ZJR	-	Harms, J.M.	2008	Dra	50S	I 222	2.91		Vacant
30	3CF5	-	Harms, J.M.	2008	Dra	50S	I 222	3.3		Thiostrepton
31	3F1F	3F1E	Korostelev, A.	2008	Tth	70S 1	$P\ 2_12_12_1$	3	P: fMet	RF2, Post-hydrolysis
32	3F1H	3F1G	Korostelev, A.	2008	Tth	70S 2	$P\ 2_12_12_1$	3	P: fMet	RF2, Post-hydrolysis
33	3D5B	3D5A	Laurberg, M.	2008	Tth	70S 1	$P\ 2_12_12_1$	3.2	P: fMet, E: fMet	RF1, Post-hydrolysis
34	3D5D	3D5C	Laurberg, M.	2008	Tth	70S 2	$P\ 2_12_12_1$	3.21	P: fMet, E: fMet	RF1, Post-hydrolysis
35	2WH2	2WH1	Weixlbaumer, A.	2008	Tth	70S 1	$P\ 2_12_12_1$	3.45	P: Phe, E: Phe	RF2, Post-hydrolysis
36	2WH4	2WH3	Weixlbaumer, A.	2008	Tth	70S 2	$P\ 2_12_12_1$	3.45	P: Phe, E: Phe	RF2, Post-hydrolysis
37	3HUX	3HUW	Blaha, G.	2009	Tth	70S 1	$P\ 2_12_12_1$	3.1	P: fMet	EF-P

#	50S PBD	30S PDB	Author	Year	Source	Subunits	Space Group	Res (Å)	tRNA	Factors / Antibiotics
38	3HUZ	3HUY	Blaha, G.	2009	Tth	70S 2	P 2_1	3.1	P: fMet	EF-P
39	2WRJ	2WRI	Gao, Y.-G.	2009	Tth	70S 1	P 2_1	3.6	P: fMet, E: fMet	EF-G·GDP/FA
40	2WRL	2WRK	Gao, Y.-G.	2009	Tth	70S 2	P 2_1	3.6	P: fMet, E: fMet	EF-G·GDP/FA
41	2WRO	2WRN	Schmeing, T.M.	2009	Tth	70S 1	P 2_1	3.6	P: Phe, A/T: Thr	TC:Cognate·GDP/ Kirro
42	2WRR	2QRQ	Schmeing, T.M.	2009	Tth	70S 2	P 2_1	3.6	P: Phe, A/T: Thr	TC:Cognate·GDP/ Kirro
44	2WDL	2WDK	Voorhees, R.M.	2009	Tth	70S 1	P $2_12_12_1$	3.5	A: aa-Phe, P: aa-Phe, E	Paro
45	2WDI	2WDG	Voorhees, R.M.	2009	Tth	70S 1	P $2_12_12_1$	3.3	A: aa-Phe, P: aa-Phe, E	Paro
46	2WDN	2WDM	Voorhees, R.M.	2009	Tth	70S 2	P $2_12_12_1$	3.5	A: aa-Phe, P: aa-Phe, E	Paro
47	2WDJ	2WDH	Voorhees, R.M.	2009	Tth	70S 2	P $2_12_12_1$	3.3	A: aa-Phe, P: fMet, E	Paro
48	3I1P	3I1O	Zhang, W.	2009	Eco	70S 1	P $2_12_12_1$	3.19	Vacant	
49	3I1R	3I1Q	Zhang, W.	2009	Eco	70S 1	P $2_12_12_1$	3.81	P: ASL-fMet	
50	3i20	3i1z	Zhang, W.	2009	Eco	70S 1	P $2_12_12_1$	3.71	A: ASL-Phe, P: ASL-Phe	
51	3I1N	3I1M	Zhang, W.	2009	Eco	70S 2	P $2_12_12_1$	3.19	Vacant	

#	50S PBD	30S PDB	Author	Year	Source	Subunits	Space Group	Res (Å)	tRNA	Factors / Antibiotics
52	3I1T	3I1S	Zhang, W.	2009	Eco	70S 2	P $2_12_12_1$	3.81	P: ASL-fMet	
53	3i22	3i21	Zhang, W.	2009	Eco	70S 2	P $2_12_12_1$	3.71	A: ASL-Phe, P: ASL-Phe	
54	3O58	3O2Z	Ben-Shem, A.	2010	Sce	80S 1	P 2_1	4	Vacant	
55	3O5H	3O30	Ben-Shem, A.	2010	Sce	80S 2	P 2_1	4	Vacant	
56	3I9E	3I9D	Jenner, L.B.	2010	Tth	70 A	P $2_12_12_1$	3.5	P: fMet, E: fMet	
57	3I8F	3I8G	Jenner, L.B.	2010	Tth	70 A	P $2_12_12_1$	3.1	A: Phe, P: Phe, E: Phe	
58	3I9C	3I9B	Jenner, L.B.	2010	Tth	70 B	P $2_12_12_1$	3.5	P: fMet, E: fMet	
59	3I8I	3I8H	Jenner, L.B.	2010	Tth	70 B	P $2_12_12_1$	3.1	A: Phe, P: Phe, E: Phe	
60	2X9S	2X9R	Jin, H.	2010	Tth	70S 1	P $2_12_12_1$	3.1	P: Phe-NH	RF2, Pre-hydrolysis
61	2X9U	2X9T	Jin, H.	2010	Tth	70S 2	P $2_12_12_1$	3.1	P: Phe-NH	RF2, Pre-hydrolysis
62	3KNI	3KNH	Stanley, R.E.	2010	Tth	70S 1	P $2_12_12_1$	3	A: Gln, P: Gln, E: Gln	Vio
63	3KNM	3KNL	Stanley, R.E.	2010	Tth	70S 1	P $2_12_12_1$	3.54	A: Gln, P: Gln, E: Gln	Capr

#	50S PBD	30S PDB	Author	Year	Source	Subunits	Space Group	Res (Å)	tRNA	Factors / Antibiotics
64	3KNK	3KNJ	Stanley, R.E.	2010	Tth	70S 2	$P\ 2_12_12_1$	3	A: Gln, P: Gln, E: Gln	Vio
65	3KNO	3KNN	Stanley, R.E.	2010	Tth	70S 2	$P\ 2_12_12_1$	3.54	A: Gln, P: Gln, E: Gln	Capr
66	2XQE	2XQD	Voorhees, R.M.	2010	Tth	70S	$P\ 2_1$	3.1		TC: Cognate·GDPNP, Paro
67	3R8S	3R8N	Dunkle, J.A.	2011	Eco	70S	$P\ 2_12_12_1$	3	P/E hybid: Phe	RRF
68	3R8T	3R8O	Dunkle, J.A.	2011	Eco	70S	$P\ 2_12_12_1$	3	P: Phe	
69	3ZVP	3ZVO	Jin, H.	2011	Tth	70S	$P\ 2_1$	3.8	P	RF3
70	2Y0V	2Y0U	Schmeing, T.M.	2011	Tth	70S 1	$P\ 2_1$	3.1	A/T: A9C-Trp	TC: Near Cognate-A9C·GDP/Kirro
71	2Y0Z	2Y12	Schmeing, T.M.	2011	Tth	70S 1	$P\ 2_1$	3.1	A/T: G24A-Trp	TC:Near cognate-G24A·GTP/Kirro
72	2Y11	2Y10	Schmeing, T.M.	2011	Tth	70S 1	$P\ 2_1$	3.1	A/T: Trp	TC:Cognate·GTP/ Kirro
73	2Y0X	2Y0W	Schmeing, T.M.	2011	Tth	70S 2	$P\ 2_1$	3.1	A/T: A9C-Trp	TC:Near Cognate-A9C·GDP/Kirro
74	2Y13	2Y12	Schmeing, T.M.	2011	Tth	70S 2	$P\ 2_1$	3.1	A/T: G24A-Trp	TC:Near cognate-G24A·GTP/Kirro

#	50S PBD	30S PDB	Author	Year	Source	Subunits	Space Group	Res (Å)	tRNA	Factors / Antibiotics
75	2Y19	2Y18	Schmeing, T.M.	2011	Tth	70S 2	P 2_1	3.1	A/T: Trp	TC: Cognate·GTP/ Kirro
76	3SGF	3SFS	Zhou, J.	2011	Tth	70S	P $2_12_12_1$	3.2		RF3·GDPNP, Vio
77	3UOS	3UOQ	Zhou, J.	2011	Tth	70S	P $2_12_12_1$	3.7		RF3·GDPNP

APPENDIX B: Depository of Aligned Ribosome Structures (D-ARS)

The Depository of Aligned Ribosome Structures (D-ARS) was developed to facilitate rapid and simultaneous manual comparison and computational analysis of multiple ribosome X-ray diffraction structures. D-ARS consists of two components: the alignment protocol (I) and the depository of structure files (.pdb) processed according to the alignment protocol (II). The alignment protocol was developed to process 30S and 50S ribosome structures into a single coordinate space. The structural alignment is based on the body 23S rRNA and excludes proteins and the flexible L1 and L11 stalks (*E. coli* 23S rRNA nucleotides 2094-2194 and 1031-1124, respectively). When a 30S ribosome is present in the reference, its coordinates are locked to those of the respective 50S subunit, thereby maintaining their exact geometries.

D-ARS is based on the PyMol platform (Delano Scientific). At present the database does not include all available 50S and 70S ribosome structures or structures of isolated 30S subunits. Aberrations exist within most .pdb files; secondary alignments are recommended.

I. Alignment Protocol

Alignments are made into the coordinate space of Korostelev et al (2006) 1VSA.pdb.

structure = 50S or 70S .pdb coordinate file. 70S ribosomes are generally deposited as separate .pdb files containing the 30S and 50S subunits.

structure.core = the 23S rRNA of *structure*, excluding the L1 and L11 stalks, nucleotides 2094-2194 and 1031-1124, respectively

1VSA = 1VSA.pdb

Step 1: Load *structure* and 1VSA .pdb files into PyMol

Step 2: For isolated 50S ribosome structures align the entire 50S ribosome to 1VSA based on coordinates of *structure.core*. For 70S ribosomes proceed to step 3.

Step 3: 70S ribosomes. An object will be made to serve as an alignment guide for positioning of the 30S subunit (Step). It contains three proteins from the 50S subunit (chains G, R, and 2) and three proteins from the 30S subunit (chains T, J, and F). Create the object GR2-TFJ from *structure* 50S chains G, R, and 2 and 30S chains T, F, and J.

Step 4: Align *structure.core* to 1VSA

Step 5: Align GR2-TFJ to *structure* chains G, R, and 2

Step 5: Align 30S chains T, F, and J to GR2-TFJ

Step 6: Save as structure_aligned.pdb

Example:

load 1vsa.pdb, 1vsa

load 2awb.pdb, *50S*

load 2aw7.pdb, *30S*

create GR2-TFJ, *50S* and chain G+R+2 + 30S and chain T+F+J

align 50S and chain A and not (resid 2094-2195+1031-1123), 1VSA

align GR2-TFJ and chain G+R+2, 50S and chain G+R+2

align 30S and chain T+F+J, GR2-TFJ and chain T+F+J

save 2awb_aligned.pdb, 50S

save 2aw7_aligned.pdb, 30S

II. D-ARS

D-ARS is provided electronically on the DVD accompanying this work.

APPENDIX C: Primer extension analysis of MS2-50S subunits

MS2-tagged 50S ribosomal subunits were analyzed by primer extension as described in Lancaster et al. (2008). Sample lanes are indicated at the top of the figure and the position of wild-type and MS2-tagged 50S ribosomal subunits is indicated on the right. ΔGAC ribosomes were analyzed in the same manner, however the data is unavailable.

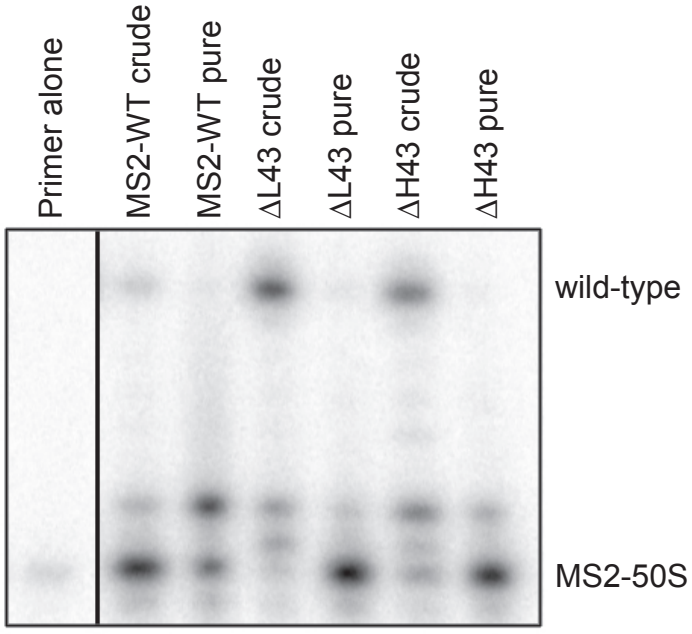

APPENDIX D: Comparison of EF-G Binding by Multiple Techniques

The binding of EF-G to ribosomes containing mutations within the L11 stalk has been studied by the techniques of ultracentrifugation (Chapter III, Figure 15B), ultrafiltration, and fluorescence quenching. Collectively, the results suggest that mutant ribosomes are capable of EF-G binding, however, that they do not support fluorescence quenching as observed for wild-type ribosomes. Below, I describe the results of two experiments and discuss potential interpretations of the results.

EF-G binding to mutant ribosomes was measured by the ultrafiltration of ribosome-EF-G complexes through a 100,000 Dalton molecular weight cutoff membrane (Amicon) in the presence or absence of GTP and fusidic acid. Retained material was resuspended and analyzed by SDS-PAGE (Panel A). Fusidic acid stalls EF-G•GDP on the ribosome by interfering with the release of inorganic phosphate. 70S ribosomes are too large to pass through the membrane, and the retained material was found to be similar to the input. Under the conditions utilized, EF-G freely passes through the membrane unless bound to ribosomes. A small amount of EF-G is retained when GTP and fusidic acid are omitted. This binding may or may not be specific in nature. ΔL43 and ΔGAC ribosomes retained approximately half as much EF-G•GDP/FA compared to wild-type ribosomes.

These results are similar to those presented in chapter III utilizing ultracentifugation of ribosome-EF-G complexes through a sucrose cushion. In that experiment, the binding of EF-G•GDPNP to ΔL43 ribosomes was very low compared to the binding observed with GTP and fusidic acid. This indicated that the complex of EF-G•GDP+P_i is stable on mutant ribosomes, and that the complex of EF-G•GDPNP is not.

The binding of EF-G•GDPNP to ΔL43, ΔH43 and ΔGAC ribosomes was investigated by fluorescence quenching as described in Lancaster et al. (2008) (Panel B). Briefly, a mutant of EF-G containing a fluorescein label at position 591 within domain IV was bound to ribosomes containing a short defined mRNA and $tRNA^{fMet}$ in the P site. Quenching of the fluorescein signal is indicative of EF-G binding, as observed for wild-type ribosomes, and occurred with a Kd of 26 nM. No quenching was detected when wild-type ribosomes were replaced with ΔL43, ΔH43 or ΔGAC ribosomes.

These results are challenging to interpret. Ultracentrifugation and fluorescence quenching techniques suggest that mutant ribosomes do not interact with EF-G in its GTP bound conformation. However, ΔL43 and ΔH43 ribosomes support EF-G-dependent GTP hydrolysis, poly(Phe) synthesis, and retain EF-G•GDP. How is it that EF-G binds to mutant ribosomes after GTP hydrolysis but not before? The lack of quenching observed for mutant ribosomes may be explained by an altered binding conformation of EF-

G•GDPNP on the ribosome. In this binding conformation the GTPase activity of EF-G is predicted to be active, however ribosomes are unable to stimulate conformational changes within the factor necessary to promote quenching of the label within domain IV. This would explain why some binding was detected by ultracentrifugation but not by the more sensitive fluorometry based approach.

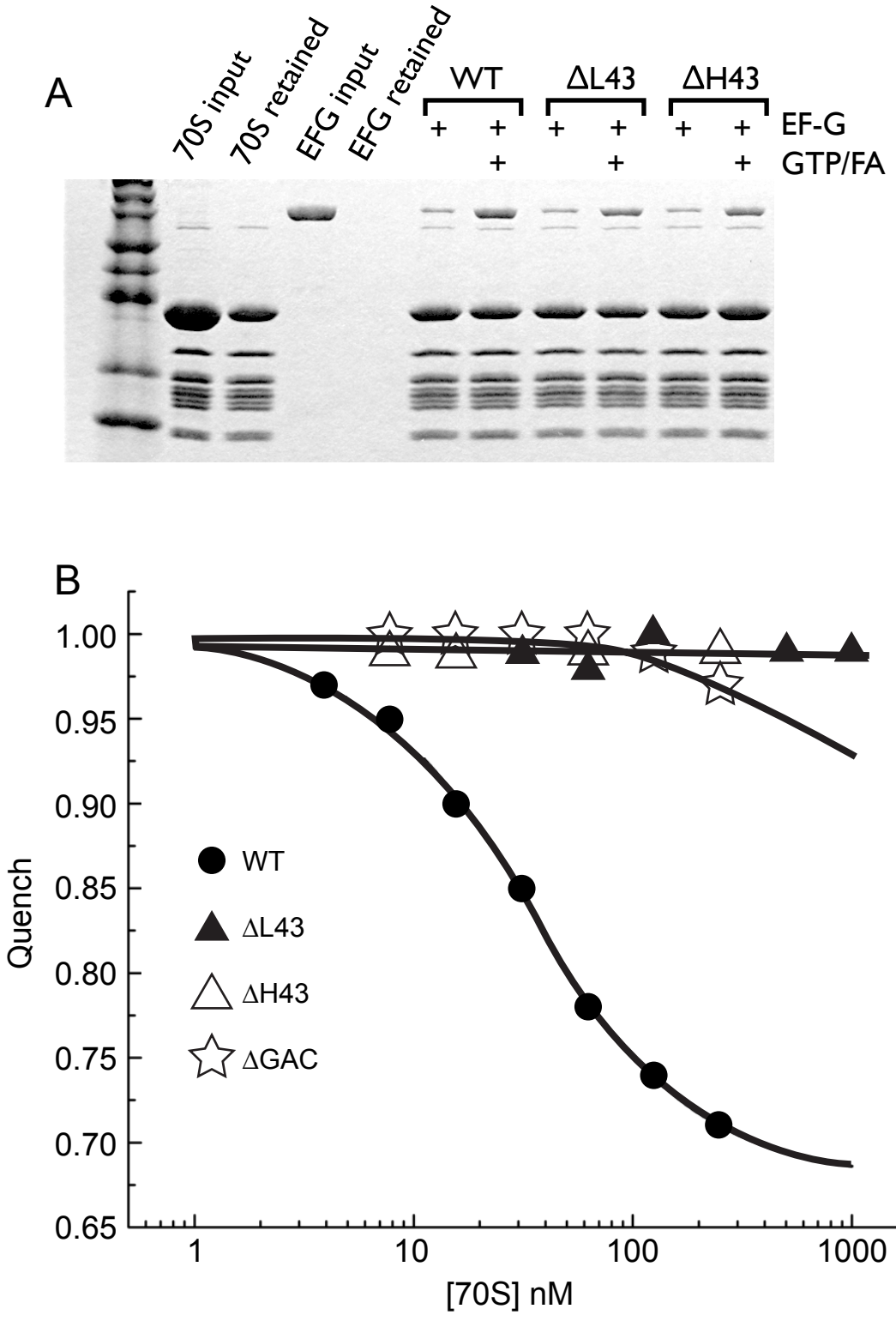
A
70S input
70S retained
EFG input
EFG retained
WT
ΔL43
ΔH43
EF-G
GTP/FA
B
Quench
1.00
0.95
0.90
0.85
0.80
0.75
0.70
0.65
WT
ΔL43
ΔH43
ΔGAC
1
10
100
1000
[70S] nM

REFERENCES

Agrawal, R.K., Heagle, A.B., Penczek, P., Grassucci, R.A. and Frank, J. 1999. EF-G-dependent GTP hydrolysis induces translocation accompanied by large conformational changes in the 70S ribosome. *Nature structural biology.* **6**: 643-7.

Agrawal, R.K., Linde, J., Sengupta, J., Nierhaus, K.H. and Frank, J. 2001. Localization of L11 protein on the ribosome and elucidation of its involvement in EF-G-dependent translocation. *J Mol Biol.* **311**: 777-87.

Ali, I.K., Lancaster, L., Feinberg, J., Joseph, S. and Noller, H.F. 2006. Deletion of a conserved, central ribosomal intersubunit RNA bridge. *Molecular cell.* **23**: 865-74.

Allen, G.S., Zavialov, A., Gursky, R., Ehrenberg, M. and Frank, J. 2005. The cryo-EM structure of a translation initiation complex from Escherichia coli. *Cell.* **121**: 703-12.

Allen, P.N. and Noller, H.F. 1991. A single base substitution in 16S ribosomal RNA suppresses streptomycin dependence and increases the frequency of translational errors. *Cell.* **66**: 141-8.

Allende, J.E., Monro, R. and Lipmann, F. 1964. Resolution of the E. Coli Amino Acyl Srna Transfer Factor into Two Complementary Fractions. *Proc Natl Acad Sci U S A.* **51**: 1211-6.

Andersson, D.I. and Kurland, C.G. 1983. Ram ribosomes are defective proofreaders. *Mol Gen Genet.* **191**: 378-81.

Antao, V.P. and Tinoco, I., Jr. 1992. Thermodynamic parameters for loop formation in RNA and DNA hairpin tetraloops. *Nucleic Acids Res.* **20**: 819-24.

Arai, N. and Kaziro, Y. 1974. Mechanism of the ribosome-dependent uncoupled GTPase reaction catalyzed by polypeptide chain elongation factor G. *J Biochem.* **2**: 439-47.

Bartetzko, A. and Nierhaus, K.H. 1988. Mg2+/NH4+/polyamine system for polyuridine-dependent polyphenylalanine synthesis with near in vivo characteristics. *Methods Enzymol.* **164**: 650-8.

Beauclerk, A.A., Hummel, H., Holmes, D.J., Bock, A. and Cundliffe, E. 1985. Studies of the GTPase domain of archaebacterial ribosomes. *Eur J Biochem.* **151**: 245-55.

Blyn, L.B., Risen, L.M., Griffey, R.H. and Draper, D.E. 2000. The RNA-binding domain of ribosomal protein L11 recognizes an rRNA tertiary structure stabilized by both thiostrepton and magnesium ion. *Nucleic Acids Res.* **28**: 1778-84.

Boon, K., Vijgenboom, E., Madsen, L.V., Talens, A., Kraal, B. and Bosch, L. 1992. Isolation and functional analysis of histidine-tagged elongation factor Tu. *Eur J Biochem.* **210**: 177-83.

Bouakaz, L., Bouakaz, E., Murgola, E.J., Ehrenberg, M. and Sanyal, S. 2006. The role of ribosomal protein L11 in class I release factor-mediated translation termination and translational accuracy. *J Biol Chem.* **281**: 4548-56.

Cannone, J.J., Subramanian, S., Schnare, M.N., Collett, J.R., D'Souza, L.M., Du, Y., Feng, B., Lin, N., Madabusi, L.V., Muller, K.M., Pande, N., Shang, Z., Yu, N. and Gutell, R.R. 2002. The comparative RNA web (CRW) site: an online database of comparative sequence and structure information for ribosomal, intron, and other RNAs. *BMC Bioinformatics.* **3**: 2.

Carter, A.P., Clemons, W.M., Brodersen, D.E., Morgan-Warren, R.J., Wimberly, B.T. and Ramakrishnan, V. 2000. Functional insights from the structure of the 30S ribosomal subunit and its interactions with antibiotics. *Nature.* **407**: 340-8.

Cate, J.H., Yusupov, M.M., Yusupova, G.Z., Earnest, T.N. and Noller, H.F. 1999. X-ray crystal structures of 70S ribosome functional complexes. *Science.* **285**: 2095-104.

Chan, Y.L., Correll, C.C. and Wool, I.G. 2004. The location and the significance of a cross-link between the sarcin/ricin domain of ribosomal RNA and the elongation factor-G. *J Mol Biol.* **337**: 263-72.

Claude, A. 1943. The Constitution of Protoplasm. *Science.* **97**: 451-6.

Clementi, N., Chirkova, A., Puffer, B., Micura, R. and Polacek, N. 2010. Atomic mutagenesis reveals A2660 of 23S ribosomal RNA as key to EF-G GTPase activation. *Nat Chem Biol.* **6**: 344-51.

Conn, G.L., Gutell, R.R. and Draper, D.E. 1998. A functional ribosomal RNA tertiary structure involves a base triple interaction. *Biochemistry.* **37**: 11980-8.

Conway, T.W. and Lipmann, F. 1964. Characterization of a Ribosome-Linked Guanosine Triphosphatase in Escherichia Coli Extracts. *Proc Natl Acad Sci U S A.* **52**: 1462-9.

Cornish, P.V., Ermolenko, D.N., Noller, H.F. and Ha, T. 2008. Spontaneous intersubunit rotation in single ribosomes. *Mol Cell.* **30**: 578-88.

Crick, F.H. 1958. On protein synthesis. *Symp Soc Exp Biol.* **12**: 138-63.

Czworkowski, J., Wang, J., Steitz, T.A. and Moore, P.B. 1994. The crystal structure of elongation factor G complexed with GDP, at 2.7 A resolution. *EMBO J.* **13**: 3661-8.

Darken, M.A. 1964. Puromycin Inhibition of Protein Synthesis. *Pharmacological reviews.* **16**: 223-43.

Diaconu, M., Kothe, U., Schlunzen, F., Fischer, N., Harms, J.M., Tonevitsky, A.G., Stark, H., Rodnina, M.V. and Wahl, M.C. 2005. Structural basis for the function of the ribosomal L7/12 stalk in factor binding and GTPase activation. *Cell.* **121**: 991-1004.

Egebjerg, J., Douthwaite, S. and Garrett, R.A. 1989. Antibiotic interactions at the GTPase-associated centre within Escherichia coli 23S rRNA. *EMBO J.* **8**: 607-11.

Endo, Y., Mitsui, K., Motizuki, M. and Tsurugi, K. 1987. The mechanism of action of ricin and related toxic lectins on eukaryotic ribosomes. The site and the characteristics of the modification in 28 S ribosomal RNA caused by the toxins. *J Biol Chem.* **262**: 5908-12.

Endo, Y. and Wool, I.G. 1982. The site of action of alpha-sarcin on eukaryotic ribosomes. The sequence at the alpha-sarcin cleavage site in 28 S ribosomal ribonucleic acid. *J Biol Chem.* **257**: 9054-60.

Ermolenko, D.N., Majumdar, Z.K., Hickerson, R.P., Spiegel, P.C., Clegg, R.M. and Noller, H.F. 2007. Observation of intersubunit movement of the ribosome in solution using FRET. *J Mol Biol.* **370**: 530-40.

Ermolenko, D.N. and Noller, H.F. 2011. mRNA translocation occurs during the second step of ribosomal intersubunit rotation. *Nat Struct Mol Biol.* **18**: 457-62.

Frank, J. and Agrawal, R.K. 2000. A ratchet-like inter-subunit reorganization of the ribosome during translocation. *Nature.* **406**: 318-22.

Frank, J., Sengupta, J., Gao, H., Li, W., Valle, M., Zavialov, A. and Ehrenberg, M. 2005. The role of tRNA as a molecular spring in decoding, accommodation, and peptidyl transfer. *FEBS Lett.* **579**: 959-62.

Fredrick, K. and Noller, H.F. 2003. Catalysis of ribosomal translocation by sparsomycin. *Science.* **300**: 1159-62.

Freistroffer, D.V., Pavlov, M.Y., MacDougall, J., Buckingham, R.H. and Ehrenberg, M. 1997. Release factor RF3 in E.coli accelerates the dissociation of release factors RF1 and RF2 from the ribosome in a GTP-dependent manner. *EMBO J.* **16**: 4126-33.

Gao, Y.G., Selmer, M., Dunham, C.M., Weixlbaumer, A., Kelley, A.C. and Ramakrishnan, V. 2009. The structure of the ribosome with elongation factor G trapped in the posttranslocational state. *Science.* **326**: 694-9.

Gavrilova, L.P., Kostiashkina, O.E., Koteliansky, V.E., Rutkevitch, N.M. and Spirin, A.S. 1976. Factor-free ("non-enzymic") and factor-dependent systems of translation of polyuridylic acid by Escherichia coli ribosomes. *J Mol Biol.* **101**: 537-52.

Gilbert, W. 1963. Polypeptide synthesis in Escherichia coli. II. The polypeptide chain and S-RNA. *Journal of molecular biology.* **6**: 389-403.

Gonzalez, R.L., Jr., Chu, S. and Puglisi, J.D. 2007. Thiostrepton inhibition of tRNA delivery to the ribosome. *RNA.* **13**: 2091-7.

Gromadski, K.B. and Rodnina, M.V. 2004. Kinetic determinants of high-fidelity tRNA discrimination on the ribosome. *Mol Cell.* **13**: 191-200.

Gutell, R.R., Schnare, M.N. and Gray, M.W. 1992. A compilation of large subunit (23S- and 23S-like) ribosomal RNA structures. *Nucleic acids research.* **20 Suppl**: 2095-109.

Hansson, S., Singh, R., Gudkov, A.T., Liljas, A. and Logan, D.T. 2005. Crystal structure of a mutant elongation factor G trapped with a GTP analogue. *FEBS Lett.* **579**: 4492-7.

Harms, J.M., Wilson, D.N., Schluenzen, F., Connell, S.R., Stachelhaus, T., Zaborowska, Z., Spahn, C.M. and Fucini, P. 2008. Translational regulation via L11: molecular switches on the ribosome turned on and off by thiostrepton and micrococcin. *Mol Cell.* **30**: 26-38.

Hausner, T.P., Atmadja, J. and Nierhaus, K.H. 1987. Evidence that the G2661 region of 23S rRNA is located at the ribosomal binding sites of both elongation factors. *Biochimie.* **69**: 911-23.

Iben, J.R. and Draper, D.E. 2008. Specific interactions of the L10(L12)4 ribosomal protein complex with mRNA, rRNA, and L11. *Biochemistry.* **47**: 2721-31.

Jenner, L.B., Demeshkina, N., Yusupova, G. and Yusupov, M. 2010. Structural aspects of messenger RNA reading frame maintenance by the ribosome. *Nat Struct Mol Biol.* **17**: 555-60.

Kavran, J.M. and Steitz, T.A. 2007. Structure of the base of the L7/L12 stalk of the Haloarcula marismortui large ribosomal subunit: analysis of L11 movements. *J Mol Biol.* **371**: 1047-59.

Kazemie, M. 1976. Binding of aminoacyl-tRNA to reconstituted subparticles of Escherichia coli large ribosomal subunits. *Eur J Biochem.* **67**: 373-8.

Keller, E.B. and Zamecnik, P.C. 1956. The effect of guanosine diphosphate and triphosphate on the incorporation of labeled amino acids into proteins. *J Biol Chem.* **221**: 45-59.

Kjeldgaard, M., Nissen, P., Thirup, S. and Nyborg, J. 1993. The crystal structure of elongation factor EF-Tu from Thermus aquaticus in the GTP conformation. *Structure.* **1**: 35-50.

Klaholz, B.P., Myasnikov, A.G. and Van Heel, M. 2004. Visualization of release factor 3 on the ribosome during termination of protein synthesis. *Nature.* **427**: 862-5.

Korostelev, A., Asahara, H., Lancaster, L., Laurberg, M., Hirschi, A., Zhu, J., Trakhanov, S., Scott, W.G. and Noller, H.F. 2008. Crystal structure of a

translation termination complex formed with release factor RF2. *Proc Natl Acad Sci U S A.* **105**: 19684-9.

Korostelev, A., Trakhanov, S., Laurberg, M. and Noller, H.F. 2006. Crystal structure of a 70S ribosome-tRNA complex reveals functional interactions and rearrangements. *Cell.* **126**: 1065-77.

Kunkel, T.A. 1985. Rapid and efficient site-specific mutagenesis without phenotypic selection. *Proceedings of the National Academy of Sciences of the United States of America.* **82**: 488-92.

Lancaster, L., Lambert, N.J., Maklan, E.J., Horan, L.H. and Noller, H.F. 2008. The sarcin-ricin loop of 23S rRNA is essential for assembly of the functional core of the 50S ribosomal subunit. *RNA.* **14**: 1999-2012.

Lancaster, L. and Noller, H.F. 2005. Involvement of 16S rRNA nucleotides G1338 and A1339 in discrimination of initiator tRNA. *Mol Cell.* **20**: 623-32.

Lee, D., Walsh, J.D., Yu, P., Markus, M.A., Choli-Papadopoulou, T., Schwieters, C.D., Krueger, S., Draper, D.E. and Wang, Y.X. 2007. The structure of free L11 and functional dynamics of L11 in free, L11-rRNA(58 nt) binary and L11-rRNA(58 nt)-thiostrepton ternary complexes. *J Mol Biol.* **367**: 1007-22.

Liljas, A. 1996. Imprinting through molecular mimicry. Protein synthesis. *Curr Biol.* **6**: 247-9.

Maden, B.E., Traut, R.R. and Monro, R.E. 1968. Ribosome-catalysed peptidyl transfer: the polyphenylalanine system. *Journal of molecular biology.* **35**: 333-45.

Matthaei, H. and Nirenberg, M.W. 1961. The dependence of cell-free protein synthesis in E. coli upon RNA prepared from ribosomes. *Biochem Biophys Res Commun.* **4**: 404-8.

Mazumder, R., Chae, Y.B. and Ochoa, S. 1969. Polypeptide chain initiation in E. coli: sulfhydryl groups and the function of initiation factor F2. *Proc Natl Acad Sci U S A.* **63**: 98-103.

Milligan, J.F., Groebe, D.R., Witherell, G.W. and Uhlenbeck, O.C. 1987. Oligoribonucleotide synthesis using T7 RNA polymerase and synthetic DNA templates. *Nucleic Acids Res.* **15**: 8783-98.

Miyoshi, T. and Uchiumi, T. 2008. Functional interaction between bases C1049 in domain II and G2751 in domain VI of 23S rRNA in Escherichia coli ribosomes. *Nucleic Acids Res.* **36**: 1783-91.

Moazed, D. and Noller, H.F. 1989. Interaction of tRNA with 23S rRNA in the ribosomal A, P, and E sites. *Cell.* **57**: 585-97.

Moazed, D. and Noller, H.F. 1989. Intermediate states in the movement of transfer RNA in the ribosome. *Nature.* **342**: 142-8.

Moazed, D., Robertson, J.M. and Noller, H.F. 1988. Interaction of elongation factors EF-G and EF-Tu with a conserved loop in 23S RNA. *Nature.* **334**: 362-4.

Mohr, D., Wintermeyer, W. and Rodnina, M.V. 2002. GTPase activation of elongation factors Tu and G on the ribosome. *Biochemistry.* **41**: 12520-8.

Monro, R.E., Celma, M.L. and Vazquez, D. 1969. Action of sparsomycin on ribosome-catalysed peptidyl transfer. *Nature.* **222**: 356-8.

Moore, P.B. 1999. Structural motifs in RNA. *Annu Rev Biochem.* **68**: 287-300.

Moore, V.G., Atchison, R.E., Thomas, G., Moran, M. and Noller, H.F. 1975. Identification of a ribosomal protein essential for peptidyl transferase activity. *Proc Natl Acad Sci U S A.* **72**: 844-8.

Morris, A.J. and Schweet, R.S. 1961. Release of soluble protein from reticulocyte ribosomes. *Biochimica et biophysica acta.* **47**: 415-6.

Munishkin, A. and Wool, I.G. 1997. The ribosome-in-pieces: binding of elongation factor EF-G to oligoribonucleotides that mimic the sarcin/ricin and thiostrepton domains of 23S ribosomal RNA. *Proc Natl Acad Sci U S A.* **94**: 12280-4.

Munro, J.B., Altman, R.B., Tung, C.S., Cate, J.H., Sanbonmatsu, K.Y. and Blanchard, S.C. 2010. Spontaneous formation of the unlocked state of the ribosome is a multistep process. *Proc Natl Acad Sci U S A.* **107**: 709-14.

Nathans, D. and Lipmann, F. 1961. Amino acid transfer from aminoacyl-ribonucleic acids to protein on ribosomes of Escherichia coli. *Proceedings of*

the National Academy of Sciences of the United States of America. **47**: 497-504.

Nirenberg, M., Leder, P., Bernfield, M., Brimacombe, R., Trupin, J., Rottman, F. and O'Neal, C. 1965. RNA codewords and protein synthesis, VII. On the general nature of the RNA code. *Proc Natl Acad Sci U S A.* **53**: 1161-8.

Nishizuka, Y. and Lipmann, F. 1966. Comparison of guanosine triphosphate split and polypeptide synthesis with a purified E. coli system. *Proc Natl Acad Sci U S A.* **55**: 212-9.

Nissen, P., Kjeldgaard, M., Thirup, S., Polekhina, G., Reshetnikova, L., Clark, B.F. and Nyborg, J. 1995. Crystal structure of the ternary complex of Phe-tRNAPhe, EF-Tu, and a GTP analog. *Science.* **270**: 1464-72.

Noller, H.F., Hoffarth, V. and Zimniak, L. 1992. Unusual resistance of peptidyl transferase to protein extraction procedures. *Science.* **256**: 1416-9.

Ogle, J.M., Brodersen, D.E., Clemons, W.M., Jr., Tarry, M.J., Carter, A.P. and Ramakrishnan, V. 2001. Recognition of cognate transfer RNA by the 30S ribosomal subunit. *Science.* **292**: 897-902.

Ogle, J.M., Murphy, F.V., Tarry, M.J. and Ramakrishnan, V. 2002. Selection of tRNA by the ribosome requires a transition from an open to a closed form. *Cell.* **111**: 721-32.

Pan, D., Kirillov, S.V. and Cooperman, B.S. 2007. Kinetically competent intermediates in the translocation step of protein synthesis. *Mol Cell.* **25**: 519-29.

Pape, T., Wintermeyer, W. and Rodnina, M. 1999. Induced fit in initial selection and proofreading of aminoacyl-tRNA on the ribosome. *EMBO J.* **18**: 3800-7.

Peske, F., Savelsbergh, A., Katunin, V.I., Rodnina, M.V. and Wintermeyer, W. 2004. Conformational changes of the small ribosomal subunit during elongation factor G-dependent tRNA-mRNA translocation. *J Mol Biol.* **343**: 1183-94.

Powers, T. and Noller, H.F. 1991. A functional pseudoknot in 16S ribosomal RNA. *EMBO J.* **10**: 2203-14.

Razga, F., Spackova, N., Reblova, K., Koca, J., Leontis, N.B. and Sponer, J. 2004. Ribosomal RNA kink-turn motif--a flexible molecular hinge. *J Biomol Struct Dyn.* **22**: 183-94.

Razga, F., Zacharias, M., Reblova, K., Koca, J. and Sponer, J. 2006. RNA kink-turns as molecular elbows: hydration, cation binding, and large-scale dynamics. *Structure.* **14**: 825-35.

Richter, D. 1972. Inability of E. coli ribosomes to interact simultaneously with the bacterial elongation factors EF Tu and EF G. *Biochem Biophys Res Commun.* **46**: 1850-6.

Robertson, J.M., Urbanke, C., Chinali, G., Wintermeyer, W. and Parmeggiani, A. 1986. Mechanism of ribosomal translocation. Translocation limits the rate of Escherichia coli elongation factor G-promoted GTP hydrolysis. *J Mol Biol.* **189**: 653-62.

Rodnina, M.V., Gromadski, K.B., Kothe, U. and Wieden, H.J. 2005. Recognition and selection of tRNA in translation. *FEBS Lett.* **579**: 938-42.

Rodnina, M.V., Savelsbergh, A., Katunin, V.I. and Wintermeyer, W. 1997. Hydrolysis of GTP by elongation factor G drives tRNA movement on the ribosome. *Nature.* **385**: 37-41.

Rodnina, M.V., Savelsbergh, A., Matassova, N.B., Katunin, V.I., Semenkov, Y.P. and Wintermeyer, W. 1999. Thiostrepton inhibits the turnover but not the GTPase of elongation factor G on the ribosome. *Proc Natl Acad Sci U S A.* **96**: 9586-90.

Roy, S. 2004. Fluorescence quenching methods to study protein-nucleic acid interactions. *Methods in enzymology.* **379**: 175-87.

Saarma, U., Remme, J., Ehrenberg, M. and Bilgin, N. 1997. An A to U transversion at position 1067 of 23 S rRNA from Escherichia coli impairs EF-Tu and EF-G function. *J Mol Biol.* **272**: 327-35.

Savelsbergh, A., Katunin, V.I., Mohr, D., Peske, F., Rodnina, M.V. and Wintermeyer, W. 2003. An elongation factor G-induced ribosome rearrangement precedes tRNA-mRNA translocation. *Mol Cell.* **11**: 1517-23.

Savelsbergh, A., Matassova, N.B., Rodnina, M.V. and Wintermeyer, W. 2000. Role of domains 4 and 5 in elongation factor G functions on the ribosome. *J Mol Biol.* **300**: 951-61.

Savelsbergh, A., Mohr, D., Kothe, U., Wintermeyer, W. and Rodnina, M.V. 2005. Control of phosphate release from elongation factor G by ribosomal protein L7/12. *EMBO J.* **24**: 4316-23.

Savelsbergh, A., Rodnina, M.V. and Wintermeyer, W. 2009. Distinct functions of elongation factor G in ribosome recycling and translocation. *RNA.* **15**: 772-80.

Schmeing, T.M., Voorhees, R.M., Kelley, A.C., Gao, Y.G., Murphy, F.V.t., Weir, J.R. and Ramakrishnan, V. 2009. The crystal structure of the ribosome bound to EF-Tu and aminoacyl-tRNA. *Science.* **326**: 688-94.

Schmeing, T.M., Voorhees, R.M., Kelley, A.C. and Ramakrishnan, V. 2011. How mutations in tRNA distant from the anticodon affect the fidelity of decoding. *Nat Struct Mol Biol.* **18**: 432-6.

Schmidt, F.J., Thompson, J., Lee, K., Dijk, J. and Cundliffe, E. 1981. The binding site for ribosomal protein L11 within 23 S ribosomal RNA of Escherichia coli. *J Biol Chem.* **256**: 12301-5.

Schuwirth, B.S., Borovinskaya, M.A., Hau, C.W., Zhang, W., Vila-Sanjurjo, A., Holton, J.M. and Cate, J.H. 2005. Structures of the bacterial ribosome at 3.5 A resolution. *Science.* **310**: 827-34.

Scott, W.G. 1998. RNA catalysis. *Curr Opin Struct Biol.* **8**: 720-6.

Selmer, M., Dunham, C.M., Murphy, F.V.t., Weixlbaumer, A., Petry, S., Kelley, A.C., Weir, J.R. and Ramakrishnan, V. 2006. Structure of the 70S ribosome complexed with mRNA and tRNA. *Science.* **313**: 1935-42.

Seo, H.S., Kiel, M., Pan, D., Raj, V.S., Kaji, A. and Cooperman, B.S. 2004. Kinetics and thermodynamics of RRF, EF-G, and thiostrepton interaction on the Escherichia coli ribosome. *Biochemistry.* **43**: 12728-40.

Sergiev, P.V., Bogdanov, A.A. and Dontsova, O.A. 2005. How can elongation factors EF-G and EF-Tu discriminate the functional state of the ribosome using the same binding site? *FEBS Lett.* **579**: 5439-42.

Sergiev, P.V., Lesnyak, D.V., Burakovsky, D.E., Kiparisov, S.V., Leonov, A.A., Bogdanov, A.A., Brimacombe, R. and Dontsova, O.A. 2005. Alteration in location of a conserved GTPase-associated center of the ribosome induced by mutagenesis influences the structure of peptidyltransferase center and activity of elongation factor G. *J Biol Chem.* **280**: 31882-9.

Shi, X., Chiu, K., Ghosh, S. and Joseph, S. 2009. Bases in 16S rRNA important for subunit association, tRNA binding, and translocation. *Biochemistry.* **48**: 6772-82.

Shine, J. and Dalgarno, L. 1974. The 3'-terminal sequence of Escherichia coli 16S ribosomal RNA: complementarity to nonsense triplets and ribosome binding sites. *Proceedings of the National Academy of Sciences of the United States of America.* **71**: 1342-6.

Sigmund, C.D., Ettayebi, M., Borden, A. and Morgan, E.A. 1988. Antibiotic resistance mutations in ribosomal RNA genes of Escherichia coli. *Methods in enzymology.* **164**: 673-90.

Spiegel, P.C., Ermolenko, D.N. and Noller, H.F. 2007. Elongation factor G stabilizes the hybrid-state conformation of the 70S ribosome. *RNA.* **13**: 1473-82.

Spirin, A.S. 1985. Ribosomal translocation: facts and models. *Progress in nucleic acid research and molecular biology.* **32**: 75-114.

Stark, M.J., Cundliffe, E., Dijk, J. and Stoffler, G. 1980. Functional homology between E. coli ribosomal protein L11 and B. megaterium protein BM-L11. *Mol Gen Genet.* **180**: 11-5.

Studer, S.M., Feinberg, J.S. and Joseph, S. 2003. Rapid kinetic analysis of EF-G-dependent mRNA translocation in the ribosome. *J Mol Biol.* **327**: 369-81.

Tate, W.P., Schulze, H. and Nierhaus, K.H. 1983. The importance of the Escherichia coli ribosomal protein L16 for the reconstitution of the peptidyl-tRNA hydrolysis activity of peptide chain termination. *J Biol Chem.* **258**: 12810-5.

Taylor, D.J., Nilsson, J., Merrill, A.R., Andersen, G.R., Nissen, P. and Frank, J. 2007. Structures of modified eEF2 80S ribosome complexes reveal the role of GTP hydrolysis in translocation. *EMBO J.* **26**: 2421-31.

Teraoka, H. and Nierhaus, K.H. 1978. Protein L16 induces a conformational change when incorporated into a L16-deficient core derived from Escherichia coli ribosomes. *FEBS Lett.* **88**: 223-6.

Thompson, J., Cundliffe, E. and Dahlberg, A.E. 1988. Site-directed mutagenesis of Escherichia coli 23 S ribosomal RNA at position 1067 within the GTP hydrolysis centre. *J Mol Biol.* **203**: 457-65.

Traut, R.R. and Monro, R.E. 1964. The Puromycin Reaction and Its Relation to Protein Synthesis. *Journal of molecular biology.* **10**: 63-72.

Valle, M., Sengupta, J., Swami, N.K., Grassucci, R.A., Burkhardt, N., Nierhaus, K.H., Agrawal, R.K. and Frank, J. 2002. Cryo-EM reveals an active role for aminoacyl-tRNA in the accommodation process. *EMBO J.* **21**: 3557-67.

Valle, M., Zavialov, A., Li, W., Stagg, S.M., Sengupta, J., Nielsen, R.C., Nissen, P., Harvey, S.C., Ehrenberg, M. and Frank, J. 2003. Incorporation of aminoacyl-tRNA into the ribosome as seen by cryo-electron microscopy. *Nat Struct Biol.* **10**: 899-906.

Vester, B. and Garrett, R.A. 1988. The importance of highly conserved nucleotides in the binding region of chloramphenicol at the peptidyl transfer centre of Escherichia coli 23S ribosomal RNA. *The EMBO journal.* **7**: 3577-87.

Voorhees, R.M., Schmeing, T.M., Kelley, A.C. and Ramakrishnan, V. 2010. The mechanism for activation of GTP hydrolysis on the ribosome. *Science.* **330**: 835-8.

Wahl, M.C. and Moller, W. 2002. Structure and function of the acidic ribosomal stalk proteins. *Curr Protein Pept Sci.* **3**: 93-106.

Watson, J.D. 1964. The Synthesis of Proteins Upon Ribosomes. *Bulletin de la Societe de chimie biologique.* **46**: 1399-425.

Wettstein, F.O. and Noll, H. 1965. Binding of Transfer Ribonucleic Acid to Ribosomes Engaged in Protein Synthesis: Number and Properties of Ribosomal Binding Sites. *Journal of molecular biology.* **11**: 35-53.

Wimberly, B.T., Guymon, R., McCutcheon, J.P., White, S.W. and Ramakrishnan, V. 1999. A detailed view of a ribosomal active site: the structure of the L11-RNA complex. *Cell.* **97**: 491-502.

Wintermeyer, W., Peske, F., Beringer, M., Gromadski, K.B., Savelsbergh, A. and Rodnina, M.V. 2004. Mechanisms of elongation on the ribosome: dynamics of a macromolecular machine. *Biochem Soc Trans.* **32**: 733-7.

Woese, C.R., Winker, S. and Gutell, R.R. 1990. Architecture of ribosomal RNA: constraints on the sequence of "tetra-loops". *Proc Natl Acad Sci U S A.* **87**: 8467-71.

Xing, Y. and Draper, D.E. 1995. Stabilization of a ribosomal RNA tertiary structure by ribosomal protein L11. *J Mol Biol.* **249**: 319-31.

Yarmolinsky, M.B. and Haba, G.L. 1959. Inhibition by Puromycin of Amino Acid Incorporation into Protein. *Proceedings of the National Academy of Sciences of the United States of America.* **45**: 1721-9.

Youngman, E.M., Brunelle, J.L., Kochaniak, A.B. and Green, R. 2004. The active site of the ribosome is composed of two layers of conserved nucleotides with distinct roles in peptide bond formation and peptide release. *Cell.* **117**: 589-99.

Yusupov, M.M., Yusupova, G.Z., Baucom, A., Lieberman, K., Earnest, T.N., Cate, J.H. and Noller, H.F. 2001. Crystal structure of the ribosome at 5.5 A resolution. *Science.* **292**: 883-96.

Yusupova, G., Jenner, L., Rees, B., Moras, D. and Yusupov, M. 2006. Structural basis for messenger RNA movement on the ribosome. *Nature.* **444**: 391-4.

Zaher, H.S. and Green, R. 2010. Hyperaccurate and error-prone ribosomes exploit distinct mechanisms during tRNA selection. *Mol Cell.* **39**: 110-20.

Zamecnik, P.C. and Keller, E.B. 1954. Relation between phosphate energy donors and incorporation of labeled amino acids into proteins. *J Biol Chem.* **209**: 337-54.

Zhou, J., Lancaster, L., Trakhanov, S. and Noller, H.F. 2011. Crystal structure of release factor RF3 trapped in the GTP state on a rotated conformation of the ribosome. *RNA.*

OM